Linköping studies in science and technology
Dissertations, No 1315

Look-ahead Control of Heavy Vehicles

Erik Hellström

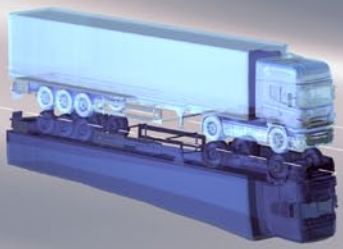

Linköping University
INSTITUTE OF TECHNOLOGY

Department of Electrical Engineering
Linköping 2010

Linköping studies in science and technology
Dissertations, No 1315

Look-ahead Control of Heavy Vehicles

Erik Hellström

Linköping University
INSTITUTE OF TECHNOLOGY

Department of Electrical Engineering
Linköping 2010

Linköping studies in science and technology
Dissertations, No 1315

Erik Hellström
hellstrom@isy.liu.se
www.vehicular.isy.liu.se
Division of Vehicular Systems
Department of Electrical Engineering
Linköping University
SE–581 83 Linköping, Sweden

Hellström, Erik
Look-ahead Control of Heavy Vehicles
ISBN 978-91-7393-389-6
ISSN 0345-7524

Cover illustration by Effektfabriken

Typeset with LaTeX 2ε
Printed by LiU-Tryck, Linköping, Sweden 2010

To Gabriella

Abstract

Trucks are responsible for the major part of inland freight and so, they are a backbone of the modern economy but they are also a large consumer of energy. In this context, a dominating vehicle is a truck with heavy load on a long trip. The aim with look-ahead control is to reduce the energy consumption of heavy vehicles by utilizing information about future conditions focusing on the road topography ahead of the vehicle.

The possible gains with look-ahead control are evaluated by performing experiments with a truck on highway. A real-time control system based on receding horizon control (RHC) is set up where the optimization problem is solved repeatedly on-line for a certain horizon ahead of the vehicle. The experimental results show that significant reductions of the fuel consumption are achieved, and that the controller structure, where the algorithm calculates set points fed to lower level controllers, has satisfactory robustness to perform well on-board in a real environment. Moreover, the controller behavior has the preferred property of being intuitive, and the behavior is perceived as comfortable and natural by participating drivers and passengers.

A well-behaved and efficient algorithm is developed, based on dynamic programing, for the mixed-integer nonlinear minimum-fuel problem. A modeling framework is formulated where special attention is given to properly include gear shifting with physical models. Fuel equivalents are used to reformulate the problem into a tractable form and to construct a residual cost enabling the use of a shorter horizon ahead of the vehicle. Analysis of errors due to discretization of the continuous dynamics and due to interpolation shows that an energy formulation is beneficial for reducing both error sources. The result is an algorithm giving accurate solutions with low computational effort for use in an on-board controller for a fuel-optimal velocity profile and gear selection.

The prevailing approach for the look-ahead problem is RHC where main topics are the approximation of the residual cost and the choice of the horizon length. These two topics are given a thorough investigation independent of the method of solving the optimal control problem in each time step. The basis for the fuel equivalents and the residual cost is formed from physical intuition as well as mathematical interpretations in terms of the Lagrange multipliers used in optimization theory. Measures for suboptimality are introduced that enables choosing horizon length with the appropriate compromise between fuel consumption and trip time.

Control of a hybrid electric powertrain is put in the framework together with control of velocity and gear. For an efficient solution of the minimum-fuel problem in this case, more fuel equivalence factors and an energy formulation are employed. An application is demonstrated in a design study where it is shown how the optimal trade-off between size and capacity of the electrical system depends on road characteristics, and also that a modestly sized electrical system achieves most of the gain.

The contributions develop algorithms, create associated design tools, and carry out experiments. Altogether, a feasible framework is achieved that pave the way for on-board fuel-optimal look-ahead control.

Populärvetenskaplig sammanfattning

Lastbilen står för majoriteten av landtransporterna av gods och är därmed en grundpelare i den moderna ekonomin men även en stor konsument av energi. Ett dominerande fordon i sammanhanget är en tung lastbil som används för långa transporter. Syftet med framförhållningsreglering (engelska: look-ahead control) är att minska denna energiförbrukning genom att använda information om framtida förhållanden, med fokus på vägtopografin framför fordonet, för energiminimal reglering.

Vägens topografi är snart tillgänglig ombord på fordon tack vare billiga enheter för satellitnavigeringssystemet GPS kombinerat med tredimensionella kartor som är under utveckling idag. Målet är att utnyttja att den här informationen är tillgänglig för att minska bränsleförbrukningen i tunga lastbilar. Dessa fordon är redan idag förhållandevis effektiva eftersom förbränningsmotorn ofta körs i fördelaktiga arbetspunkter på grund av stor last i förhållande till motoreffekten. Samtidigt förbrukar de mycket bränsle totalt sett och därför har även små framsteg stor effekt; enligt industrin är en möjlig förbättring om 0.5% i bränsleekonomi värd att utforska. I en serie experiment med framförhållningsreglering på en svensk motorväg visas att förbättringspotentialen är 3.5%, utan ökad körtid, jämfört med traditionell reglering.

Principen för framförhållningsreglering beskrivs i figuren nedan med hjälp av bilder från den video om projektet som finns på YouTube.[†]

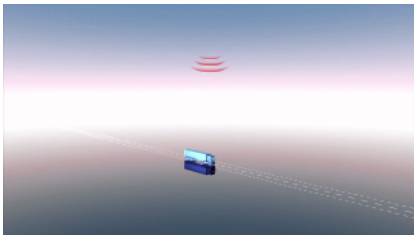

(a) Koordinater för den aktuella positionen tas emot med en GPS-enhet ombord på fordonet.

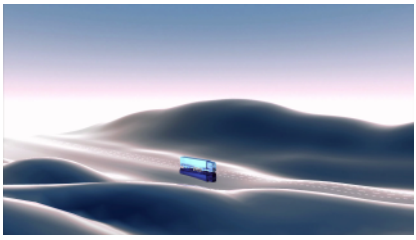

(b) Med hjälp av positionen och en databas med vägtopografin fås information om vägens lutning.

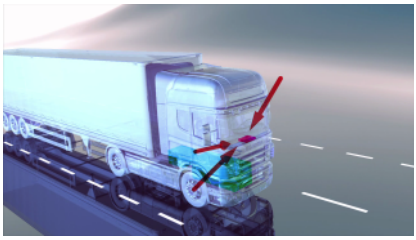

(c) Algoritmen beräknar den mest bränsleeffektiva regleringen utifrån tillgänglig information.

(d) Lösningen kommuniceras till fordonet där den verkställs och förfarandet börjar om.

[†] Videon hittas genom att söka på frasen *look-ahead control* på `http://www.youtube.com/` eller genom följande länk: `http://www.youtube.com/watch?v=waCxqRys6v8`

De besparingar som är möjliga att uppnå med framförhållningsreglering utvärderas genom att utföra experiment med en lastbil på motorväg. Ett realtidssystem för reglering, baserat på prediktionsreglering, tas fram där optimeringsproblemet löses ombord i ett iterativt schema som, i varje iteration, betraktar en viss horisont framför fordonet. Resultaten från experimenten visar att en betydande minskning i bränsleförbrukning är möjlig och att reglerstrukturen, där algoritmen beräknar börvärden för regulatorer på lägre nivå i en regulatorhierarki, har den robusthet som krävs för att fungera väl ombord under verkliga förhållanden. Beteendet hos regleringen har den önskvärda egenskapen att vara intuitivt, och det uppfattas också som naturligt och bekvämt för de förare och passagerare som deltar i test och demonstrationer.

En väl fungerande och effektiv algoritm har utvecklats, baserad på dynamisk programmering, för bränsleminimeringsproblemet som är ett olinjärt optimeringsproblem med både kontinuerliga och diskreta inslag. En modellstruktur formuleras där speciell vikt läggs vid att, på ett adekvat sätt, inkludera fysikaliska modeller för växlingar. Bränsleekvivalenter används för att formulera problemet på en lätthanterlig form och för att skapa en restkostnad som gör det möjligt att använda en kortare horisont framför fordonet. En analys av de numeriska fel som uppstår på grund av att kontinuerlig dynamik görs diskret och på grund av interpolation visar att båda felkällorna minskar genom att använda en energiformulering. Resultatet är en algoritm som ger noggranna lösningar med låg beräkningsinsats för ombordanvändning i en regulator för bränsleminimal hastighetsprofil och växelval.

Prediktionsreglering är den etablerade övergripande metoden för framförhållningsproblemet. Väsentliga frågeställningar gäller därför approximationen av restkostnaden och valet av horisontlängden. Dessa två frågor ägnas en ingående analys som är oberoende av hur optimeringsproblemet löses i varje iteration. Fundamenten för bränsleekvivalenterna och restkostnaden byggs på fysikalisk intuition såväl som på matematiska tolkningar i termer av de Lagrange-multiplikatorer som används i optimeringsteori. Mått för suboptimalitet introduceras som ger verktyg för att välja horisontlängden med en ändamålsenlig kompromiss mellan bränsleförbrukning och körtid.

Reglering av en hybrid drivlina, där ett elektriskt system också kan driva fordonet, kombineras med reglering av hastighet och växel. För att effektivt lösa bränsleminimeringsproblemet för det här fallet används fler bränsleekvivalenter och en energiformulering. En användning demonstreras i en designstudie där det visas hur den optimala kompromissen mellan storlek och kapacitet för det elektriska systemet beror av vägens karaktäristik där det visar sig att ett relativt litet system uppnår större delen av vinsten.

Bidragen utvecklar algoritmer, skapar relaterade designverktyg och utför experiment. Sammantaget åstadkommes ett realiserbart ramverk som banar väg för energiminimal framförhållningsreglering ombord på fordon.

Acknowledgments

This work has been carried out at the division of Vehicular Systems, department of Electrical Engineering at Linköping University. First of all, I would like to express my gratitude to my supervisor Professor Lars Nielsen for letting me join the group and all of his encouragement and valuable input during the project. I am fortunate to have had such a dedicated supervisor who always made me feel that our work was important and who always stand by me at critical times.

My second supervisor Jan Åslund is a great thinker and I am utterly thankful for the time he put into the project. Anders Fröberg and Maria Ivarsson have been valued colleagues and co-authors; we have had interesting discussions and fruitful collaborations on the subject of look-ahead control. Per Sahlholm, Anders Jensen, and Nils-Gunnar Vågstedt at Scania are appreciated for their efforts concerning the realization of the demonstrator vehicle and the experiments. Erik Frisk is thanked for helping me scrutinize the layout of the dissertation.

The work was funded by the Swedish Foundation for Strategic Research SSF through the research center MOVIII. The support is gratefully acknowledged.

The many dinners together with my dear friends Frisk and Janne really brightened up everyday life, and I look forward to many more. Everyone at the division is appreciated for jointly creating a positive and nice atmosphere to work in.

I will forever owe a debt of gratitude to my parents, Britta and Svenny, for always supporting me. I am also blessed with my sisters and brothers Karin, Andreas, and John. My love goes to family, friends and to my wife Gabriella.

Erik Hellström
Linköping, April 2010

Contents

Chapter 1

Introduction

Efficient transportation is a matter of vital importance in the modern economy and the backbone is road vehicles that, e.g., in Europe and in the United States account for more than 70% of inland freight transport (Noreland, 2008; Bradley, 2000). It is therefore attractive to reduce the energy consumption of vehicles, both from an environmental and an economical point of view. To reduce the energy consumption, the losses in the chain of steps from a basic energy source to a completed drive mission should be targeted. This chain starts at a basic energy source, from which a fuel is extracted that can be converted, on-board the vehicle, into mechanical energy.

One approach to reduce the losses of the on-board energy conversion is look-ahead control where knowledge about future conditions is utilized to increase fuel efficiency. A source of such information is the combination of road topography maps with the global positioning system (GPS). This has become economically viable with the decreasing cost of GPS devices, and road databases including elevation are now emerging from map providers. The road topography naturally has a large influence on the motion of vehicles with low engine power compared to the vehicle mass. The topic of this dissertation is how the knowledge of the road topography ahead of such a vehicle can be utilized for reducing the fuel consumption. This is achieved by longitudinal control that, for example for a conventional powertrain means controlling velocity and gear in the most fuel-efficient way with respect to the upcoming topography.

A common heavy vehicle is a class 8 truck, weighing more than 15 tonnes. For such a truck, about $1/3$ of the life cycle cost comes from the cost of fuel, see Figure 1.1. These trucks typically travel on open road and have a high annual mileage making them a large consumer of fuel. For example, an average European class 8 truck travels 150,000 km with a fuel consumption of 32.5 $\mathrm{l}/100\mathrm{km}$ (Schittler, 2003). In the U.S. the average fuel consumption is 37.9 $\mathrm{l}/100\mathrm{km}$ (Vyas et al., 2003) and class 8 trucks consume about 68% of all commercial truck fuel used where 70% of this amount is spent operating on open road with a trip length of more than 161 km (Bradley, 2000). For this type of vehicles, a technology improving fuel efficiency will thus have good benefit.

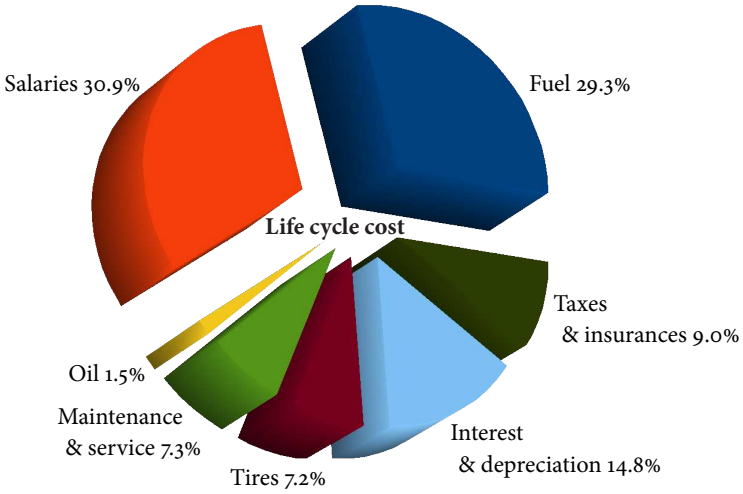

Figure 1.1: Life cycle cost of a class 8 truck in Europe (Schittler, 2003).

The main challenges faced when trying to reduce the fuel consumption of heavy trucks by control are coupled to the current fuel efficiency of these vehicles and the real-time requirements of an algorithm. Due to the large mass compared to the engine power, heavy trucks on open road typically run at engine operating points with high load and high efficiency. This is also indicated by the fact that, according to the industry, any technology for long-haulage having the promise of saving 0.5% of fuel is considered worthwhile to explore. Further, for a minimum-fuel control to be feasible on-board, an efficient solution of a complex optimization problem is required. These challenges are taken up in this dissertation and the contributions develop computationally efficient algorithms and show that significant fuel savings are possible.

1.1 Outline and contributions

The continuous link in the contributions is the successive development of the framework for look-ahead control in Paper A through C and the transfer of the methodology for also studying hybrid electric vehicles in Paper D.

Paper A describes an implementation and evaluation of look-ahead control in a demonstrator vehicle. A real-time control system is implemented based on receding horizon control (RHC) where the optimization problem is solved repeatedly on-line for a given horizon. The controller structure, where the algorithm calculates set points fed to lower level controllers, is proven to perform well on-board in a real environment. An experimental evaluation, on Swedish highway in normal traffic, shows a significant fuel consumption reduction of 3.5%, without increased trip time, compared to traditional cruise control. The controller behavior is characterized and found to be intuitive, and is appreciated by drivers and passengers.

The development is continued in Paper B where an efficient algorithm, based on dynamic programming (DP), is designed for the on-line optimization problem. A model structure is defined that allows general velocity dynamics and proper physical modeling of gear shifts through a set of functions describing the shift process. Fuel equivalence factors for time and kinetic energy are introduced, and these are used to reformulate the problem into a tractable form and to construct a residual cost to be used at the end of the horizon. Furthermore, analysis of the errors due to discretization of the continuous dynamics and due to interpolation shows that an energy formulation is beneficial for reducing both error sources. The result is a computationally efficient algorithm giving accurate solutions for use in an on-board controller for a fuel-optimal velocity profile and gear selection.

The main topics in RHC, the prevailing approach for the look-ahead problem, are choosing a residual cost and selecting a proper horizon length, and these are addressed in Paper C. The basis for the fuel equivalents and the residual cost is substantiated by adding mathematical interpretations in terms of the Lagrange multipliers used in optimization theory. Measures for suboptimality, independent of the optimization method, are introduced that enables choosing horizon lengths with the appropriate compromise between fuel consumption and trip time. A subsequent evaluation shows how the road characteristics and the vehicle mass influence the choice of horizon length.

In Paper D, control of a hybrid electric powertrain is put together with control of velocity and gear which gives a framework for the simultaneous management of kinetic and electric energy. An efficient solution is obtained by employing more fuel equivalence factors and an energy formulation. The formulation is applied to a design study where it is shown how the optimal trade-off between size and capacity of the electrical system depends on road characteristics.

The contributions altogether achieve a feasible framework for look-ahead control by developing algorithms, creating associated design tools, and carrying out experiments. A theme is the exploration of physically intuitive approaches. These have lend themselves to mathematical analysis where important ideas have been an energy formulation and the use of fuel equivalents.

1.2 Publications

In the research work leading to this dissertation, the author has published the following conference and journal papers.

- E. Hellström, J. Åslund, and L. Nielsen. Horizon length and fuel equivalents for fuel-optimal look-ahead control. In *6th IFAC Symposium on Advances in Automotive Control*, Munich, Germany, 2010.
- E. Hellström, J. Åslund, and L. Nielsen. Management of kinetic and electric energy in heavy trucks. In *SAE World Congress*, number 2010-01-1314 in SAE Technical Paper Series, Detroit, MI, USA, 2010.
- E. Hellström, J. Åslund, and L. Nielsen. Design of an efficient algorithm for fuel-optimal look-ahead control. *Control Engineering Practice*, in press, 2010.

- ⋆ E. Hellström, M. Ivarsson, J. Åslund, and L. Nielsen. Look-ahead control for heavy trucks to minimize trip time and fuel consumption. *Control Engineering Practice*, 17(2):245–254, 2009.
- ⋆ E. Hellström, J. Åslund, and L. Nielsen. Design of a well-behaved algorithm for on-board look-ahead control. In *IFAC World Congress*, Seoul, Korea, 2008.
- ⋆ E. Hellström, M. Ivarsson, J. Åslund, and L. Nielsen. Look-ahead control for heavy trucks to minimize trip time and fuel consumption. In *5th IFAC Symposium on Advances in Automotive Control*, Monterey, CA, USA, 2007.
- ⋆ A. Fröberg, E. Hellström, and L. Nielsen. Explicit fuel optimal speed profiles for heavy trucks on a set of topographic road profiles. In *SAE World Congress*, number 2006-01-1071 in SAE Technical Paper Series, Detroit, MI, USA, 2006.
- ⋆ E. Hellström, A. Fröberg, and L. Nielsen. A real-time fuel-optimal cruise controller for heavy trucks using road topography information. In *SAE World Congress*, number 2006-01-0008 in SAE Technical Paper Series, Detroit, MI, USA, 2006.

Chapter 2

Prelude

As a prelude to the publications, some additional background is given in this chapter with the purpose of putting the contributions of the papers into perspective. The main challenges for look-ahead control, the high fuel efficiency of heavy trucks and the requirements for real-time control, were briefly presented in Chapter 1 together with the contributions. This chapter elaborates on these topics, and first an examination of the energy use in a heavy diesel truck is made in Section 2.1 to indicate the potential increase in fuel efficiency. In Section 2.2, the possibility for on-board control is examined and examples are used for showing how fuel-optimal control differs from traditional control. Finally, in Section 2.3, the literature in the field is surveyed more comprehensively than there was room for in the included papers, and the contributions are put into this perspective.

2.1 Energy audit

In a heavy diesel truck, the chemical energy w_c stored in the fuel is converted, with an efficiency η, into mechanical energy through the combustion process in the engine. Some of the mechanical energy is consumed by auxiliary loads, such as the alternator and cooling fan, and by losses in the driveline, such as friction in the transmission and wheel bearings. After these losses w_l, the remaining energy w_p is transmitted to the wheels. For an interval of distance Δs, this energy balance is thus

$$\Delta w_p = \eta \Delta w_c - \Delta w_l \tag{2.1}$$

The propulsive energy w_p is partly consumed by the work d from the drag forces due to air drag and rolling resistance. Energy is also stored in the vehicle in form of kinetic energy e when accelerating and potential energy p when climbing grades. When braking, energy b is dissipated from the system. The energy balance becomes

$$\Delta w_p = \Delta e + \Delta p + \Delta d + \Delta b \tag{2.2}$$

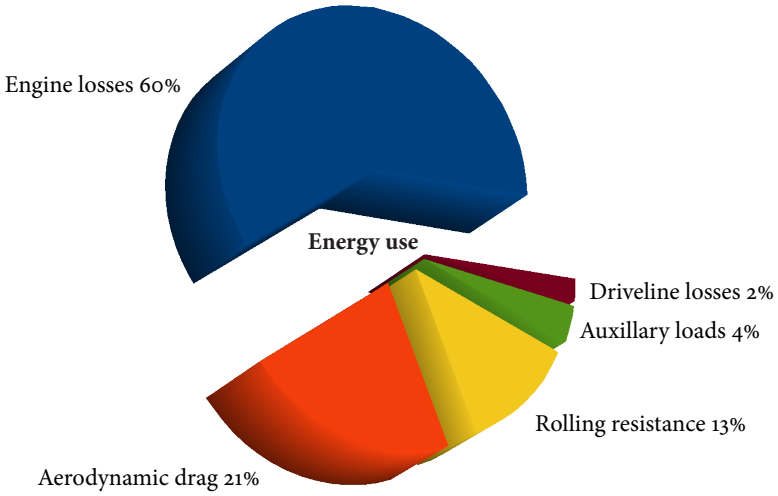

Figure 2.1: Energy use for a class 8 truck on level road (Bradley, 2000).

for a distance Δs.

When cruising at constant speed on level road, $\Delta e = \Delta p = \Delta b = 0$. The energy balance obtained by combining (2.1)–(2.2) for these conditions, considering a typical current class 8 vehicle traveling at 105 km/h (65 mph) with a gross weight of 36.3 t (80,000 lb), is shown in Figure 2.1. These numbers correspond to $\eta = 40\%$ that is a representative overall efficiency; the peak efficiency may reach 46% but engine losses remain the largest individual share among these categories (Bradley, 2000).

For a heavy truck operating on a real road, constant speed is typically not possible. In downhills, the truck may accelerate without engine propulsion due to the large mass and it can be necessary to use the brakes for safety or legal reasons. Clearly, when using the brakes, Δb becomes positive and energy is lost to the ambient. To investigate the brake usage, the integral of the energy balance (2.2) over three different routes is calculated, see Figure 2.2. The results are obtained with a model for a truck with a 360 hp powertrain controlled by a cruise controller, and a gross weight of 40 t. The initial and terminal velocity are the same and the routes are traveled back and forth, hence the integral of $\Delta e + \Delta p$ is zero. The set speed is 80 km/h and the extra speed allowed in downhills, before braking limits the speed, is varied along the horizontal axis in the figure. It is seen that considerable amounts of energy are wasted by braking, there is a intuitively negative correlation with the extra speed allowed in downhills, and the values are dependent on the road characteristics.

2.1.1 Potential benefits

Knowledge of the upcoming road topography gives a better prediction of the future load and this can be utilized by look-ahead control to improve the fuel economy. Among the categories in the analysis of energy use in Figures 2.1 and 2.2; brake energy, auxiliary

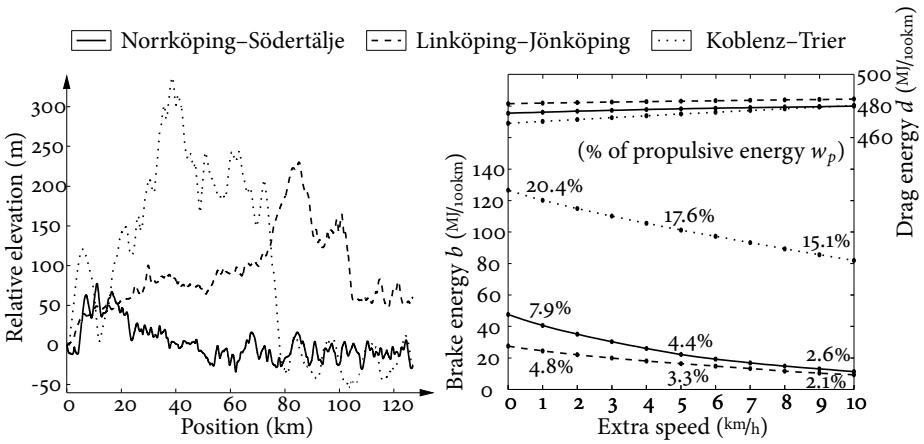

Figure 2.2: Energy use for a 40 t truck is shown to the right, with different values for the extra speed allowed in downhills, on the three routes shown to the left.

loads, and engine losses are the primary possible targets for look-ahead control. These are shortly discussed below. The other categories can be targeted by, e.g., improved lubricants and innovative design of the vehicle and the tires.

The energy wasted in braking can be reduced by slowing down prior to steep downhills, by using a hybrid powertrain for recovering some of the energy, and by utilizing some of the energy for driving auxiliary units. Electrically driven auxiliary units can also use the conventional battery as an energy buffer for fuel-optimal planning of the load. Moreover, there is a possibility to reduce engine losses since the peak engine efficiency is higher than the overall efficiency on a typical cycle. This can be achieved by controlling the engine to more efficient operating points taking nonlinear engine characteristics and gear shifting into account. A hybrid powertrain gives further possibilities to reduce engine losses by optimizing the energy distribution, between the combustion engine and electrical motor in a hybrid electric vehicle, and by downsizing the engine.

The gains that are possible to obtain in reality by controlling the engine, the brakes, and the transmission are investigated and quantified in Paper A through experiments. The benefits of a hybridization are evaluated in Paper D in a design study performed by computer simulations.

2.2 Realization of look-ahead control

A controller working on-board in a real environment requires a complexity that is manageable in real-time and robustness towards disturbances and uncertainties.

The algorithm in Paper A requires tenths of a second on a laptop computer to compute the optimal feedback solution for about 1 min ahead which enabled the realization in a demonstrator vehicle and the experimental evaluation. The development in Paper B increases the numerical soundness of the algorithm and reduces the computation time

with about a factor of 10. Moreover, the results in Paper C are guiding for choosing a well-founded residual cost and choosing a horizon length with a desired trade-off between suboptimality and complexity. The result is an algorithm feasible to run on an embedded system, this has been verified by an implementation on an embedded system based on a 200 MHz ARM processor with 32 Mb RAM.

The experimental results in Paper A show that the controller structure has satisfactory robustness towards disturbances for performing well in a real environment. Regarding uncertainties, the vehicle mass is an important parameter typically estimated on-line. Simulations have shown that typical estimation errors of about 10% have only minor effects on the performance of the look-ahead algorithm (Krahwinkel, 2010). In conclusion, the contributions in Paper A through C pave the way for on-board fuel-optimal look-ahead control.

2.2.1 Characteristics of fuel-optimal solutions

To get an impression of how look-ahead control differs from traditional control, examples of fuel-optimal solutions, obtained by the algorithm in Paper B, are computed for a typical truck weighing 40 t and equipped with a 360 hp diesel engine. The elevation data for the road segment, shown in Figure 2.3, come from measurements on the trial route between Norrköping and Södertälje used in the experiments in Paper A, see Figure 2.6. For a characterization of the controller behavior in practical driving, see Paper A.

The result from the algorithm is the optimal feedback law for fueling, braking, and gear choice as a function of current position, velocity, and gear. In traditional cruise control, the velocity is controlled towards a given set point and the gear is selected based on current engine speed and load. This strategy is only dependent on the current state of the vehicle whereas the optimal control law also depends on the future topography as can be seen in Figure 2.4 where the optimal fueling level and gear choice are shown. The figure shows the optimal feedback law for the highest gear, and the color represents the control value. The colors dark blue, cyan, yellow, and dark red represent gears 9 through 12. The fueling level ranges through these colors where dark blue is zero throttle and dark red is full throttle. The engine model used is an approximation that is affine in fueling, and the solution in Figure 2.4 for the fueling has the expected bang-singular-bang characteristics where large regions are at the constraint of either zero throttle or full throttle (see, e.g., Fröberg et al. (2006) or Paper C). For the nonlinear engine model using measured data, with the solution in Figure 2.5, there are still large regions at the constraints but the boundary area between them is widened and smoothed. The gear choice is rather similar in the figures, e.g., it is noted that in the uphill after 6 km the solution is, depending on the velocity, either to downshift from gear 12 to 11 or to keep gear 12 and then, if the velocity decreases, to downshift two steps to gear 10.

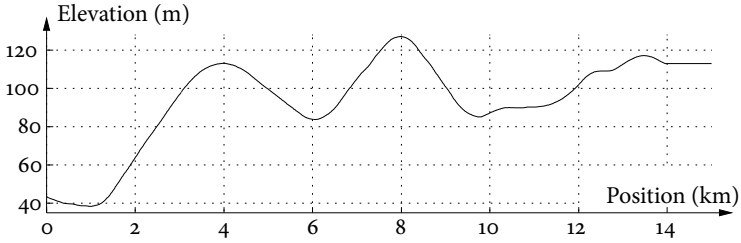

Figure 2.3: A road segment close to Norrköping.

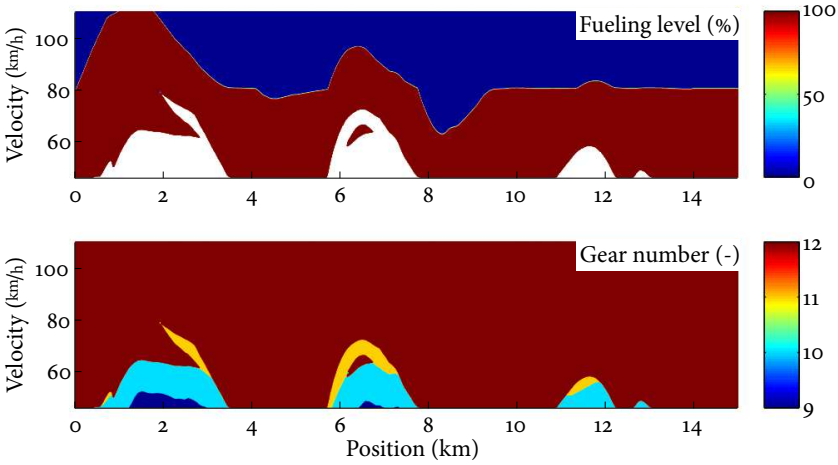

Figure 2.4: Optimal control law for gear 12, computed with an affine engine model.

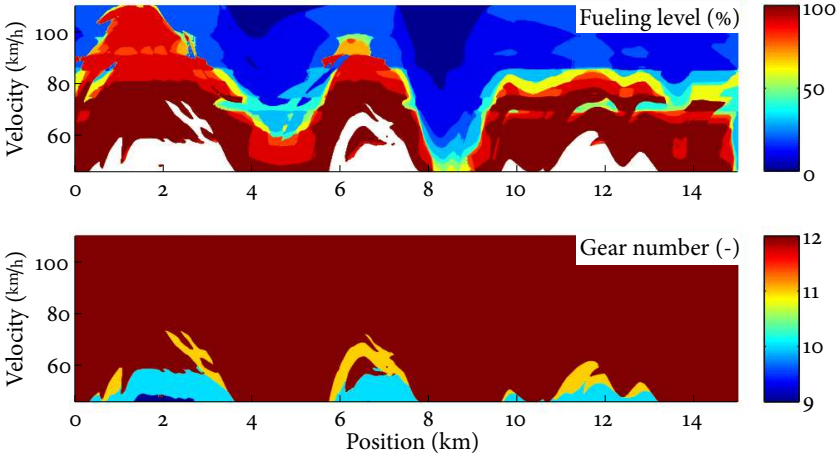

Figure 2.5: Optimal control law for gear 12, computed with measured engine data.

Figure 2.6: The route between Norrköping and Södertälje is marked in blue and the road segment in Figure 2.3 is marked in red. Map data used with permission (MEDGIV-2010-25084) from Sverigekartan © Lantmäteriverket, Gävle 2010.

2.3 Literature overview

An overview of related work is made that is more comprehensive than there was room for in the included papers, and the contributions in this dissertation are put into that perspective.

In the early work by Schwarzkopf and Leipnik (1977), a minimum-fuel problem for a nonlinear vehicle model is formulated and explicit solutions for constant road slopes are obtained by aid of the maximum principle. References to other early works are given by Stoicescu (1995) who also studied analytical solutions. More recent studies are reported in Chang and Morlok (2005); Fröberg et al. (2006); Fröberg and Nielsen (2007); Ivarsson et al. (2009) where the latter two works focus on the connection between the engine nonlinearities and the characteristics of the solution. Fuel-optimal strategies for approaching a leading vehicle are derived analytically by Sciaretta and Guzzella (2005). The related problem of traveling in a slowly moving car queue is treated in Jonsson and Jansson (2004) where numerical results from a DP algorithm are reported.

The analytical studies treat simplistic road profiles while different numerical algorithms have been proposed to solve the problem for a general road profile. Results from a forward DP approach are reported in Hooker et al. (1983); Hooker (1988). Such a technique is also used by Monastyrsky and Golownykh (1993) but the problem is formu-

lated as dependent on distance instead of time and trip time is added to the objective function besides the fuel use. Later developments, focused on heavy trucks, are reported in Lattemann et al. (2004); Neiss et al. (2004); Terwen et al. (2004) who consider cruise control, by adding a quadratic penalty on deviations from a cruise speed, rather than pure fuel-optimal control. This approach was also taken by Hellström et al. (2006) but in later works by the same authors, e.g., Paper A and B, the method to include time in the objective is adopted. This is basically also the procedure in Huang et al. (2008); Passenberg et al. (2009).

2.3.1 Heavy trucks

The transmission in a heavy truck is typically of the automated manual type due to cost, durability and efficiency in comparison with an automatic transmission (Pettersson and Nielsen, 2000). This has been treated with several approaches, such as assuming that the shift process is autonomous and instantaneous (Lattemann et al., 2004; Neiss et al., 2004; Passenberg et al., 2009) or making a continuous relaxation of the discrete signal (Huang et al., 2008). Analytical and numerical studies have shown that the optimal shift strategy depends on the model (Fröberg and Nielsen, 2008; Ivarsson et al., 2010). These works have suggested that a instantaneous model is too simple and that it is important to model the losses during a shift. Explicit physical models for the shift process are used by Terwen et al. (2004) and in Paper A. In Paper B, an algorithmic framework is proposed that allows a general physical model of the gear shift by specifying functions for the velocity change and the required time, distance, and fuel, respectively, during the shift.

On-board control

When considering on-board control the prevailing approach for managing the complexity, due to changing conditions during a drive mission, is RHC. This approach is taken in Paper A and B as well as in other recent studies on the minimum-fuel problem, e.g., Terwen et al. (2004); Hellström et al. (2006); Huang et al. (2008); Passenberg et al. (2009). RHC is a general method for approximating the optimal control law by solving on-line, at each time step, a finite horizon optimal control problem (see, e.g., the survey paper Mayne et al., 2000). Main topics in RHC are how to select the residual cost at the end of the horizon and how to select a proper horizon length. A residual cost, based on physical intuition, is proposed and justified in Paper B, and the theoretical support for this residual cost is strengthened in Paper C. The choice of horizon length is treated in Paper C where measures are introduced, independent of the particular optimization method used in each time step in RHC, that quantifies the basic compromise between suboptimality and computational complexity when choosing the horizon length.

Demonstrated concepts

In Paper A, experimental results with look-ahead control, first published in Hellström et al. (2007), with significant fuel consumption reductions are reported. Recently, a system adapting the velocity to the road topography was introduced by Daimler Trucks

North America in collaboration with Navteq (Daimler Trucks North America press release, 2009). A related system, although without look-ahead, has been launched by Volvo (Volvo press release, 2006). The system senses the current road slope and utilizes that for controlling the truck powertrain, e.g., engaging neutral gear in certain conditions.

Other approaches

The information about road topography has also been used, in other ways than control of velocity and gear selection, with the aim of reducing the energy consumption. Strategies for electrically driven auxiliary units are studied by Pettersson and Johansson (2004) and the control of neutral gear is investigated in Fröberg et al. (2005); Hellström et al. (2006).

2.3.2 Hybrid electric vehicles

The control of hybrid electric vehicles for minimum energy consumption has received a lot of attention since the nineties see, e.g., the overview by Sciarretta and Guzzella (2007), the dissertation Back (2006), and the monograph by Guzzella and Sciarretta (2007). The focus has been on vehicles where the largest gain of hybridization is expected, such as passenger cars (Paganelli et al., 2000; Sciarretta et al., 2004) and light-duty trucks (Lin et al., 2003, 2004). These vehicles have a driving pattern rather different than long-haulage trucks and they are not as much affected by the road slope. Therefore, the approaches have mainly focused on the management of the electrical energy and have not considered the potential energy and management of kinetic energy. Long-haulage trucks are treated in Paper D where hybridization, velocity control, and gear control are put in a common framework with equivalence factors for each degree of freedom. By utilizing the formulation for computational efficiency from Paper B, an optimization algorithm is applied on the evaluation of the size of the electrical system.

2.3.3 Rail vehicles

The problem of optimal control for energy minimization of rail vehicles seems to have been studied earlier than for road vehicles with papers appearing in the late fifties see, e.g., the work by Kokotovic et al. (1972); Liu and Golovitcher (2003) and references therein. These problems are closely related but road vehicles typically have a transmission making the optimal control problem more complicated. The train problem is however still an important problem of its own as indicated by recent publications see, e.g., Khmelnitsky (2000); Franke et al. (2002); Howlett et al. (2009). The dynamic models for train used in these publications fit well into the algorithmic framework in Paper B as the special case without gear shifts.

References

M. Back. *Prädiktive Antriebsregelung zum energieoptimalen Betrieb von Hybridfahrzeugen*. PhD thesis, Universität Karlsruhe, Karlsruhe, Germany, 2006.

R. Bradley. Technology roadmap for the 21st century truck program. Technical Report 21CT-001, U.S. Department of Energy, December 2000.

D.J. Chang and E.K. Morlok. Vehicle speed profiles to minimize work and fuel consumption. *Journal of transportation engineering*, 131(3):173–181, 2005.

Daimler Trucks North America press release, 2009. Freightliner Trucks Launches RunSmart Predictive Cruise for Cascadia. http://daimler-trucksnorthamerica.com/, March 19, 2009.

R. Franke, M. Meyer, and P. Terwiesch. Optimal control of the driving of trains. *Automatisierungstechnik*, 50(12):606–613, December 2002.

A. Fröberg and L. Nielsen. Optimal fuel and gear ratio control for heavy trucks with piece wise affine engine characteristics. In *5th IFAC Symposium on Advances in Automotive Control*, Monterey, CA, USA, 2007.

A. Fröberg and L. Nielsen. Optimal control utilizing analytical solutions for heavy truck cruise control. Technical Report LiTH-ISY-R-2842, Department of Electrical Engineering, Linköping University, Linköping, Sweden, 2008.

A. Fröberg, L. Nielsen, L-G. Hedström, and M. Pettersson. Controlling gear engagement and disengagement on heavy trucks for minimization of fuel consumption. In *IFAC World Congress*, Prague, Czech Republic, 2005.

A. Fröberg, E. Hellström, and L. Nielsen. Explicit fuel optimal speed profiles for heavy trucks on a set of topographic road profiles. In *SAE World Congress*, number 2006-01-1071 in SAE Technical Paper Series, Detroit, MI, USA, 2006.

L. Guzzella and A. Sciarretta. *Vehicle Propulsion Systems*. Springer, Berlin, 2nd edition, 2007.

E. Hellström, A. Fröberg, and L. Nielsen. A real-time fuel-optimal cruise controller for heavy trucks using road topography information. In *SAE World Congress*, number 2006-01-0008 in SAE Technical Paper Series, Detroit, MI, USA, 2006.

E. Hellström, M. Ivarsson, J. Åslund, and L. Nielsen. Look-ahead control for heavy trucks to minimize trip time and fuel consumption. In *5th IFAC Symposium on Advances in Automotive Control*, Monterey, CA, USA, 2007.

E. Hellström, J. Åslund, and L. Nielsen. Design of a well-behaved algorithm for on-board look-ahead control. In *IFAC World Congress*, Seoul, Korea, 2008.

E. Hellström, M. Ivarsson, J. Åslund, and L. Nielsen. Look-ahead control for heavy trucks to minimize trip time and fuel consumption. *Control Engineering Practice*, 17(2): 245–254, 2009.

E. Hellström, J. Åslund, and L. Nielsen. Horizon length and fuel equivalents for fuel-optimal look-ahead control. In *6th IFAC Symposium on Advances in Automotive Control*, Munich, Germany, 2010a.

E. Hellström, J. Åslund, and L. Nielsen. Design of an efficient algorithm for fuel-optimal look-ahead control. *Control Engineering Practice*, in press, 2010b. doi: 10.1016/j.conengprac.2009.12.008.

E. Hellström, J. Åslund, and L. Nielsen. Management of kinetic and electric energy in heavy trucks. In *SAE World Congress*, number 2010-01-1314 in SAE Technical Paper Series, Detroit, MI, USA, 2010c.

J.N. Hooker. Optimal driving for single-vehicle fuel economy. *Transportation Research*, 22A(3):183–201, 1988.

J.N. Hooker, A.B. Rose, and G.F. Roberts. Optimal control of automobiles for fuel economy. *Transportation Science*, 17(2):146–167, 1983.

P.G. Howlett, P.J. Pudney, and X. Vu. Local energy minimization in optimal train control. *Automatica*, 45(11):2692–2698, 2009.

W. Huang, D.M. Bevly, S. Schnick, and X. Li. Using 3D road geometry to optimize heavy truck fuel efficiency. In *11th International IEEE Conference on Intelligent Transportation Systems*, pages 334–339, 2008.

M. Ivarsson, J. Åslund, and L. Nielsen. Look ahead control - consequences of a non-linear fuel map on truck fuel consumption. *Proceedings of the Institution of Mechanical Engineers, Part D, Journal of Automobile Engineering*, 223(D10):1223–1238, 2009.

M. Ivarsson, J. Åslund, and L. Nielsen. Impacts of amt gear-shifting on fuel-optimal look-ahead control. In *SAE World Congress*, number 2010-01-0370 in SAE Technical Paper Series, Detroit, MI, USA, 2010.

J. Jonsson and Z. Jansson. Fuel optimized predictive following in low speed conditions. In *4th IFAC Symposium on Advances in Automotive Control*, Salerno, Italy, 2004.

E. Khmelnitsky. On an optimal control problem of train operation. *IEEE Transactions on Automatic Control*, 45(7):1257–1266, 2000.

P. Kokotovic, , and G. Singh. Minimum-energy control of a traction motor. *Automatic Control, IEEE Transactions on*, 17(1):92–95, Feb 1972.

W. Krahwinkel. Robustness analysis of look-ahead control for heavy trucks. Master's thesis, Institut für Fahrzeugtechnik, TU-Braunschweig, 2010.

F. Lattemann, K. Neiss, S. Terwen, and T. Connolly. The predictive cruise control - a system to reduce fuel consumption of heavy duty trucks. In *SAE World Congress*, number 2004-01-2616 in SAE Technical Paper Series, Detroit, MI, USA, 2004.

C. Lin, H. Peng, J.W. Grizzle, and J. Kang. Power management strategy for a parallel hybrid electric truck. *Control Systems Technology, IEEE Transactions on*, 11(6):839–849, 2003.

C. Lin, H. Peng, and J.W. Grizzle. A stochastic control strategy for hybrid electric vehicles. In *American Control Conference*, volume 5, pages 4710–4715, 2004.

R. Liu and I.M. Golovitcher. Energy-efficient operation of rail vehicles. *Transportation Research*, 37A:917–932, 2003.

D. Q. Mayne, J. B. Rawlings, C. V. Rao, and P. O. M. Scokaert. Constrained model predictive control: Stability and optimality. *Automatica*, 36(6):789–814, 2000.

V.V Monastyrsky and I.M. Golownykh. Rapid computations of optimal control for vehicles. *Transportation Research*, 27B(3):219–227, 1993.

K. Neiss, S. Terwen, and T. Connolly. Predictive speed control for a motor vehicle, 2004. United States Patent Application Publication 2004/0068359.

J. Noreland. Modal split in the inland transport of the EU. Technical Report 35, Eurostat, 2008.

G. Paganelli, T.M. Guerra, S. Delprat, J-J. Santin, M. Delhom, and E. Combes. Simulation and assessment of power control strategies for a parallel hybrid car. *Proceedings of the Institution of Mechanical Engineers – Part D – Journal of Automobile Engineering*, 214 (7):705–717, 2000.

B. Passenberg, P. Kock, and O. Stursberg. Combined time and fuel optimal driving of trucks based on a hybrid model. In *European Control Conference*, Budapest, Hungary, 2009.

M. Pettersson and L. Nielsen. Gear shifting by engine control. *IEEE Transactions on Control Systems Technology*, 8(3):495–507, 2000.

N. Pettersson and K.H. Johansson. Modelling and control of auxiliary loads in heavy vehicles. *International Journal of Control*, 79(5):479–495, 2004.

M. Schittler. State-of-the-art and emerging truck engine technologies for optimized performance, emissions, and life-cycle costing. In *9th Diesel Engine Emissions Reduction Conference*, Rhode Island, USA, August 2003.

A.B. Schwarzkopf and R.B. Leipnik. Control of highway vehicles for minimum fuel consumption over varying terrain. *Transportation Research*, 11(4):279–286, 1977.

A. Sciaretta and L. Guzzella. Fuel-optimal control of rendezvous maneuvers for passenger cars. *Automatisierungstechnik*, 53(6):244–250, 2005.

A. Sciarretta and L. Guzzella. Control of hybrid electric vehicles. *IEEE Control Systems Magazine*, 27(2):60–70, 2007.

A. Sciarretta, M. Back, and L. Guzzella. Optimal control of parallel hybrid electric vehicles. *IEEE Transactions on Control Systems Technology*, 12(3):352–363, 2004.

A.P. Stoicescu. On fuel-optimal velocity control of a motor vehicle. *Int. J. of Vehicle Design*, 16(2/3):229–256, 1995.

S. Terwen, M. Back, and V. Krebs. Predictive powertrain control for heavy duty trucks. In *4th IFAC Symposium on Advances in Automotive Control*, Salerno, Italy, 2004.

Volvo press release, 2006. Volvo delivers I-shift automated transmission for North America. http://www.volvo.com/, September 20, 2006.

A. Vyas, C. Saricks, and F. Stodolsky. The potential effect of future energy-efficiency and emissions-improving technologies on fuel consumption of heavy trucks. Technical Report ANL/ESD/02-4, Argonne National Lab., March 2003.

Publications

Paper A

Look-ahead control for heavy trucks to minimize trip time and fuel consumption[☆]

A

[☆] Published in *Control Engineering Practice*, 17(2):245–254, 2009. Modifications are made to notation, language, and layout.

Look-ahead control for heavy trucks to minimize trip time and fuel consumption

Erik Hellström[a], Maria Ivarsson[b], Jan Åslund[a], and Lars Nielsen[a]

[a] *Linköping University, Linköping, Sweden*
[b] *Scania CV AB, Södertälje, Sweden*

Abstract

The scenario studied is a drive mission for a heavy diesel truck. With aid of an on-board road slope database in combination with a GPS unit, information about the road geometry ahead is extracted. This look-ahead information is used in an optimization of the velocity trajectory with respect to a criterion formulation that weighs trip time and fuel consumption. A dynamic programming algorithm is devised and used in a predictive control scheme by constantly feeding the conventional cruise controller with new set points. The algorithm is evaluated with a real truck on a highway, and the experimental results show that the fuel consumption is significantly reduced.

1 Introduction

As much as about 30% of the life cycle cost of a heavy truck comes from the cost of fuel. Further, the average mileage for a (European class 8) truck is 150,000 km per year and the average fuel consumption is 32.5 $^{l}/_{100km}$ (Schittler, 2003). Lowering the fuel consumption with only a few percent will thus translate into significant cost reductions. These facts make a system which can reduce the fuel consumption appealing to owners and manufacturers of heavy trucks. The problem scenario in the present work is a drive mission for a truck where the route is considered to be known. It is, however, not assumed that the vehicle constantly operates on the same route. Instead, it is envisioned that there is road information on-board and that the current heading is predicted or supplied by the driver. In the current work, information about the road slope is exploited aiming at a fuel consumption reduction.

One early work (Schwarzkopf and Leipnik, 1977) formulates an optimal control problem for a nonlinear vehicle model with the aim at minimizing fuel consumption and explicit solutions are obtained for constant road slopes. A dynamic programming (DP) approach is taken from Monastyrsky and Golownykh (1993) to obtain solutions for a number of driving scenarios on shorter road sections. Inspired of some of the results indicated in these and other works it was shown in Chang and Morlok (2005); Fröberg et al. (2006) with varying vehicle model complexity that constant speed is optimal on a constant road slope within certain bounds on the slope. The result relies on that there is an affine relation between the fuel consumption and the produced work. Analytical studies of the situation when this relation is nonlinear were conducted in Fröberg and Nielsen (2007). Predictive cruise control is investigated through computer simulations in, e.g., Lattemann et al. (2004); Terwen et al. (2004), but constructing an optimizing controller that works on-board in a real environment puts additional demands on the system in terms of robustness and complexity.

In Hellström et al. (2006) a predictive cruise controller (CC) is developed where discrete DP is used to numerically solve the optimal control problem. The current paper is a continuation where an improved approach is realized and evaluated in actual experiments. One objective is to evaluate the order of fuel reduction that can be obtained in practical driving. The strategies to achieve fuel reductions may be intuitive, but only in a qualitatively manner. Another objective is therefore to find the optimal solution and thereby quantify the characteristics of the best possible strategy. The purpose is also to analyze controller behavior in real trial runs and evaluate potential benefits.

To perform this study a chain of elements is needed. Section 2 presents a vehicle model of standard type. Section 3 deals with the DP algorithm, and it is described how the problem characteristics are utilized to reduce the complexity, to determine penalty parameters, and efficiently compute the criterion by an inverse technique. In Section 4 the experimental setup is presented, and finally the quantitative evaluation concludes the study.

2 Truck model

The modeling follows Kiencke and Nielsen (2005); Sandberg (2001), and the resulting model is then reformulated and adapted for the numerical optimization that is performed.

The engine torque T_e is modeled as

$$T_e(\omega_e, u_f) = a_e\omega_e + b_e u_f + c_e \tag{1}$$

where ω_e is the engine speed and u_f is the control signal which determines the fueling level.

The control u_f is assumed to be bounded by

$$0 \le u_f \le u_{f,max}(\omega_e) \tag{2}$$

where the upper limit $u_{f,max}(\omega_e)$ is modeled by a second-order polynomial in engine speed ω_e,

$$u_{f,max}(\omega_e) = a_f\omega_e^2 + b_f\omega_e + c_f.$$

When a gear is engaged, the engine transmits a torque T_c to the clutch and

$$J_e\dot{\omega}_e = T_e - T_c \tag{3}$$

where J_e is the engine inertia and ω_e is the engine speed. The clutch, propeller shafts and drive shafts are assumed stiff and their inertia are lumped into one together with the wheel inertia, denoted by J_l. The resulting conversion ratio of the transmission and final drive is denoted by i and energy losses are modeled by an efficiency η. When a gear is engaged, this gives

$$\begin{aligned} \omega_e &= i\omega_w, \;\; T_w = i\eta T_c \\ J_l\dot{\omega}_w &= T_w - T_b - r_w F_w \end{aligned} \tag{4}$$

where T_w is the torque transmitted to the wheel, T_b is the braking torque and r_w is the wheel radius. F_w is the resulting friction force.

When neutral gear is engaged, the engine transmits zero torque to the driveline. The driveline equations (3) and (4) then become

$$\begin{aligned} J_e\dot{\omega}_e &= T_e, \;\; T_c = T_w = 0 \\ J_l\dot{\omega}_w &= -T_b - r_w F_w. \end{aligned} \tag{5}$$

The motion of the truck is governed by

$$m\frac{dv}{dt} = F_w - F_a(v) - F_r(\alpha) - F_N(\alpha) \tag{6}$$

where α is the road slope. The models of the longitudinal forces are explained in Table 1.

It is assumed that the transmission is of the automated manual type and that gear shifts are accomplished through engine control, see Pettersson and Nielsen (2000). A shift is modeled by a constant period of time τ_{shift} where the neutral gear is engaged

Table 1: Longitudinal forces.

Force	Explanation	Expression
$F_a(v)$	Air drag	$\frac{1}{2}c_w A_a \rho_a v^2$
$F_r(\alpha)$	Rolling resistance	$mgc_r \cos\alpha$
$F_N(\alpha)$	Gravitational force	$mg\sin\alpha$

before the new gear is engaged. The number of the currently engaged gear is denoted by g. The ratio i and efficiency η then becomes functions of the integer g. The control signal that selects gear is denoted by u_g. Neutral gear corresponds to gear zero, equivalent with a ratio and efficiency of zero.

The vehicle velocity v is

$$v = r_w \omega_w \tag{7}$$

where ω_w is the wheel speed of revolution and r_w is the effective wheel radius. Equations (3)-(7) are combined into

$$\frac{dv}{dt}(x,u,\alpha) = \frac{r_w}{J_l + mr_w^2 + \eta(g)i(g)^2 J_e}\Big(i(g)\eta(g)T_e(v,u_f) - T_b(u_b) - r_w\left(F_a(v) + F_r(\alpha) + F_l(\alpha)\right)\Big) \tag{8}$$

where

$$x = \left[v, g\right]^T \quad u = \left[u_f, u_b, u_g\right]^T \tag{9}$$

denote the state and control vector, respectively. The states are the velocity v and currently engaged gear g and the controls are fueling u_f, braking u_b and gear selector u_g.

The mass flow of fuel is determined by the fueling level u_f (g/cycle) and the engine speed ω_e (rad/s). The flow in (g/s) is then

$$\frac{n_{cyl}}{2\pi n_r}\omega_e u_f \tag{10}$$

where n_{cyl} is the number of cylinders and n_r is the number of crankshaft revolutions per cycle. Using (4) and (7) in (10) gives

$$\dot{m}(x,u) = \frac{n_{cyl}}{2\pi n_r}\frac{i}{r_w} v u_f, \; g \neq 0 \tag{11}$$

whereas in the case of neutral gear, $g = 0$, the fuel flow is assumed constant and equal to an idle fuel flow $\dot{m}_{idle}$.

2.1 Reformulation

Models (8) and (11) are transformed to be dependent on position rather than time. Denoting traveled distance by s and the trip time by t, then for a function $f(s(t))$

$$\frac{df}{dt} = \frac{df}{ds}\frac{ds}{dt} = \frac{df}{ds}v \tag{12}$$

is obtained using the chain rule where $v > 0$ is assumed. By using (12), the models can be transformed as desired.

The approach in this work is numerical and therefore the model equations should be made discrete. The quantization step in position is constant and equal to h. The control signals are considered piece-wise constant during a discretization step. Denote

$$\begin{aligned} x_k &= x(kh),\ u_k = u(kh) \\ \alpha_k &= \frac{1}{h}\int_{kh}^{(k+1)h} \alpha(s)ds \end{aligned} \tag{13}$$

where the road slope α_k is set to the mean value over the discretization step. The trapezoidal rule is used to make the truck model (8) discrete. If a gear shift occurs during a step, a second-order Runge-Kutta method is used for a time step equal to the delay τ_{shift} to modify the initial values and the step length. The system dynamics is finally

$$x_{k+1} = f(x_k, u_k, \alpha_k) \tag{14}$$

where $f(x_k, u_k, \alpha_k)$ is given by (8).

The discretized problem is incorporated into the algorithm and thus affects the algorithm complexity. The simplest Euler method do, however, not yield satisfactory results due to truncation errors, see Hellström (2007). For this reason second-order methods were chosen.

3 Look-ahead control

Look-ahead control is a predictive control scheme with additional knowledge about some of the future disturbances, here focusing on the road topography ahead of the vehicle. An optimization is thus performed with respect to a criterion that involves predicted future behavior of the system, and this is accomplished through DP (Bellman and Dreyfus, 1962).

The conditions change during a drive mission due to disturbances, e.g., delays due to traffic, or changed parameters such as the vehicle mass. The robustness is increased by feedback and the approach taken here is therefore to repeatedly calculate the fuel-optimal control on-line. The principle is shown in Figure 1. At point A, the optimal solution is sought for the problem that is defined over the look-ahead horizon. This horizon is obtained by truncating the entire drive mission horizon. Only the first optimal control is applied to the system and the procedure is repeated at point B.

This section will first deal with the identification of the control objectives. Based on these, a suitable criterion is devised and the tuning of its parameters is discussed. At the end, the DP algorithm is outlined.

3.1 Objective

The objectives are to minimize the energy and time required for a given drive mission. The vehicle velocity is desired to be kept inside an interval

$$v_{min} \leq v \leq v_{max} \tag{15}$$

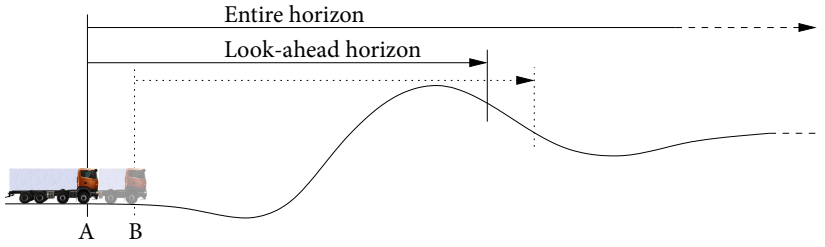

Figure 1: Illustration of the look-ahead control strategy.

where v denotes the vehicle velocity. These bounds are set with respect to the desired behavior of the controller. For example, the lower bound will be the lowest velocity the controller would deliberately actuate. The upper bound can be set by, e.g., safety reasons or legal considerations.

The brake system is assumed to be powerful enough to keep the upper bound in (15). On the other hand, the lower bound is not expected to be physically reachable on all road profiles. It is assumed though, that it is possible to keep a velocity, denoted by v_{lim}, which is positive at all times. If Equation (15) were to be used, it would not be certain to find any feasible solution. Therefore the constraints on the vehicle speed v are expressed as follows:

$$0 < \min\{v_{min}, v_{lim}(s)\} \leq v \leq v_{max} \tag{16}$$

3.2 Criterion

The fundamental trade-off when studying minimization of energy required for a drive mission is between the fuel use and the trip time. The fuel use on a trip from $s = s_0$ to $s = s_f$ is

$$M = \int_{s_0}^{s_f} \frac{1}{v}\dot{m}(x,u)ds \tag{17}$$

where $\frac{1}{v}\dot{m}(x,u)$ is the mass flow per unit length as function of the state x and control u. The trip time T is simply

$$T = \int_{s_0}^{s_f} \frac{dt}{ds}ds = \int_{s_0}^{s_f} \frac{ds}{v}. \tag{18}$$

To weigh fuel and time use, the cost function proposed is

$$I = M + \beta T \tag{19}$$

using (17) and (18) and where β is a scalar factor which can be tuned to receive the desired trade-off.

Criterion (19) is then made suitable for discrete DP by dividing the look-ahead horizon into N steps of length h (m) and transforming the cost function. Denote

$$m_k = \int_{kh}^{(k+1)h} \dot{m}(x,u)ds, \quad t_k = \int_{kh}^{(k+1)h} \frac{ds}{v},$$
$$a_k = |v_k - v_{k+1}| \tag{20}$$

and the cost function can be expressed as

$$J = \sum_{k=0}^{N-1} \zeta_k(x_k, x_{k+1}, u_k, \alpha_k) \tag{21}$$

where

$$\zeta_k = [1, \beta, \varepsilon] \begin{bmatrix} m_k \\ t_k \\ a_k \end{bmatrix}, \quad k = 0, 1, \ldots, N-1 \tag{22}$$

and β, ε are scalar penalty parameters for controlling the properties of solutions. The difference in the criterion between neighboring discretization points is typically very small. In order to receive a smoother control, the term a_k is added with a small value of ε.

3.3 Penalty parameters

The size of the factor ε is chosen for smoothing but still such that the term εa_k becomes considerable smaller than the others.

One way to determine the parameter β, i.e. the trade-off between fuel and time, is to study a stationary solution to the criterion in Equation (19). Assume that a gear is engaged and there exists at least one control $\hat{u}$, for which (2) holds and that gives a stationary velocity $\hat{v}$, i.e. $dv/dt = 0$. From the equations (1), (8), and Table 1 it is concluded that $\hat{u}$ can be written as

$$\hat{u} = c_1\hat{v}^2 + c_2\hat{v} + f(\alpha) \tag{23}$$

where, for a given gear, c_1 and c_2 are constants and $f(\alpha)$ is a function corresponding to the rolling resistance and gravity, and thus being a function of the road slope α. With (11) and (12), the fuel flow is written as

$$\frac{1}{v}\dot{m}(x, u) = c_4\hat{u}_f \tag{24}$$

where c_4 is the proportionality constant. The cost function (19) is thus

$$\hat{I}(\hat{v}) = \int_{s_0}^{s_f} \left(c_4 \left(c_1\hat{v}^2 + c_2\hat{v} + f(\alpha) \right) + \frac{\beta}{\hat{v}} \right) ds \tag{25}$$

where the integrand is constant with respect to s if constant slope is assumed. A stationary point to $\hat{I}$ is found by setting the derivative equal to zero,

$$\frac{d\hat{I}}{d\hat{v}} = \int_{s_0}^{s_f} \left(c_4 \left(2c_1\hat{v} + c_2 \right) - \frac{\beta}{\hat{v}^2} \right) ds = 0. \tag{26}$$

Solving the equation for β gives

$$\beta = c_4\hat{v}^2 \left(2c_1\hat{v} + c_2 \right) \tag{27}$$

that can be interpreted as the value of β such that a stationary velocity $\hat{v}$ is the solution to (26). Note that the value of β neither depends on the vehicle mass m nor the slope α. The calculated β will thus give the solution $\hat{v}$ of the criterion for any fixed mass and slope as long as there exists a control $\hat{u}_f$ satisfying the bounds in (2).

3.4 Preprocessing

The ambition with the present work is a real-time algorithm and hence the complexity plays an important role. The subset of the state space over which the optimization is applied, the search space, is one determining factor for the complexity. If the search space is reduced without loosing any solutions, obvious gains are made. A preprocessing algorithm is therefore developed with this aim.

Since DP is used in an predictive control setting, the current velocity can be measured and used for limiting the set of possible initial states. In order to handle terminal effects, the final velocities are also constrained. By using the model and traversing the horizon forward and backward before the optimization is started, the search space is downsized, see Hellström (2007).

The preprocessing algorithm gives, for each stage, an interval of velocities which are to be considered. For every stage the interval $\left[v_{lo}, v_{up}\right]$ is discretized in constant steps of δ. This makes up a set V_k,

$$V_k = \left\{v_{lo}, v_{lo} + \delta, v_{lo} + 2\delta, \ldots, v_{up}\right\}. \tag{28}$$

3.5 DP algorithm

To summarize, the optimal control problem at hand is the minimization of the objective,

$$\min_{u,g} \sum_{k=0}^{N-1} \zeta_k(x_k, x_{k+1}, u_k, \alpha_k)$$

where ζ_k is given in (22). The system dynamics is given by

$$x_{k+1} = f(x_k, u_k, \alpha_k) \quad k = 0, 1, \ldots, N-1$$

according to (14). The constraints are

$$0 < \min\left\{v_{min}, v_{lim}(kh)\right\} \leq v_k \leq v_{max} \ \forall k$$

according to (16). Due to the predictive control setting, the initial state x_0 is given.

With a given velocity, only a subset of the gears in the gearbox is feasible. If the operating region of the engine is defined with bounds on the engine speed $[\omega_{e,min}, \omega_{e,max}]$, it is easy to select the set of feasible gears. Only gears with a ratio that gives an engine speed in the allowed range are then considered. In a state with velocity v, the set of usable gears G_v is thus defined as

$$G_v = \left\{g \mid \omega_{e,min} \leq \omega_e(v, g) \leq \omega_{e,max}\right\} \tag{29}$$

where $\omega_e(v, g)$ is the engine speed at vehicle velocity v and gear number g.

Braking is only considered in the algorithm if the upper velocity bound is encountered. Braking without recuperation is an inherent waste of energy and therefore braking will only occur when the velocity bounds would otherwise be violated. This reduces the complexity since the number of possible control actions lessens.

Table 2: Truck specifications.

Component	Type	Characteristics
Engine	DC9	Cylinders: 5
		Displacement: 9 dm^3
		Max.torque: 1,550 Nm
		Max.power: 310 hp
Gearbox	GRS890R	12 gears
Vehicle	-	Total weight: 39,410 kg

A state x is made up of velocity v and gear number g. The possible states in stage k are denoted with the set S_k and it is generated from the velocity range V_k given in (28) and the set of gears G_v given in (29). This yields

$$S_k = \{\{v, g\} \,|v \in V_k, g \in G_v\}\,. \tag{30}$$

At a stage k, feasible control actions $u_k^{i,j}$ that transform the system from a state $x^i \in S_k$ to another state $x^j \in S_{k+1}$ are sought. The control is found by an inverse simulation of the system equations, see e.g. Fröberg and Nielsen (2008). Here this means that for a given state transition, x_k to x_{k+1}, the control u_k is solved from (14). Interpolation is thereby avoided. If there are no fueling level u_f and gear u_g that transforms the system from state x^i to x^j at stage k, there are two possible resolutions. If there exist a feasible braking control u_b it is applied, but if there is no feasible braking control the cost is set to infinity.

The algorithm is outlined as follows:

1. Let $J_N(i) = 0$.
2. Let $k = N - 1$.
3. Let
$$J_k(x^i) = \min_{x^j \in S_{k+1}} \left\{\zeta_k^{i,j} + J_{k+1}(x^j)\right\},\ x^i \in S_k.$$
4. Repeat (3) for $k = N-2, N-3, \ldots, 0$.
5. The optimal cost is J_0 and the sought control is the optimal control set from the initial state.

4 Trial run

The experiments are performed on the highway E4 between the cities of Södertälje and Norrköping in Sweden, see Figure 4. The truck used is a Scania tractor and trailer, see Figure 2. The specifications are given in Table 2.

Following in this section, the experimental setup and road slope data are presented. The last part of the section will present some results from the trial runs that have been undertaken.

Figure 2: The vehicle used in the experiments.

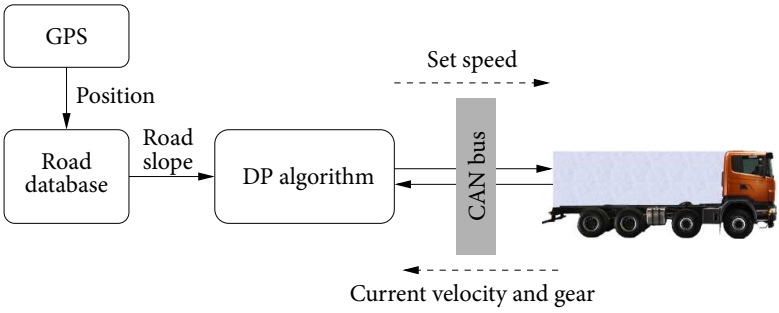

Figure 3: Information flow.

4.1 Setup

The information flow in the experimental setup is shown schematically in Figure 3. Due to adjustments for the demonstrator vehicle, gear shifts were not directly controlled by the algorithm. This is handled by including a prediction model of the gear control system and take it into account when calculating the running costs. In the optimization algorithm, a shift that is not predicted is assigned an infinite cost. As depicted in Figure 3 the algorithm controls the vehicle by adjusting the set speed to the conventional CC. The fueling level is therefore only controlled indirectly. The standard CC available from Scania is used, which is basically a PI-regulator. All communications are done over the CAN bus.

The algorithm parameters used are stated in Table 3 and the penalty factors are shown in Table 4. The factors are adjusted in order to receive a stationary solution in the middle of the desired velocity interval (15).

All software run on a portable computer with an Intel Centrino Duo processor at 1.20 GHz and 1 Gb RAM. With the stated parameters, a solution on a road stretch of level road is calculated in tenths of a second on this computer.

The truck has a legislative speed limiter at 89 $^{km}/_{h}$. Propulsion above this limit is not possible. When the truck accelerates due to gravity above 89 $^{km}/_{h}$, the brake control

Table 3: User parameters

Parameter	Function	Value
h	Step length	50 m
N	Number of steps	30
$h \cdot N$	Horizon	1500 m
δ	Velocity discret.	0.2 km/h
v_{min}	Min. allowed vel.	79 km/h
v_{max}	Max. allowed vel.	89 km/h

Table 4: Penalty factors

Factor	Penalizes	Value
	Fuel use	1.0
β	Time use	6.2
ε	Velocity changes	0.1

system is activated at a set maximum speed. In the trial run this limit is set to be 91 km/h.

Database

The slope in front of the vehicle for the length of the look-ahead horizon is needed to be known. It is expected that such data will be commercially available soon. But for now, the road slope along the trial route is estimated off-line prior to any experiments. This is done by aid of a non-stationary forward-backward Kalman filter (Sahlholm et al., 2007). The estimated slope and elevation are shown in Figure 4. The measurements were obtained at 20 Hz from a GPS unit. The filter inputs are vertical and horizontal velocity of the vehicle, elevation and the number of reachable GPS satellites.

4.2 Performance

In total, five comparative trial runs were made. All runs were done in light to moderate traffic, and each consisted of one drive with look-ahead control and one with standard cruise control. The algorithm parameters, see Table 3 and 4, were the same for all runs. The trip time thus became about the same for all drives with the look-ahead control. The set point for the CC was chosen in order to achieve a trip time close to the one obtained with look ahead.

4.3 Overall results

The relative changes in fuel consumption and trip time (Δfuel, Δtime) are shown in Figure 5 and Figure 6 for each direction on the trial road. A negative value means that the look-ahead controller (LC) has lowered the corresponding value. The set point for the CC increases along the horizontal axis. The left-most result is maybe the most convincing since it reduces both fuel use and trip time in both directions.

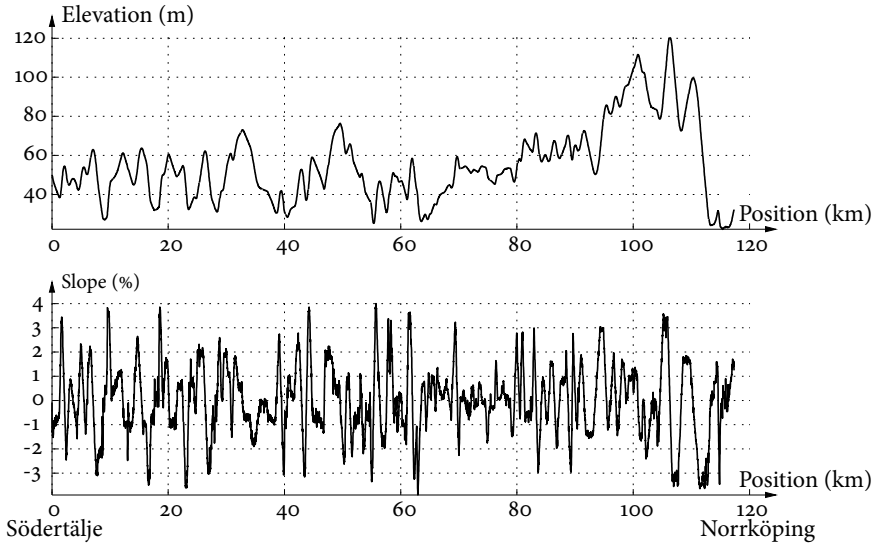

Figure 4: Estimated road topography.

The average results in both directions that are made with the same set speed are also calculated. For these mean values the fuel consumption was lowered with 3.53%, from 36.33 $^{L}/_{100km}$ to 35.03 $^{L}/_{100km}$, with a negligible reduction of the trip time (0.03%) in comparison with the CC. Also interesting to note is that the mean number of gear shifts on this route decreases from 20 to 12 with the LC.

4.4 Control characteristics

With the intention to give a representative demonstration of more detailed controller characteristics, two road segments have been chosen. The first is a 2.5 km segment close to Södertälje and is named *the Järna segment*. The second one is a 3.5 km segment about halfway on the trial route and called *the Hållet segment*.

Each figure, see, e.g., Figure 7, is divided into four subfigures, all having the position as the horizontal axis. The road topography is shown at the top and the coordinates for the start and final position are also given on the horizontal axis. The next subfigure shows the velocity trajectories for the LC and the standard CC. The third part shows normalized fueling (acc) and auxiliary brake (brake) levels with thick and thin lines, respectively. At the bottom, both the engaged gear number and the fuel use are shown. Data related to the LC are displayed in solid lines and data associated to the CC are displayed with dashed lines in these figures. Above the figures, the time and fuel spent on the section are shown together with the relative change (Δfuel, Δtime) in these values between the two controllers. A negative value means that the value is lowered by the LC.

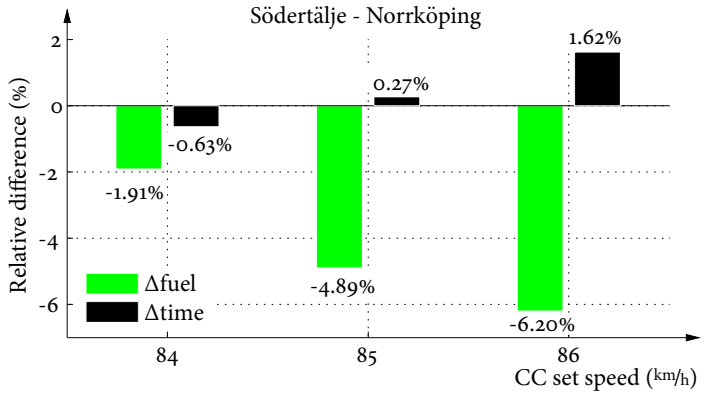

Figure 5: Trial run results on the road from Södertälje to Norrköping with varying cruise controller (CC) set speed.

The Hållet segment

Figures 7 and 8 show the Hållet segment. In Figure 7, the LC accelerates at 500 m prior to the uphill that begins at 750 m. At the top of the hill at 1750 m, the LC slows down in contrast to the CC. The truck is thus let to accelerate by gravity alone. The CC will, however, use a non-zero fueling as long as the truck is going slower than the set point. The LC slow down reduces the need for braking later in the downslope and thereby the inherent waste of energy is lessened. From the fuel integral at the bottom, it is seen that the LC consumes more fuel the first 1.5 km owing to the acceleration, but then gains.

The trip in the other direction, see Figure 8, gives similar features. A gain of speed at 250 m and then a slow down at the top of the hill at 2250 m. In both directions, time as well as fuel are saved.

Note that the sections in Figure 7 and 8 are not exceptionally steep. The uphill and downhill slope is at most about 4% for short intervals. However, they become significant for the truck due to the large vehicle mass.

The Järna segment

In Figures 9 and 10 the Järna segment is shown. Figure 9 shows that the LC begins to gain speed at 200 m and thereby avoids the gear shift that the CC is forced to do around 1 km. At 1400 m, the LC slows down and lets the truck accelerate in the downslope.

In Figure 10, a drive in the other direction is shown. The LC accelerates at 500 m and starts to slow down at 1400 m. The slow down lessen the braking effort needed at about 2000 m.

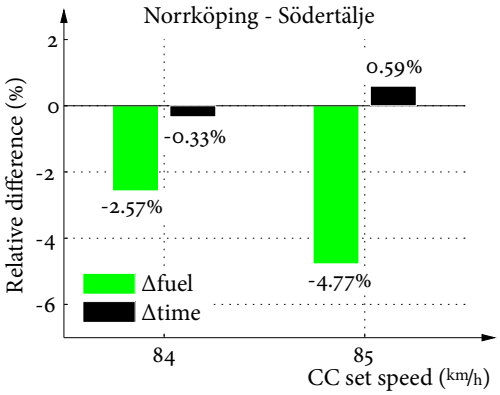

Figure 6: Trial run results on the road from Norrköping to Södertälje with varying cruise controller (CC) set speed.

5 Conclusions

The control algorithm was proven to perform well on-board in a real environment. Using the standard cruise controller as an inner loop and feeding it with new set points is advantageous considering robustness against model errors and disturbances.

The gearbox consists of a set of discrete gears and there is no propulsion force during a gear shift. Taking these facts into account renders a challenging optimization problem. A discrete dynamic programming algorithm is devised where the search space is reduced by a preprocessing algorithm. The algorithm computes a solution in tenths of a second on a modern laptop computer and this allows evaluation in a real environment on-board a truck.

The trial runs show that significant reductions of the fuel consumption can be achieved. A fuel consumption reduction of about 3.5% on the 120 km route without an increase in trip time was obtained. The mean number of gear shifts was reduced with 42% due to shifts avoided by gaining speed prior to uphills.

The look-ahead control mainly differs from conventional cruise control near significant downhills and uphills where the look-ahead control in general slows down or gains speed prior to the hill. Slowing down prior to downhills is intuitively saving fuel. There is, however, no challenge in saving fuel by traveling slower, so if the vehicle is let to slow down at some point, the lost time must thus be gained at another point. Accelerating prior to uphills is one way which, at least for shorter hills, gives a higher velocity throughout the hill and will reduce the need for lower gears. These strategies are intuitive but the crucial issue is the detailed shape of the solution and its actuation such that a positive end result is obtained, and this is shown to be handled well by the algorithm.

A final comment is that the controller behavior has been perceived as comfortable and natural by drivers and passengers that have participated in tests and demonstrations.

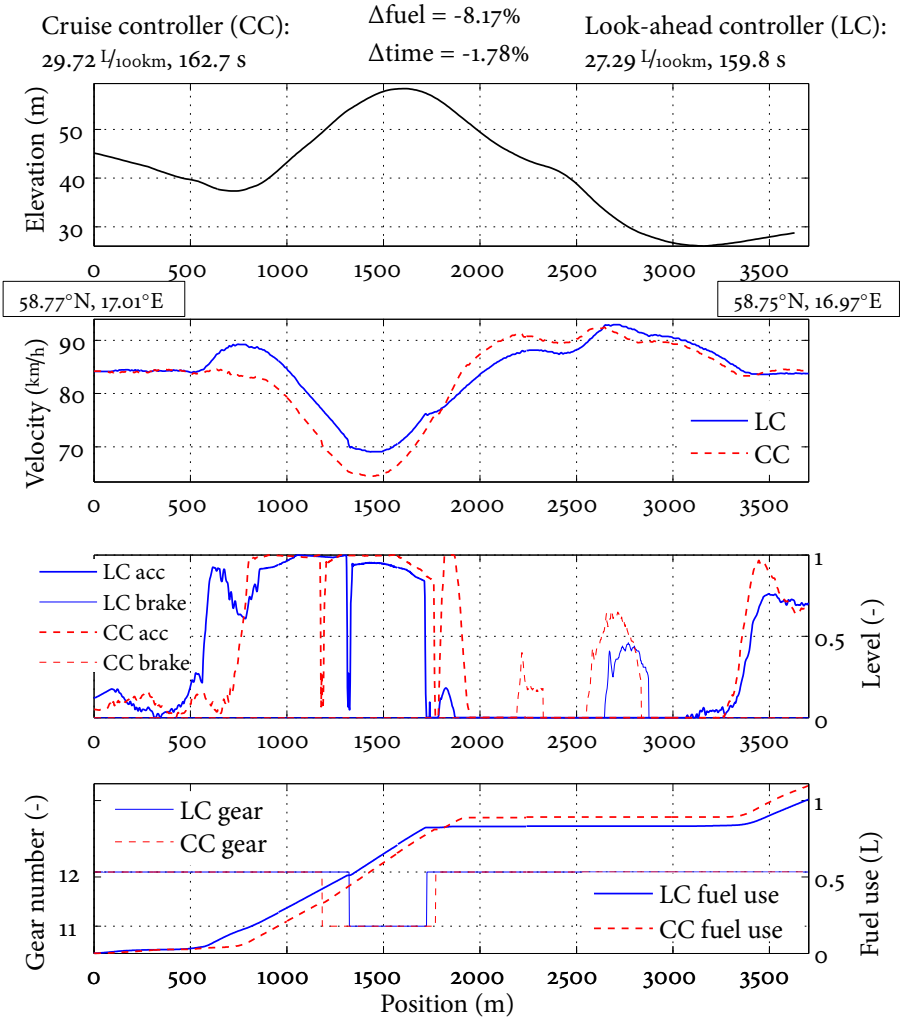

Figure 7: The Hållet segment. The LC accelerates at 500 m prior to the uphill and slows down at 1750 m when the top is reached.

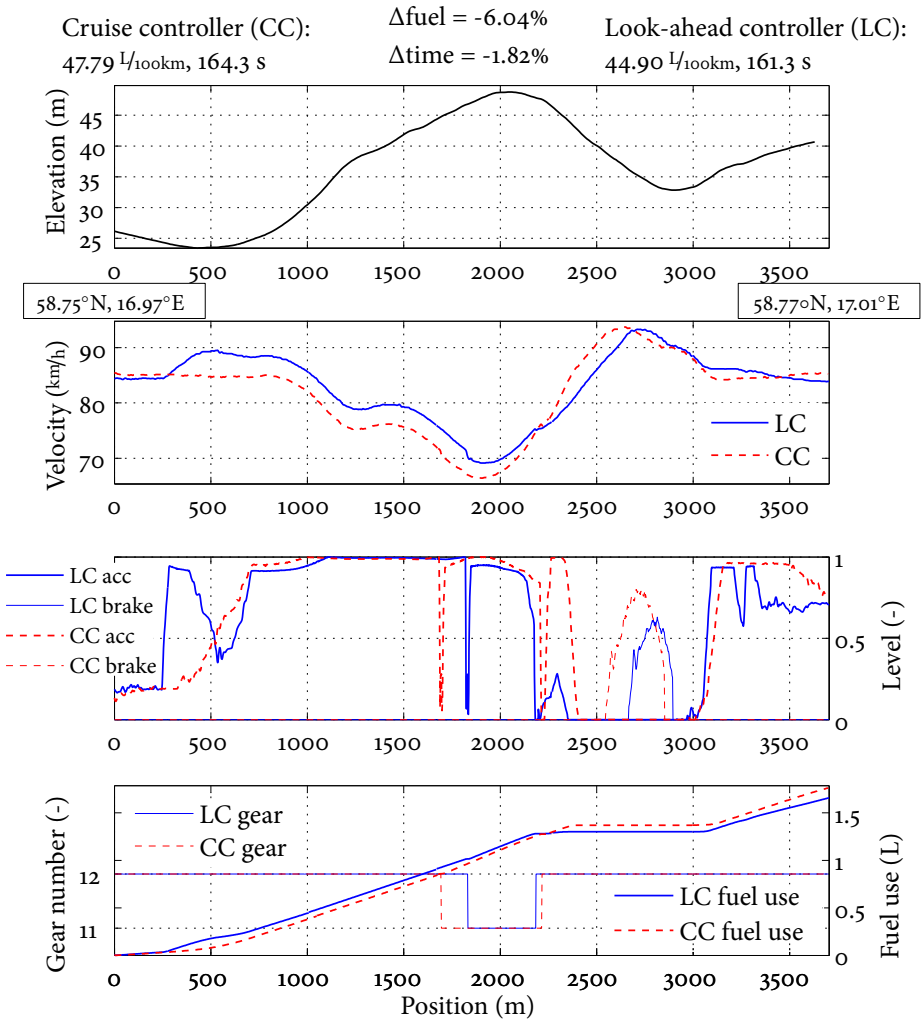

Figure 8: The Hållet segment. The LC gains speed at 250 m prior to the uphill and slows down at 2250 m prior to the downhill.

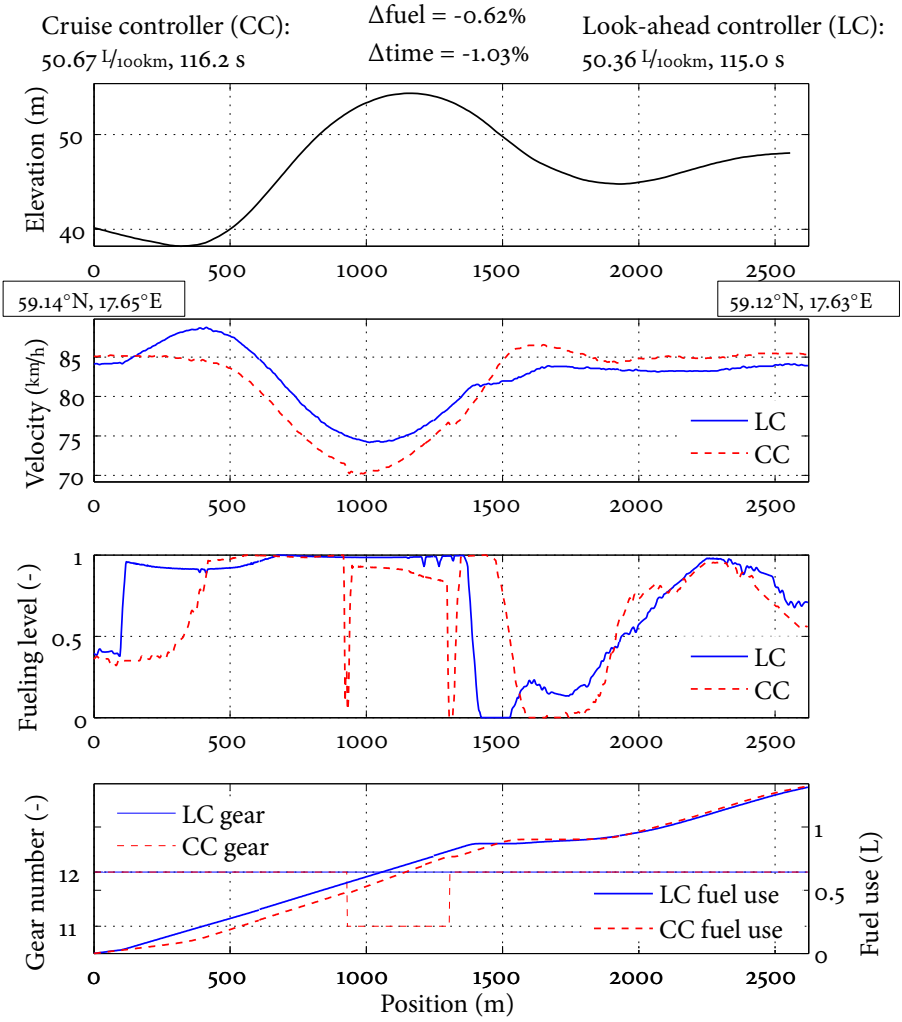

Figure 9: The Järna segment. The LC gains speed at 200 m prior to the uphill and avoids a gear shift. At 1400 m the LC slows down and the truck is let to accelerate in the downslope.

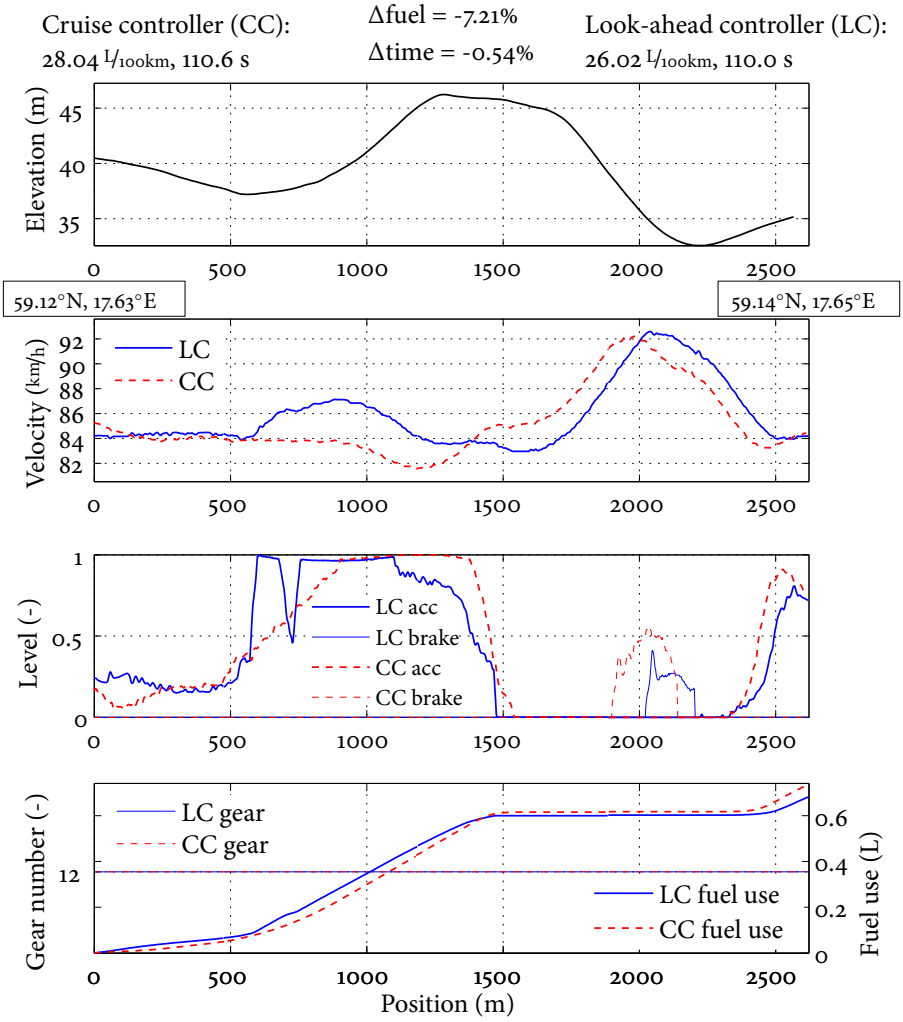

Figure 10: The Järna segment. The LC accelerates at 500 m and slows down at 1400 m thereby reducing the braking effort needed later on.

References

R.E. Bellman and S.E. Dreyfus. *Applied Dynamic Programming*. Princeton University Press, Princeton, New Jersey, 1962.

D.J. Chang and E.K. Morlok. Vehicle speed profiles to minimize work and fuel consumption. *Journal of transportation engineering*, 131(3):173–181, 2005.

A. Fröberg and L. Nielsen. Optimal fuel and gear ratio control for heavy trucks with piece wise affine engine characteristics. In *5th IFAC Symposium on Advances in Automotive Control*, Monterey, CA, USA, 2007.

A. Fröberg and L. Nielsen. Efficient drive cycle simulation. *IEEE Transactions on Vehicular Technology*, 57(2), 2008.

A. Fröberg, E. Hellström, and L. Nielsen. Explicit fuel optimal speed profiles for heavy trucks on a set of topographic road profiles. In *SAE World Congress*, number 2006-01-1071 in SAE Technical Paper Series, Detroit, MI, USA, 2006.

E. Hellström. *Look-ahead Control of Heavy Trucks utilizing Road Topography*. Licentiate thesis LiU-TEK-LIC-2007:28, Linköping University, 2007.

E. Hellström, A. Fröberg, and L. Nielsen. A real-time fuel-optimal cruise controller for heavy trucks using road topography information. In *SAE World Congress*, number 2006-01-0008 in SAE Technical Paper Series, Detroit, MI, USA, 2006.

U. Kiencke and L. Nielsen. *Automotive Control Systems, For Engine, Driveline, and Vehicle*. Springer-Verlag, Berlin, 2nd edition, 2005.

F. Lattemann, K. Neiss, S. Terwen, and T. Connolly. The predictive cruise control - a system to reduce fuel consumption of heavy duty trucks. In *SAE World Congress*, number 2004-01-2616 in SAE Technical Paper Series, Detroit, MI, USA, 2004.

V.V Monastyrsky and I.M. Golownykh. Rapid computations of optimal control for vehicles. *Transportation Research*, 27B(3):219–227, 1993.

M. Pettersson and L. Nielsen. Gear shifting by engine control. *IEEE Transactions on Control Systems Technology*, 8(3):495–507, 2000.

P. Sahlholm, H. Jansson, E. Kozica, and K.H. Johansson. A sensor and data fusion algorithm for road grade estimation. In *5th IFAC Symposium on Advances in Automotive Control*, Monterey, CA, USA, 2007.

T. Sandberg. Simulation tool for predicting fuel consumption for heavy trucks. In *IFAC Workshop: Advances in Automotive Control*, Karlsruhe, Germany, 2001.

M. Schittler. State-of-the-art and emerging truck engine technologies for optimized performance, emissions, and life-cycle costing. In *9th Diesel Engine Emissions Reduction Conference*, Rhode Island, USA, August 2003.

A.B. Schwarzkopf and R.B. Leipnik. Control of highway vehicles for minimum fuel consumption over varying terrain. *Transportation Research*, 11(4):279–286, 1977.

S. Terwen, M. Back, and V. Krebs. Predictive powertrain control for heavy duty trucks. In *4th IFAC Symposium on Advances in Automotive Control*, Salerno, Italy, 2004.

Paper B

Design of an efficient algorithm for fuel-optimal look-ahead control[☆]

B

[☆] Accepted for publication in *Control Engineering Practice* and currently in press, doi: 10.1016/j.conengprac.2009.12.008. Modifications are made to language and layout. Corrections are made to Section 6.2.

Design of an efficient algorithm for fuel-optimal look-ahead control

Erik Hellström, Jan Åslund, and Lars Nielsen

Linköping University, Linköping, Sweden

Abstract

A fuel-optimal control algorithm is developed for a heavy diesel truck that utilizes information about the road topography ahead of the vehicle when the route is known. A prediction model is formulated where special attention is given to properly include gear shifting. The aim is an algorithm with sufficiently low computational complexity. To this end, a dynamic programming algorithm is tailored, and complexity and numerical errors are analyzed. It is shown that it is beneficial to formulate the problem in terms of kinetic energy in order to avoid oscillating solutions and to reduce linear interpolation errors. A residual cost is derived from engine and driveline characteristics. The result is an on-board controller for an optimal velocity profile and gear selection.

1 Introduction

A drive mission for a heavy truck is studied where there is road data on-board and the road slope ahead of the vehicle is known. The mission is given by a route and a desired maximum trip time, and the objective is to minimize the energy required for a given mission. Experimental results (Hellström et al., 2009) have confirmed that the fuel economy is improved with this approach, and the current main challenge is the efficient solution of the optimal control problem.

Related works for energy optimal control are found in other application areas such as trains (Howlett et al., 1994; Franke et al., 2002; Liu and Golovitcher, 2003) and hybrid electric vehicles (Sciarretta et al., 2004; Back, 2006; Guzzella and Sciarretta, 2007). Fuel-optimal solutions for vehicles on basic topographic road profiles are obtained in Schwarzkopf and Leipnik (1977); Monastyrsky and Golownykh (1993); Chang and Morlok (2005); Fröberg et al. (2006); Ivarsson et al. (2009). Predictive cruise control is investigated through computer simulations in, e.g., Lattemann et al. (2004); Terwen et al. (2004); Huang et al. (2008); Passenberg et al. (2009). In Hellström et al. (2006) a predictive cruise controller is developed where discrete dynamic programming is used to numerically solve the optimal control problem. In Hellström et al. (2009) the approach was evaluated in real experiments where the road slope was estimated by the method in Sahlholm and Johansson (2009).

The purpose of the present paper is to develop an optimization algorithm that finds the optimal control law for a finite horizon. The algorithm should be sufficiently robust and simple in order to be used on-board a vehicle in a real environment, and with reduced computational effort compared to previous works. Some distinguishing features of the optimization problem are that it contains both real and integer variables, and that the dimension of the state space is low. Here, an algorithm based on dynamic programming (DP) (Bellman, 1957) that finds the optimal control law is developed. Applying DP for high order systems is usually unfeasible due to exponential increase of the complexity due to the discretization of the continuous variables (Bellman, 1961), but this is not an issue in this application, since the dimension is low. Alternatively, an open-loop optimal control problem can be solved on line repeatedly for the current state to achieve feedback. These approaches are generally indirect methods based on the maximum principle (Bryson and Ho, 1975) or direct methods based on transcription (Betts, 2001). For mixed-integer nonlinear optimization, a complex combinatorial problem typically arises with the open-loop approaches due to the integer variables (Floudas, 1995). For DP, however, the computational complexity is linear in the horizon length which is beneficial for this application since a rather long horizon is needed (Hellström, 2007; Hellström et al., 2009).

Starting out the paper, a generic analysis is presented, and the model structure is defined. The first idea to reduce complexity is to obtain a better estimate of the residual cost at the end of the horizon, so that a shorter horizon can be used. By reducing the search space at each position the computational complexity can be improved further. Based on an energy formulation of the dynamics and an analysis of the discretization errors, it is shown that a coarser grid for numerical interpolation together with a simple integration method can be used.

2 Objective

The objective is to minimize the fuel M required for a drive mission with a given maximum trip time T_0:

$$\begin{aligned} &\text{minimize } M \\ &\text{s.t.} \quad T \leq T_0 \end{aligned} \tag{P1}$$

It is possible to control accelerator, brake and gear shift. Constraints on, e.g., velocity and control signals may also be included in the problem statement.

Since the road slope is a function of position, it is natural to formulate the vehicle model using spatial coordinates. A simple model may have gear and, e.g., velocity as states. Studying (P1), the time spent so far also has to be considered. A straightforward way to handle this is to include the trip time as an additional state.

The model is discretized and dynamic programming (DP) is used for the optimization. The complexity in DP grows exponentially with the number of states which is known as the *Curse of dimensionality* (Bellman, 1961). The first step to avoid this is to consider an alternative formulation of the optimization problem (P1). This is obtained by adjoining the trip time to the criterion in (P1) yielding

$$\text{minimize } M + \beta T \tag{P2}$$

where β is a scalar representing the trade-off between fuel consumption and trip time. This is the approach taken in Monastyrsky and Golownykh (1993). With this formulation, it is no longer necessary to introduce time as an additional state. Instead, there is an additional issue tuning the parameter β.

For a given β, the solution for (P2) gives a trip time $T(\beta)$. This function is not known explicitly in general. The optimal policy for (P2), for a given β, is also the optimal policy for (P1) with $T_0 = T(\beta)$, since the minimum is attained in the limit for a realistic setup. Thus, problem (P1) can be solved through (P2) if β is found such that $T(\beta) = T_0$. The function $T(\beta)$ is monotonically decreasing and β may be found by, e.g., using simple shooting methods.

The conditions may change during a drive mission due to disturbances, e.g., delays due to traffic, or changed parameters such as the vehicle mass. New optimal solutions must then be computed during the drive mission. An efficient approach is to only consider a truncated horizon in each optimization. This method gives an approximate solution to problem (P1) where the accuracy depends on the length of the truncated horizon.

3 A generic analysis

Consider the motion of a vehicle in one dimension, see Figure 1. The propelling force is F_p. The drag force is dependent on the position s and the velocity v, and is given by the function $F_d(s, v)$. It is assumed that this function is monotonically increasing for

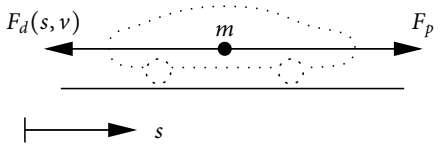

Figure 1: A vehicle moving in one dimension.

positive v, that is

$$\frac{\partial F_d}{\partial v} \geq 0, v > 0 \tag{1}$$

which should hold for any physically plausible resistance function. The problem of finding the velocity trajectory, that minimizes the work required to move the vehicle from one point $s = 0$ to another point $s = S$, is now studied.

Newton's second law of motion in spatial coordinates is

$$mv\frac{dv}{ds} = F_p - F_d(s,v) \tag{2}$$

The propulsive work equals

$$\begin{aligned} W &= \int_0^S F_p\, ds = \int_0^S \left(mv\frac{dv}{ds} + F_d(s,v) \right) ds \\ &= \frac{m}{2}\left(v(S)^2 - v(0)^2 \right) + \int_0^S F_d(s,v)\, ds \end{aligned} \tag{3}$$

that is, the sum of the difference in kinetic energy and the work due to the resisting force along the path.

The problem objective is now stated as

$$\min_{v(s)} \int_0^S \left(mv(s)\frac{dv(s)}{ds} + F_d(s, v(s)) \right) ds \tag{4}$$

with the time constraint expressed as

$$\int_0^S \frac{ds}{v(s)} \leq T_0 \tag{5}$$

where T_0 denotes the desired maximum time.

If the inequality in (5) is replaced by an equality, the resulting problem is an isoperimetric problem. For a functional $\int F(s,v,v')\, ds$ and a constraint $\int G(s,v,v')\, ds = C$ the Euler–Lagrange equation in the calculus of variations is

$$\frac{\partial F^*}{\partial v} - \frac{d}{ds}\frac{\partial F^*}{\partial v'} = 0, \quad F^* = F + \lambda G \tag{6}$$

where λ is a constant (Gelfand and Fomin, 1963). Only smooth solutions will be considered, so it is assumed that the studied functional has continuous first and second order

derivatives in the considered interval for arbitrary v and v'. In the present problem (4) and (5), the functional

$$\int_0^S \left(mv\frac{dv}{ds} + F_d + \frac{\lambda}{v} \right) ds \tag{7}$$

is formed where λ is a constant. Then, according to the Euler equation

$$m\frac{dv}{ds} + \frac{\partial F_d}{\partial v} - \frac{d}{ds}(mv) + \lambda\left(-\frac{1}{v^2}\right) = 0 \tag{8}$$

should be satisfied which yields that

$$v^2\frac{\partial}{\partial v}F_d(s,v) = \lambda \tag{9}$$

is a necessary condition for the objective to have an extremum for a function $v(s)$. Due to the assumption (1), the multiplier λ will be positive. Relaxing the equality constraint to the inequality (5) does not alter the solution. Every $v(s)$ that becomes admissible when the equality constraint is replaced with an inequality will have a higher value of the objective (4) due to (1).

In order to proceed, assume that the resistance function is a sum of two functions with explicit dependency on s and v respectively, that is

$$F_d(s,v) = f_1(s) + f_2(v) \tag{10}$$

The condition (9) then becomes

$$v^2\frac{\partial}{\partial v}f_2(v) = \lambda. \tag{11}$$

For a given λ, the solution to (11) is constant velocity. To minimize the work for moving the body from one point to another point, the extremum is thus a constant speed level adjusted to match the desired trip time.

3.1 Observations

For the general longitudinal vehicle model, depicted in Figure 1, constant speed is the solution to the problem of minimizing the needed work to move from one point to another with a trip time constraint. The assumptions are that the velocity and acceleration are smooth and that (1), (2), and (10) holds. However, due to the large mass of a heavy truck, it is not possible to keep a desired cruising speed, and the thereby unavoidable gear shifts have a noteworthy influence on vehicle motion. Therefore, the mass is the most important parameter in the current context and gear selection should be considered.

4 Truck model

The physical models are now presented. First, in the general form that is treated by the algorithm. Explicit models in this form are then given in Section 4.1–4.4. In the last section, an approximation of the explicit models is discussed.

Table 1: Longitudinal forces.

Force	Explanation	Expression
$F_a(v)$	Air drag	$\frac{1}{2}c_w A_a \rho_a v^2$
$F_r(s)$	Rolling resistance	$mg_0 c_r \cos\alpha(s)$
$F_g(s)$	Gravitational force	$mg_0 \sin\alpha(s)$

With constant gear number, i.e., between gear shifts, the vehicle acceleration is given by

$$\frac{dv}{ds} = f(s, v, g, u) \tag{12}$$

where s is the position, v is the velocity, u is the control signals and g is the gear number. The fuel mass flow is given by

$$\dot{m} = h(v, g, u) \tag{13}$$

and the consumption is obtained by integrating the flow.

A gear shift, from g_1 to g_2 with initial speed v_1, is modeled by the required time for the shift,

$$\Delta t = \xi(s, v_1, g_1, g_2) \tag{14}$$

the required distance,

$$\Delta s = \varphi(s, v_1, g_1, g_2) \tag{15}$$

the change in velocity,

$$\Delta v = v_2 - v_1 = \chi(s, v_1, g_1, g_2) \tag{16}$$

and the consumed fuel

$$\Delta m = \psi(s, v_1, g_1, g_2) \tag{17}$$

The model structure given by (12)–(17) is used in the optimization. Now, explicit models are given.

4.1 Longitudinal model

A model for the longitudinal dynamics of a truck is formulated (Kiencke and Nielsen, 2005). The vehicle is considered as a point mass moving in one dimension, see Figure 1.

The engine torque T_e is given by

$$T_e = f_e(\omega_e, u_{\mathrm{f}}) \tag{18}$$

where ω_e is the engine speed and u_{f} is the fueling control signal. The function f_e is a look-up table originating from measurements. The clutch, propeller shafts and drive shafts are stiff. The resulting conversion ratio of the transmission and final drive $i(g)$ and their efficiency $\eta(g)$ are functions of the engaged gear number, denoted by g. The models of the resisting forces are explained in Table 1.

The relation

$$v = r_w \omega_w = \frac{r_w}{i} \omega_e \tag{19}$$

Table 2: Truck model parameters.

I_l	Lumped inertia	c_w	Air drag coefficient
I_e	Engine inertia	A_a	Cross section area
m	Vehicle mass	ρ_a	Air density
r_w	Wheel radius	c_r	Rolling res. coeff.
g_0	Gravity constant		

is assumed to hold where r_w is the effective wheel radius. Introduce the mass factor

$$c = 1 + \frac{I_l + \eta i^2 I_e}{m r_w^2}$$

Now, when a gear is engaged the forces in (2) are

$$F_p = \frac{1}{c r_w} \left(i \eta T_e(v, g, u_\mathrm{f}) - T_b(u_\mathrm{b}) \right) \tag{20a}$$

$$F_d(s, v) = \frac{1}{c} \left(F_a(v) + F_r(s) + F_g(s) \right) \tag{20b}$$

Note that the conditions (1) and (10) hold for (20b). The model (12) is now defined by

$$mv \frac{dv}{ds} = mv f(s, v, g, u) = F_p - F_d(s, v) \tag{21}$$

The states are the velocity v and currently engaged gear g, and the controls are fueling u_f, braking u_b and gear u_g. The road slope is given by $\alpha(s)$ and the brake torque is denoted by T_b. All model parameters are explained in Table 2.

4.2 Fuel consumption

The mass flow of fuel $\dot{m}$ is determined by the fueling level u_f and the engine speed ω_e. With (19), the mass flow is

$$\dot{m} = h(v, g, u) = \frac{n_{cyl}}{2\pi n_r} \omega_e u_\mathrm{f} = \frac{n_{cyl}}{2\pi n_r} \frac{i}{r_w} v u_\mathrm{f} \tag{22}$$

where n_{cyl} is the number of cylinders and n_r is the number of engine revolutions per cycle.

4.3 Neutral gear modeling

When neutral gear is engaged $g = 0$, the engine transmits zero torque to the driveline. The ratio i and efficiency η are undefined since the engine is decoupled from the rest of the powertrain. The approach taken here is to define the ratio and efficiency of neutral gear to be zero. Then, Equation (21) with $i(0) = \eta(0) = 0$ describes the vehicle motion.

4.4 Gear shift modeling

The transmission is of the automated manual type and gear shifts are carried out by engine control. In order to engage neutral gear without using the clutch, the transmission should first be controlled to a state where no torque is transmitted. The engine torque should then be controlled to a state where the input and output revolution speeds of the transmission are synchronized when the new gear is engaged. In the case of a truck with a large vehicle mass, the influence of the time with no engine propulsion becomes significant. Therefore, a model is formulated that is simple but also includes this effect.

Consider a gear shift from g_1 to g_2 with vehicle initial speed v_1. The currently engaged gear $g(t)$ is then described by

$$g(t) = \begin{cases} g_1 & t < 0 \\ 0 & 0 \le t \le \tau \\ g_2 & t > \tau \end{cases} \tag{23}$$

where τ is chosen to be constant, and hence the function in (14) is

$$\Delta t = \xi(s, v_1, g_1, g_2) = \tau \tag{24}$$

The vehicle motion $v(t)$ is given by solving the initial value problem given by (21) with $g = 0$ on $t \in [0, \tau]$ where $v(0) = v_1$. The required distance (15) is then given by integrating $v(t)$ over the interval,

$$\Delta s = \varphi(s, v_1, g_1, g_2) = \int_0^\tau v(t)\, dt \tag{25}$$

and the function in (16) becomes

$$\Delta v = \chi(s, v_1, g_1, g_2) = v(\tau) - v_1 \tag{26}$$

Fueling is required to synchronize the engine speed with the corresponding speed of the next gear in case of a down-shift. When neutral gear is engaged,

$$I_e \dot{\omega}_e = T_e = f_e(\omega_e, u_\mathrm{f}) \tag{27}$$

holds. Since the velocity trajectory is known through (21), the initial value ω_0 and desired final value ω_1 of the engine speed are also known through (19). Synchronizing the engine speed is thus equivalent to changing the rotational energy for the engine inertia by $I_e(\omega_1^2 - \omega_0^2)/2$. The consumed fuel is then estimated by

$$\Delta m = \psi(s, v_1, g_1, g_2) = \gamma \frac{1}{2} I_e(\omega_1^2 - \omega_0^2) \tag{28}$$

where γ (g/J) is introduced in Section 6.

4.5 Energy formulation

The model can be reformulated in terms of energy. Introduce the kinetic energy

$$e = \frac{1}{2} mv^2 \tag{29}$$

With the relation

$$\frac{dv}{dt} = v\frac{dv}{ds} = \frac{1}{2}\frac{d}{ds}v^2$$

a model with the structure (2) then becomes

$$\frac{de}{ds} = F_p - F_d\left(s, \sqrt{2e/m}\right) \tag{30}$$

4.6 Basic model

A basic model is derived as an approximation of the explicit model (21) for the purpose of analytical calculations later on. The speed dependence in engine torque is neglected, i.e., $T_e(v, g, u_f) \approx T(u_f)$. The approximation is typically reasonable, see Section 6 and Figure 4. For a given gear and without braking the propelling force in (2) becomes

$$F_p = \frac{i\eta}{cr_w} T(u_f) \tag{31}$$

The drag force $F_d(s, v)$ in (2) is still given by (20b).

5 Look-ahead control

Look-ahead control is a control scheme with knowledge about some of the future disturbances, here focusing on the road topography ahead of the vehicle. An optimization is performed with respect to a criterion that involves predicted future behavior of the system, and this is accomplished through DP (Bellman, 1961; Bertsekas, 1995).

5.1 Discretization

The models (12)–(17) are discretized in order to obtain a discrete process model

$$x_{k+1} = F_k(x_k, u_k)$$

where x_k, u_k denotes the state and control vectors.

Dividing the distance of the entire drive mission into M steps, the problem faced is to find

$$J_0^*(x_0) = \min_{u_0,\ldots,u_{M-1}} \zeta_M(x_M) + \sum_{k=0}^{M-1} \zeta_k(x_k, u_k) \tag{32}$$

where ζ_k and ζ_M defines the step cost and the terminal cost, respectively. The step cost is defined in Equations (38)–(40) and (44)–(45), see Section 5.4–5.5. The terminal cost is handled by introducing a residual cost in the following section.

5.2 Receding horizon

The approach taken here is to construct a look-ahead horizon by truncating the entire drive mission horizon of M steps to $N < M$ steps and approximating the cost-to-go at stage N. The shorter horizon is used in the on-line optimization. Rewrite problem (32) as

$$\begin{aligned} J_0^*(x_0) &= \min_{u_0,\ldots,u_{M-1}} \left\{ \zeta_M(x_M) + \sum_{k=0}^{M-1} \zeta_k(x_k, u_k) \right\} \\ &= \min_{u_0,\ldots,u_{N-1}} \left\{ \sum_{k=0}^{N-1} \zeta_k(x_k, u_k) + \min_{u_N,\ldots,u_{M-1}} \left\{ \zeta_M(x_M) + \sum_{k=N}^{M-1} \zeta_k(x_k, u_k) \right\} \right\} \end{aligned}$$

and define the residual cost

$$J_N^*(x_N) = \min_{u_N,\ldots,u_{M-1}} \zeta_M(x_M) + \sum_{k=N}^{M-1} \zeta_k(x_k, u_k) \tag{33}$$

as the cost-to-go function at stage N. Replace this function with an approximation $\tilde{J}_N^*(x_N)$ that should be available at a low computational effort. The problem is now only defined over the look-ahead horizon and

$$\min_{u_0,\cdots,u_{N-1}} \tilde{J}_N^*(x_N) + \sum_{k=0}^{N-1} \zeta_k(x_k, u_k) \tag{34}$$

is to be solved.

5.3 Dynamic programming algorithm

Denote by U_k the set of allowed controls and by S_k the set of allowed states at stage k. The DP solution to the look-ahead problem (34) is as follows.

1. For $x \in S_N$, let $J_N(x) = \tilde{J}_N^*(x)$.
2. Let $k = N - 1$.
3. For $x \in S_k$, let
$$J_k(x) = \min_{u \in U_k} \left\{ \zeta_k(x, u) + J_{k+1}(F_k(x, u)) \right\} \tag{35}$$
4. Repeat (3) for $k = N - 2, N - 3, \ldots, 0$.
5. The solution is made up of the policy with the optimal cost $J_0^*(x_0) = J_0(x_0)$.

The basic principle in the algorithm above is that if the cost-to-go $J_l(x)$ is known for $l \geq n$, then the cost-to-go $J_l(x)$ for $l = n - 1$ can be computed as a function of $J_l(x)$, $l \geq n$.

Now consider the model in Section 4. Introduce the discretized position $s_n = nh_s$ and velocity $v_m = mh_v$, where h_s, h_v are the respective step lengths. The gear number g is assumed to be discrete.

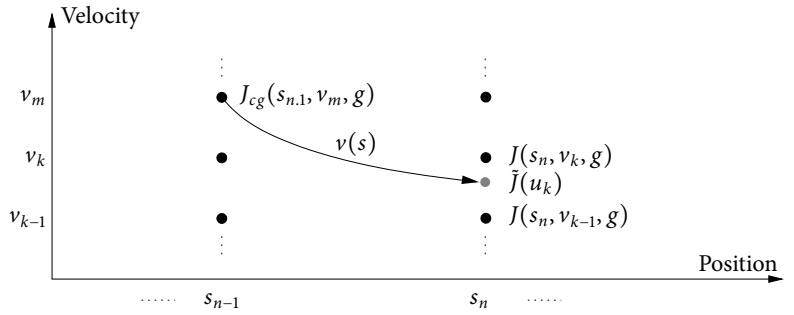

Figure 2: Cost-to-go for constant gear.

For a given velocity v_m and gear number g, the cost-to-go is $J_l(x) = J(s_l, v_m, g)$. The cost-to-go is first computed under the assumption that there is no gear shift and the result is denoted by $J_{cg}(s_{n-1}, v_m, g)$. After that, gear shifts are considered and the cost-to-go with a gear shift, $J_{gs}(s_{n-1}, v_m, g)$, is calculated. Finally, the cost-to-go is given by

$$J(s_{n-1}, v_m, g) = \min\left\{J_{cg}(s_{n-1}, v_m, g), J_{gs}(s_{n-1}, v_m, g)\right\} \tag{36}$$

The expressions for the cost-to-go for the respective case are derived in the following.

5.4 Cost-to-go for constant gear

Consider the case of constant gear g. For every discretized value u_k of the control, the solution to

$$\begin{aligned} \frac{dv}{ds} &= f(s, v(s), g, u_k), \quad s \in (s_{n-1}, s_n) \\ v(s_{n-1}) &= v_m \end{aligned} \tag{37}$$

gives a trajectory $v(s)$. The cost-to-go at the position s_n and velocity $v(s_n)$ is given by linear interpolation of $J(s_n, v_{k-1}, g)$ and $J(s_n, v_k, g)$ where $v_{k-1} \le v(s_n) \le v_k$, see Figure 2. The interpolated value is denoted by $\tilde{J}(u_k)$. The consumed fuel is

$$\Delta M = \int_{s_{n-1}}^{s_n} h(v(s), g, u_k) \frac{ds}{v(s)} \tag{38}$$

and the time spent is

$$\Delta T = \int_{s_{n-1}}^{s_n} \frac{ds}{v(s)} \tag{39}$$

where $v(s)$ is the solution of (37). The step cost is

$$\zeta_{cg}(u_k) = \Delta M + \beta \Delta T \tag{40}$$

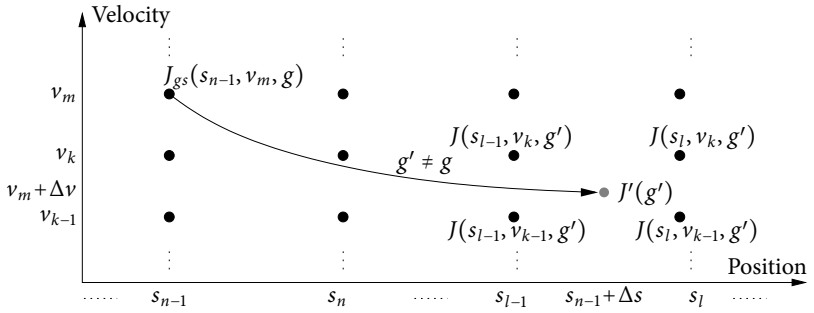

Figure 3: Cost-to-go for a gear shift.

where the terms are given by (38)–(39). The cost-to-go at position s_{n-1} and velocity v_m is obtained by finding the control signal u_k that minimizes the sum of the cost-to-go at position s_n and the step cost:

$$J_{cg}(s_{n-1}, v_m, g) = \min_{u_k} \left\{ \zeta_{cg}(u_k) + \tilde{J}(u_k) \right\} \tag{41}$$

5.5 Cost-to-go with gear shift

Consider a gear shift from gear g to $g' \neq g$ where the shift is initiated at position s_{n-1}. The gear shift model equations (15) and (16) give

$$\Delta v = \chi(s_{n-1}, v_m, g, g') \tag{42}$$
$$\Delta s = \varphi(s_{n-1}, v_m, g, g') \tag{43}$$

The cost-to-go at position $s_{n-1} + \Delta s$ and the velocity $v_m + \Delta v$ is obtained by using bilinear interpolation of the values $J(s_{l-1}, v_{k-1}, g')$, $J(s_{l-1}, v_k, g')$, $J(, s_l, v_{k-1}, g')$, and $J(s_l, v_k, g')$. An illustration is given in Figure 3. The interpolated value is denoted by $J'(g')$. The step cost is

$$\zeta_{gs}(g') = \Delta M + \beta \Delta T \tag{44}$$

where the terms are given by (17) and (14),

$$\Delta M = \psi(s_{n-1}, v_m, g, g') \tag{45}$$
$$\Delta T = \xi(s_{n-1}, v_m, g, g') \tag{46}$$

The cost-to-go at position s_{n-1} and the velocity v_m is obtained by minimizing the sum of the cost-to-go at position $s_{n-1} + \Delta s$ and the step cost:

$$J_{gs}(s_{n-1}, v_m, g) = \min_{g' \neq g} \left\{ \zeta_{gs}(g') + J'(g') \right\} \tag{47}$$

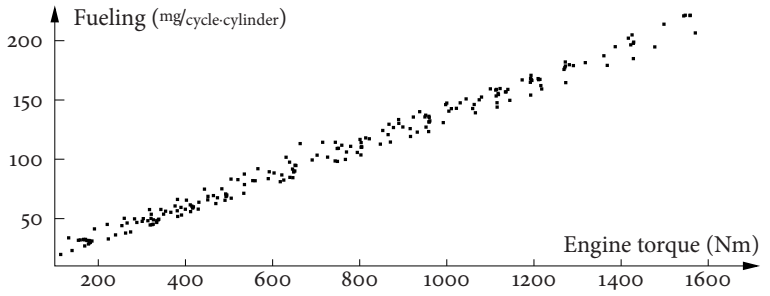

Figure 4: The relation between fueling and engine torque for a truck engine.

6 Residual cost

An approximation $\tilde{J}_N^*(x_N)$ of the residual cost (33) is now presented. The measured relation between engine torque and injected fuel mass per cycle and cylinder, for a truck engine with typical characteristics, is shown in Figure 4.

As can be seen in the figure, the function is approximately an affine function and using the method of least squares, the gradient can be calculated. By multiplying the quantities by the scaling factors $2\pi n_r \eta$ and n_{cyl}, respectively, the relation between energy (J/cycle) and fueling (g/cycle) is obtained. The gradient of the scaled function is denoted by γ, (g/J), and it indicates how much additional fuel ΔM is needed, approximately, in order to obtain a given increase of the kinetic energy Δe, i.e.

$$\Delta M \approx \gamma \Delta e$$

The basic idea in the computation of the approximate residual cost is that it is assumed that kinetic energy can be calculated to an equivalent fuel energy and conversely, at the final stage N, using the proportionality constant γ. This reflects that kinetic energy at the end of the current horizon can be used to save fuel in the future. With this assumption, the residual cost is in the form

$$\tilde{J}_N^*(x_N) = C - \gamma e \tag{48}$$

where C is an arbitrary constant that can be omitted when the optimal driving strategy is sought. In the following section, it will be shown that this approximation is accurate when no control constraint is active. It will be seen in Section 9 that this is a reasonable approximation of the residual cost in a more general case.

6.1 Cost-to-go gradient

Upper and lower bounds are derived for the difference between the cost-to-go of two neighboring states. First, introduce some short-hand notation. Denote the neighboring states at stage k by x_k^i for $i \in \{0,1\}$. The step cost is denoted by $\zeta^i = \zeta_k(x_k^i, u_k^i)$ and the cost-to-go (35) is

$$J^i = J_k(x_k^i) = \min_{u_k^i \in U_k} \left\{ \zeta^i + J_{k+1}(x_{k+1}^i) \right\}$$

where $x_{k+1}^i = F_k(x_k^i, u_k^i)$.

Now, assume that minimum is attained for u_k^0 and let $\zeta^* = \zeta^0$, then

$$J^0 = \zeta^* + J_{k+1}(x_{k+1}^0)$$

hold. Further, for any $u_k^1 \in U_k$,

$$J^1 \leq \zeta^1 + J_{k+1}(x_{k+1}^1)$$

holds. In particular, if there is an $u_k^1 \in U_k$ such that $x_{k+1}^0 = x_{k+1}^1$ then

$$\Delta J = J^1 - J^0 \leq \zeta^1 - \zeta^* \tag{49}$$

is an upper bound on the difference between the neighboring values of the cost-to-go. A lower bound can be derived analogously by assuming that the minimum is attained for u_k^1 and that there is a $u_k^0 \in U_k$ such that $x_{k+1}^0 = x_{k+1}^1$. Let $\zeta^* = \zeta^1$, then $J^1 = \zeta^* + J_{k+1}(x_{k+1}^1)$ and

$$J^0 \leq \zeta^0 + J_{k+1}(x_{k+1}^0) = \zeta^0 + J_{k+1}(x_{k+1}^1)$$

hold which can be combined into

$$\Delta J = J^1 - J^0 \geq \zeta^* - \zeta^0 \tag{50}$$

as a lower bound.

6.2 Cost-to-go gradient for basic model

The bounds in (49) and (50) are evaluated for the basic model, see Section 4.6, with the energy formulation according to (30).

Assume that constants k_1, k_2 are chosen such that the relation between fueling u and torque T fulfills

$$k_1 \leq \frac{du}{dT} \leq k_2 \tag{51}$$

Consider the upper bound (49), the difference between the step costs is given by (40) and (22),

$$\zeta^1 - \zeta^* = h_s \left[\frac{n_{cyl}}{2\pi n_r} \frac{i}{r_w} \Delta u + \beta \left(\frac{1}{v_k^1} - \frac{1}{v_k^0} \right) \right]$$

where $\Delta u = u_k^1 - u_k^0$. Assuming that $\Delta u \leq k \Delta T$ yields

$$\zeta^1 - \zeta^* \leq h_s \left[\frac{n_{cyl}}{2\pi n_r} \frac{i}{r_w} k \Delta T_e + \beta \left(\frac{1}{v_k^1} - \frac{1}{v_k^0} \right) \right] \tag{52}$$

where $\Delta T_e = T_e(u_k^1) - T_e(u_k^0)$. Applying Euler forward to (30) and solving for ΔT_e yields

$$\Delta T_e = \frac{c r_w}{i \eta} \frac{\Delta e}{h_s} \left(-1 + h_s \frac{c_w A_a \rho_a}{cm} \right)$$

where $\Delta e = e_k^1 - e_k^0$ and the value inside the parenthesis is negative for reasonable parameter values. Note that it is assumed that there is a feasible control for the required state transition. Insertion into (52), using (51), and rewriting yields

$$\zeta^1 - \zeta^* \leq \Delta e \left[\underline{\gamma} \left(-c + h_s \frac{c_w A_a \rho_a}{m} \right) - \beta \frac{h_s}{m} \frac{2}{v^0 v^1 (v^0 + v^1)} \right] \tag{53}$$

where $\underline{\gamma} = \frac{n_{cyl}}{2\pi n_r \eta} k_1$ and $v^i = \sqrt{\frac{2e_k^i}{m}}$. Thus, for a discretization where $\underline{v} \leq v \leq \overline{v}$,

$$\frac{\Delta J}{\Delta e} \leq -\underline{\gamma} \left[c - \frac{h_s}{m} \left(c_w A_a \rho_a - \frac{\beta}{\underline{\gamma} \overline{v}^3} \right) \right] \tag{54}$$

holds.

The lower bound (50) is analogously treated. This yields

$$\frac{\Delta J}{\Delta e} \geq -\overline{\gamma} \left[c - \frac{h_s}{m} \left(c_w A_a \rho_a - \frac{\beta}{\overline{\gamma} \underline{v}^3} \right) \right] \tag{55}$$

where $\overline{\gamma} = \frac{n_{cyl}}{2\pi n_r \eta} k_2$.

For a large mass, $c \approx 1$. The other two terms in the parentheses in (54) and (55) are in the order of 10^{-3} for typical parameters. Thus, the gradient of the value function with respect to kinetic energy is approximately equal to the scaled gradient γ of the fueling with respect to engine torque.

7 Complexity analysis

In the DP algorithm, the state x_k and the control signal u_k are discretized. If there are no restrictions on the search space, the number of step costs $\zeta_k(x_k, u_k)$ that have to be computed, at each gear and position, is equal to the product of the number of grid points and the number of discrete control signals.

The number of possible control signals is reduced due to physical limitations, such as limits on available propulsive force and braking force. In Figure 5 these limitations are the dashed lines. The number of control signals can be reduced even further by taking into account that different optimal trajectories never intersect. This principle is illustrated in Figure 5. First, assume that the grid is uniform, and that the optimal control for a state in the middle of the interval is computed, as shown to the left in the figure. After that the interval is divided into two the subintervals of equal length, and the optimal control is computed for the states in the middle of these subintervals. In these two computations, the possible control signals, not taking physical limitations into account, are reduced by half in average, as indicated by the gray areas in the right figure.

The interval is then divided into four subintervals of equal length and the number of computations can once again be reduced by half in average. By continuing in the same

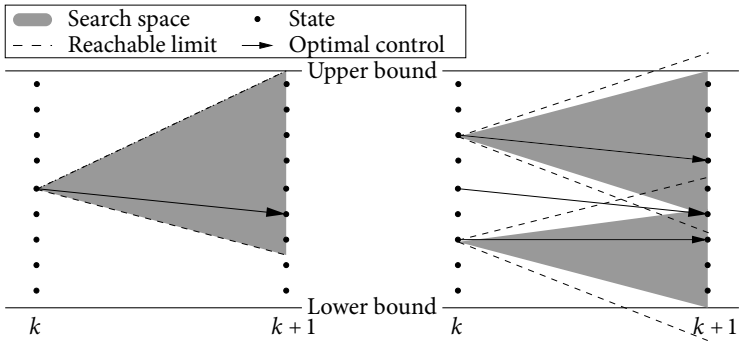

Figure 5: Reducing the possible control signals.

way and divide the state space into smaller and smaller subintervals and reducing the search space, the number of computations can be significantly reduced.

In Section 9 it will be shown that also the number of grid points can be reduced by choosing kinetic energy as a state in comparison to using velocity.

8 Discretization analysis

Performing numerical optimization of dynamical systems inevitable leads to errors such as rounding and truncation errors. It is of course desirable, but hard to guarantee, that such errors do not lead to that the numerical solution differ from the solution of the original problem.

In the following illustrating examples are presented. The observed features are then investigated by continuing the generic analysis in Section 3.

8.1 Generic analysis continued

Consider the problem of minimizing the fuel consumption, on a given gear, for a trip with a constraint on the trip time. Without other constraints, braking is intuitively never optimal and the only control left is the fueling. To study this problem the basic model is used, see Section 4.6.

Study the objective to minimize the work needed to bring the system from $s = 0,\ v(0) = v_0$ to $s = S,\ v(S) = v_0$. According to (3), the work needed is

$$W = \int_0^S F_p \, ds = \int_0^S F_d(s, v) \, ds \tag{56}$$

since the kinetic energy at the start and the end of the interval is the same. The time is constrained by

$$\int_0^S \frac{ds}{v} \leq T_0 \tag{57}$$

The engine torque is approximately an affine function in u_f, see Section 6 and Figure 4. With this approximation, the criterion (56) is equivalent to minimizing the fuel consumption. Without bounds on the control, the solution is constant speed according to Section 3. However, the fueling has natural bounds. If constant speed is feasible and the constraints are inactive then, clearly, the solution is still constant speed. Considering that the constraints possibly are active, the optimal control is analytically known to be of the type bang-singular-bang (Fröberg et al., 2006). It consists of constrained arcs with maximum or minimum fueling, and singular arcs with partial fueling such that constant speed is maintained.

In the following, the problem given by (2) and (56)–(57) is used as a test problem. Numerical solutions given by DP are presented and basic analytical calculations are performed.

For the analytical calculations three mesh points, $0 < h_s < 2h_s$ are studied. The control is assumed constant on each subinterval,

$$u_f(s) = \begin{cases} u_0 & s \in [0, h_s) \\ u_1 & s \in [h_s, 2h_s) \end{cases}$$

The objective can then be stated as

$$J = \min_{u_0, u_1} h_s \left(F_p(u_0) + F_p(u_1) \right) \tag{58}$$

using Equation (56) and where $v(0) = v_0$, $v(h) = v_1$. The maximum time T_0 is chosen as $T_0 = 2h_s/v_0$. For flat road, constant speed is feasible and the expected solution is constant speed, that is $v_1 = v_0$.

8.2 The Euler forward method

The DP solution for the test problem, using velocity as state and the Euler forward method for discretization, is shown in Figure 6. An oscillating solution appears on the flat segment where the solution is expected to be constant speed. The forward method applied to the dynamic model for simulation is stable for the step lengths used, hence such a stability analysis cannot explain the behavior. In the following, the test problem is used to investigate the oscillating behavior of the solution to the optimization problem.

The forward Euler method applied on the model (2) gives

$$\frac{v_{i+1} - v_i}{h_s} = \frac{1}{m v_i} \left(F_p(u_i) - F_d(s_i, v_i) \right) \tag{59}$$

Now, solve (59) for $F_p(u_i)$ where $i \in \{0, 1\}$ and note that, due to the terminal constraints, $v_2 = v_0$. Insertion into the objective (58) gives

$$W_{ef}(v_1) = h_s \left(F_d(s_0, v_0) + F_d(s_1, v_1) \right) - m \left(v_1 - v_0 \right)^2 \tag{60}$$

where v_1 now is the only free parameter.

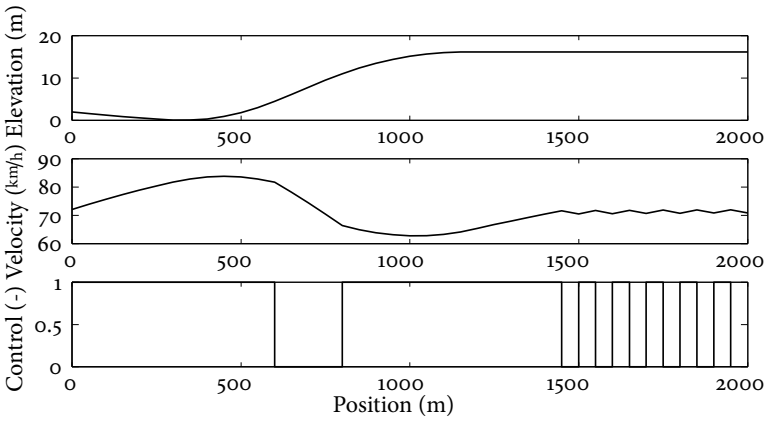

Figure 6: DP solution using velocity as state and Euler forward for discretization.

For flat road, the minimum of the objective is expected to occur for $v_1 = v_0$. Therefore,

$$W_{\text{ef}}(v_0) < W_{\text{ef}}(v_1) \quad \forall\ v_1 > v_0 \tag{61}$$

should hold. By inserting (60) into (61),

$$\frac{F_d(s_1, v_1) - F_d(s_1, v_0)}{v_1 - v_0} > m\frac{v_1 - v_0}{h_s} \tag{62}$$

is obtained. Approximating the differences with the corresponding derivatives yields

$$\frac{\partial F_d}{\partial v} > m\frac{dv}{ds} \tag{63}$$

Using (20b) and the models in Table 1 give $\partial F_d/\partial v = c_w A_a \rho_a v/c$. For typical values of a heavy truck with $m = 40 \cdot 10^3$ kg at $v = 20$ m/s, $c_w A_a \rho_a / c \approx 0.6 \cdot 10 \cdot 1.2/1 = 7.2 < 8$. Then according to (63),

$$\frac{dv}{dt} = v\frac{dv}{ds} < \frac{c_w A_a \rho_a v^2}{cm} < \frac{8 \cdot 20^2}{40 \cdot 10^3} = 0.08 \text{ m/s}^2$$

should hold but such a truck typically has a larger maximum acceleration. Therefore, the discrete optimization algorithm using this method may find these oscillating solutions.

8.3 The Euler backward method

With velocity as state and the Euler backward method for discretization, the DP solution for the test problem is shown in Figure 7. There is no longer an oscillating solution but the expected control switches between singular and constrained arcs are damped.

Applying the backward Euler method on the model (2) gives

$$\frac{v_{i+1} - v_i}{h_s} = \frac{1}{mv_{i+1}}\left(F_p(u_i) - F_d(s_{i+1}, v_{i+1})\right) \tag{64}$$

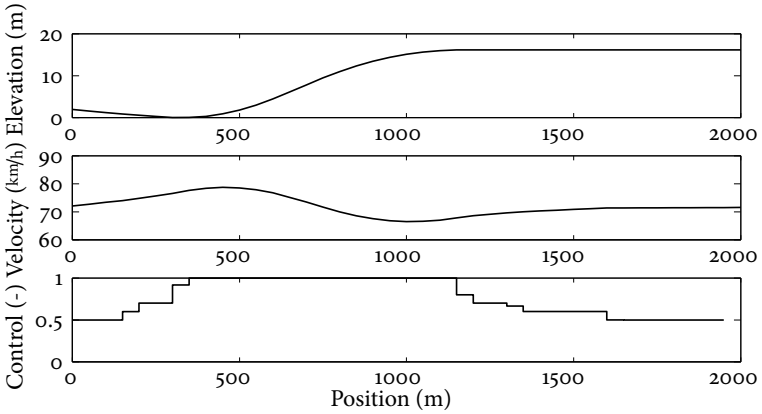

Figure 7: DP solution using velocity as state and Euler backward for discretization.

Proceed as for the Euler forward method earlier. Solve for $F_p(u_i)$ from (64) where $i \in \{0,1\}$ and use that $v_2 = v_0$. Insertion into the objective (58) gives

$$W_{\text{eb}}(v_1) = h_s \left(F_d(s_1, v_1) + F_d(s_2, v_0)\right) + m \left(v_1 - v_0\right)^2 \tag{65}$$

When using this method, it is seen that there is no $v_1 > v_0$ such that the objective (65) becomes lower than when $v_1 = v_0$. Thus, the method guarantees that the solution for flat road, i.e., constant speed, to the test problem is preserved. However, changes in velocity $v_1 \neq v_0$ are always penalized with the last term in (65). This is consistent with the results in Figure 7 where the expected control switches are smoothed out.

8.4 Energy formulation

With the energy formulation in (30), kinetic energy e is used as state variable instead of the velocity v. The DP solutions for the test problem, with this reformulation and the same number of grid points as before, for both Euler methods are shown in Figure 8. The bang-singular-bang characteristics now appear clearly and there are only small differences between the two Euler methods.

Performing similar calculations as previously, the objective value (58) becomes

$$W_{\text{ef}}(v_1) = h_s \left(F_d(s_0, v_0) + F_d(s_1, v_1)\right)$$
$$W_{\text{eb}}(v_1) = h_s \left(F_d(s_1, v_1) + F_d(s_2, v_0)\right)$$

Due to (1), $F_d(s, v_1) > F_d(s, v_0)$ if $v_1 > v_0$ and thus, the expected solution $v_1 = v_0$ for flat road is obtained. The objective values only consist of the resisting force evaluated in different points and there is no extra term as in (60) and (65). In conclusion, with the energy formulation, the simple Euler forward method can be used with adequate solution characteristics.

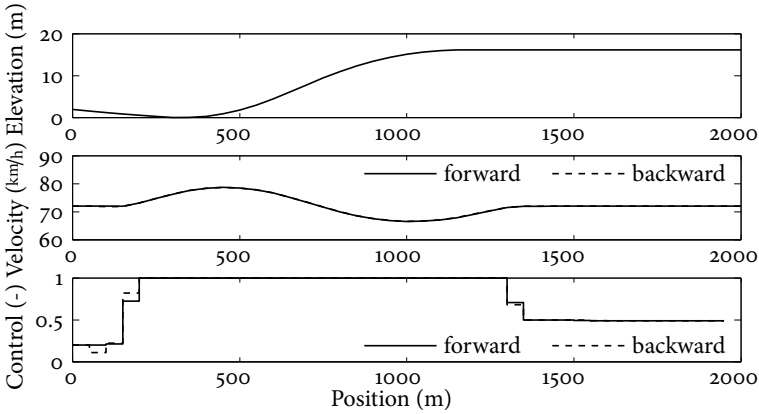

Figure 8: DP solution using kinetic energy as state and Euler methods for discretization.

9 Interpolation error

The DP algorithm is now applied on an illustrating example. The explicit truck model (21) and the energy formulation is used. The model thus has the structure (30) with forces given by (20). The road segment comes from measurements on a Swedish highway, see Figure 9.

Figure 10 shows the value function at 16 different positions with a distance between them of 200 m. The value function at position $s = 3000$ m is the proposed residual cost (48) and it can be seen that the shape of the cost function is approximately preserved for the other positions. Hence, the value function is dominated by a linear function with the gradient γ introduced in Section 6. As can be expected, the distance between the lines is smaller in the downhill segment compared to the uphill segment.

In the optimization algorithm it is the small deviations from the dominating straight line that are important. A consequence of this is that the linear interpolation error is significantly reduced if kinetic energy is used as state, instead of velocity, since the interpolation error of the dominating linear part is zero. This means that a coarser grid can be used and the complexity of the algorithm is reduced.

In Figure 11 the deviation from the linear function (48) is shown at four positions. It

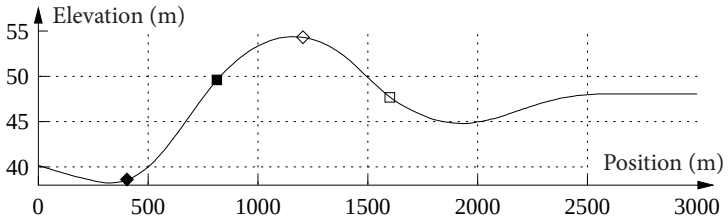

Figure 9: A road segment. The markers show the positions for the curves in Figure 11.

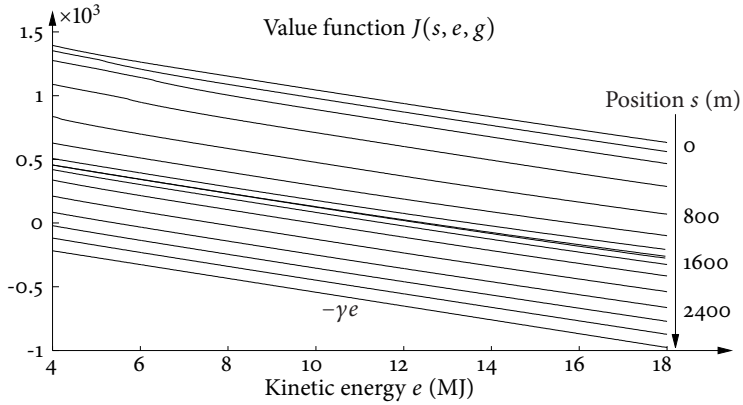

Figure 10: Value function $J(s, e, g)$ for $g = 12$.

is clearly seen that high velocities are most favorable at the beginning of the uphill slope, at 400 m, and least favorable at the top of the hill, at 1200 m. The curve for $s = 400$ m has a knee at 6 MJ, and the reason is that below this point a gear-shift is required. Low velocities are most beneficial at the top of the hill and in the downhill slope, at 1200 m and 1600 m.

10 Experimental data

A demonstrator vehicle, developed in collaboration with Scania, has been used to drive optimally according to (P2). Detailed description of the experimental situation is given in Hellström et al. (2009), and sensitivity to, e.g., mass and horizon length, is found in Hellström (2007). The trial route is a 120 km segment of a Swedish highway. In average, the fuel consumption is decreased about 3.5% without increasing the trip time and the number of gear shifts is decreased with 42% traveling back and forth, compared to the standard cruise controller. The tractor and trailer have a gross weight of about 40 tonnes. In Figure 12, measurements from a 6 km segment of the trial route are shown. The experience from the work with look-ahead is that the control is intuitive, in a qualitatively manner. The main characteristics are slowing down or gaining speed prior to significant hills. Slowing down will intuitively save fuel and reduce the need for braking. The lost time is gained by accelerating prior to uphills which also reduces the need for lower gears. However, to reduce the fuel consumption the detailed shape of the optimal solution is crucial.

The energy formulation together with the discretization and interpolation theory from Sections 8 and 9 leads to that the required resolution of the state grid is reduced compared to the straightforward velocity formulation. Note that the obtained solution is still optimal according to (P2). Furthermore, the use of simple Euler forward integration is possible since oscillations are avoided and the residual cost enables the use of a shorter horizon. Although a completely fair comparison is hard to make, all these factors reduce

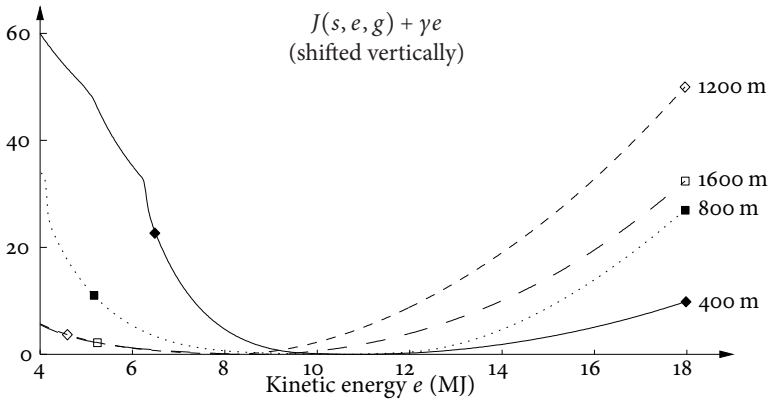

Figure 11: $J(s, e, g) + \gamma e$ for $g = 12$ and different positions s. Each curve is shifted vertically such that its minimum is zero. The markers are also shown in Figure 9.

the computation time significantly, in total approximately a factor of 10 compared to the previous implementation.

11 Conclusions

A DP algorithm for fuel-optimal control has been developed. Gear shifting is modeled by functions for the velocity change and the required time, distance, and fuel, respectively, during the shift process. A formulation that the algorithmic framework is well suited for, since it allows a proper physical model of the gear shift and can be easily handled in the algorithm by using interpolation. Furthermore, it was shown that a residual cost can be derived from engine and driveline characteristics, and the result is a linear function in energy.

The errors due to discretization and interpolation have been analyzed in order to assure a well-behaved algorithm. Depending on the choice of integration method, oscillating solutions may appear, and for that the interplay between the objective and the errors was shown to be crucial. A key point is that it is beneficial to reformulate the problem in terms of energy. It was shown that this both avoids oscillating solutions and reduces interpolation errors. A consequence is that a simple Euler forward method can be used together with a coarse grid and linear interpolation. This gives an accurate solution with low computational effort, thereby paving the way for efficient on-board fuel-optimal look-ahead control.

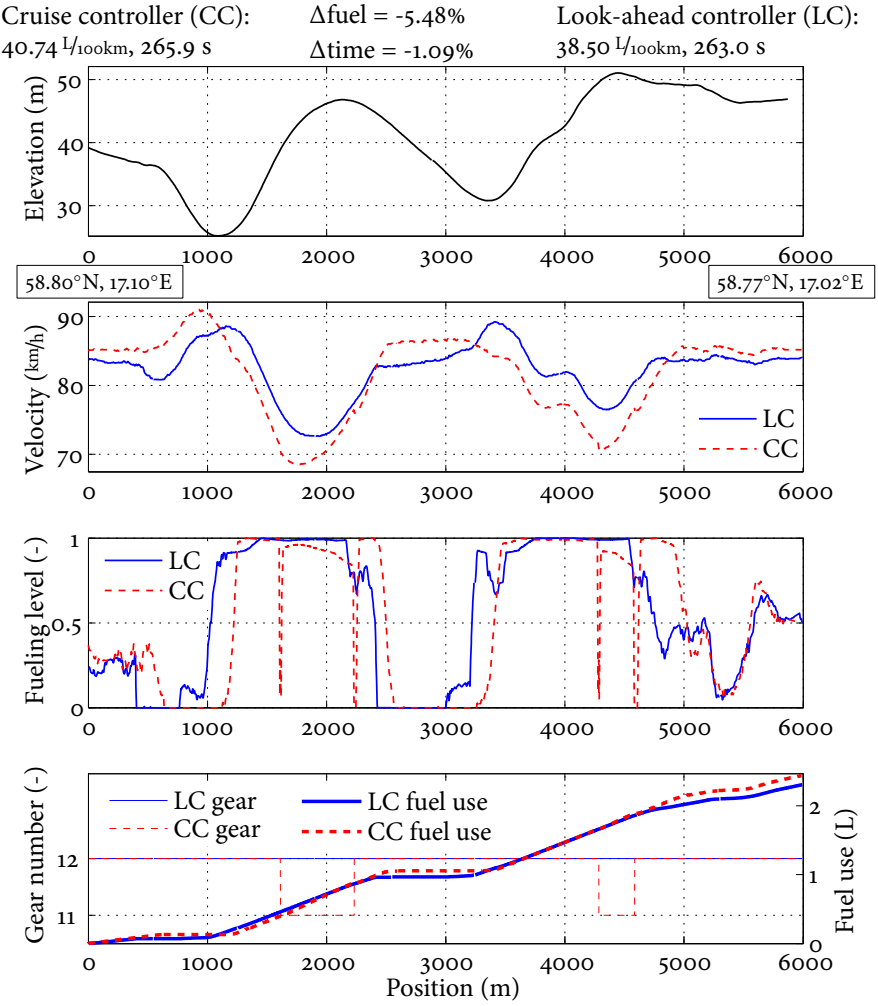

Figure 12: Measured data from one road segment. The LC travels slower prior to downhills and saves fuel. Gaining speed prior to uphills gains the lost time and also avoids gear shifts.

References

M. Back. *Prädiktive Antriebsregelung zum energieoptimalen Betrieb von Hybridfahrzeugen*. PhD thesis, Universität Karlsruhe, Karlsruhe, Germany, 2006.

R.E. Bellman. *Dynamic Programming*. Princeton University Press, Princeton, New Jersey, 1957.

R.E. Bellman. *Adaptive Control Processes: A Guided Tour*. Princeton University Press, Princeton, New Jersey, 1961.

D.P. Bertsekas. *Dynamic Programming and Optimal Control*, volume I. Athena Scientific, Belmont, Massachusetts, 1995.

J.T. Betts. *Practical methods for otpimal control using nonlinear programming*. SIAM, Philadelphia, 2001.

A.E. Bryson and Y. Ho. *Applied Optimal Control*. Taylor and Francis, 1975.

D.J. Chang and E.K. Morlok. Vehicle speed profiles to minimize work and fuel consumption. *Journal of transportation engineering*, 131(3):173–181, 2005.

C.A. Floudas. *Nonlinear and mixed-integer optimization*. Oxford Univ. Press, New York, 1995.

R. Franke, M. Meyer, and P. Terwiesch. Optimal control of the driving of trains. *Automatisierungstechnik*, 50(12):606–613, December 2002.

A. Fröberg, E. Hellström, and L. Nielsen. Explicit fuel optimal speed profiles for heavy trucks on a set of topographic road profiles. In *SAE World Congress*, number 2006-01-1071 in SAE Technical Paper Series, Detroit, MI, USA, 2006.

I.M. Gelfand and S.V. Fomin. *Calculus of variations*. Prentice-Hall, Englewood Cliffs, New Jersey, 1963.

L. Guzzella and A. Sciarretta. *Vehicle Propulsion Systems*. Springer, Berlin, 2nd edition, 2007.

E. Hellström. *Look-ahead Control of Heavy Trucks utilizing Road Topography*. Licentiate thesis LiU-TEK-LIC-2007:28, Linköping University, 2007.

E. Hellström, A. Fröberg, and L. Nielsen. A real-time fuel-optimal cruise controller for heavy trucks using road topography information. In *SAE World Congress*, number 2006-01-0008 in SAE Technical Paper Series, Detroit, MI, USA, 2006.

E. Hellström, M. Ivarsson, J. Åslund, and L. Nielsen. Look-ahead control for heavy trucks to minimize trip time and fuel consumption. *Control Engineering Practice*, 17(2): 245–254, 2009.

P.G. Howlett, I.P. Milroy, and P.J. Pudney. Energy-efficient train control. *Control Engineering Practice*, 2(2):193–200, 1994.

W. Huang, D.M. Bevly, S. Schnick, and X. Li. Using 3D road geometry to optimize heavy truck fuel efficiency. In *11th International IEEE Conference on Intelligent Transportation Systems*, pages 334–339, 2008.

M. Ivarsson, J. Åslund, and L. Nielsen. Look ahead control - consequences of a non-linear fuel map on truck fuel consumption. *Proceedings of the Institution of Mechanical Engineers, Part D, Journal of Automobile Engineering*, 223(D10):1223–1238, 2009.

U. Kiencke and L. Nielsen. *Automotive Control Systems, For Engine, Driveline, and Vehicle*. Springer-Verlag, Berlin, 2nd edition, 2005.

F. Lattemann, K. Neiss, S. Terwen, and T. Connolly. The predictive cruise control - a system to reduce fuel consumption of heavy duty trucks. In *SAE World Congress*, number 2004-01-2616 in SAE Technical Paper Series, Detroit, MI, USA, 2004.

R. Liu and I.M. Golovitcher. Energy-efficient operation of rail vehicles. *Transportation Research*, 37A:917–932, 2003.

V.V Monastyrsky and I.M. Golownykh. Rapid computations of optimal control for vehicles. *Transportation Research*, 27B(3):219–227, 1993.

B. Passenberg, P. Kock, and O. Stursberg. Combined time and fuel optimal driving of trucks based on a hybrid model. In *European Control Conference*, Budapest, Hungary, 2009.

P. Sahlholm and K.H. Johansson. Road grade estimation for look-ahead vehicle control using multiple measurement runs. *Control Engineering Practice*, 2009. doi: 10.1016/j.conengprac.2009.09.007.

A.B. Schwarzkopf and R.B. Leipnik. Control of highway vehicles for minimum fuel consumption over varying terrain. *Transportation Research*, 11(4):279–286, 1977.

A. Sciarretta, M. Back, and L. Guzzella. Optimal control of parallel hybrid electric vehicles. *IEEE Transactions on Control Systems Technology*, 12(3):352–363, 2004.

S. Terwen, M. Back, and V. Krebs. Predictive powertrain control for heavy duty trucks. In *4th IFAC Symposium on Advances in Automotive Control*, Salerno, Italy, 2004.

Paper C

Horizon length and fuel equivalents for fuel-optimal look-ahead control[☆]

C

[☆] Accepted for *6th IFAC Symposium Advances in Automatic Control*, 2010. Modifications are made to the layout.

Horizon length and fuel equivalents for fuel-optimal look-ahead control

Erik Hellström, Jan Åslund, and Lars Nielsen

Linköping University, Linköping, Sweden

Abstract

Recent studies from several authors show that it is possible to lower the fuel consumption for heavy trucks by utilizing information about the road topography ahead of the vehicle. The approach in these studies is receding horizon control where horizon length and residual cost are main topics. To approach these topics, fuel equivalents previously introduced based on physical intuition are given a mathematical interpretation in terms of Lagrange multipliers. Measures for the suboptimality, caused by the truncated horizon and the residual cost approximation, are defined and evaluated for different routes and parameters.

1 Introduction

The scenario of look-ahead control is a heavy truck operating on varying terrain, and there is road data on-board so that the road slope ahead of the vehicle is known. The objective used is to minimize the fuel mass M required for a drive mission with a given maximum trip time T_0:

$$\begin{aligned} &\text{minimize } M \\ &\text{subject to } T \le T_0 \end{aligned} \tag{P1}$$

A receding horizon control (RHC) approach has successfully been used for the solution, and experimental evidence confirms that it is possible to improve the fuel economy of heavy trucks by this approach (Hellström et al., 2009). RHC is a general method to find an approximation for the optimal control law by solving on-line, at each time step, a finite horizon optimal control problem (see, e.g., the survey paper Mayne et al., 2000). In this method, it is crucial how to select the residual cost at the end of the finite horizon and how to select a proper horizon length to balance between computational complexity and suboptimality. These two topics are in this paper given a thorough investigation that is independent of the method of solving the optimal control problem in each time step.

The line of investigation is to consider (P1) but also the reformulation

$$\text{minimize } M + \beta T \tag{P2}$$

where β determines the compromise between fuel mass and trip time. Problem (P1) is solved in Hellström et al. (2010a) by developing an efficient algorithm for (P2). The RHC approach is taken in recent papers on the problem (P1) for heavy trucks (Terwen et al., 2004; Hellström et al., 2007, 2009; Huang et al., 2008; Passenberg et al., 2009). These works utilize the reformulation (P2) except for Terwen et al. (2004) where cruise control rather than fuel-optimal control is considered by adding a quadratic penalty on deviations from a cruise speed in (P1). Although the method of solution in each time step differs in these studies, the length of the horizon and the residual cost are important common issues. A residual cost is selected and explained by Hellström et al. (2010a) that is linear in kinetic energy where the gradient γ represents the trade-off between fuel mass and kinetic energy at the end of the horizon. The deviation from optimality thus depends on the length of the horizon and the choice of the fuel equivalence factors (β, γ), and the issue of suboptimality is studied here.

The paper starts out by formulating models of the longitudinal vehicle dynamics that follows the treatment in previous papers (Hellström et al., 2009, 2010a). Next look-ahead control is recalled, and measures are introduced for the suboptimality due to the truncated horizon. The following two sections treat the fuel equivalents. These were based on physical intuition in the prior papers but a clear mathematical interpretation is added here by relating to well established optimal control theory. A quantitative study is then performed to evaluate how the degree of suboptimality depends on the horizon length, vehicle mass, and road characteristics.

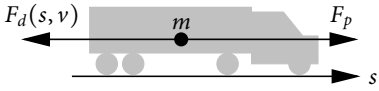

Figure 1: A vehicle moving in one dimension.

2 Model

The dynamics of the vehicle is modeled by considering the motion in one dimension, see Figure 1. The propelling force is denoted by F_p. The drag force is denoted by $F_d(s,v)$ and is dependent on position s and velocity v. The velocity dynamics is given by Newton's second law of motion,

$$mv\frac{dv}{ds} = F_p - F_d(s,v) \tag{1}$$

In the following, the full model and the basic model are presented. The full model has two states and three control signals whereas the basic model is an approximation of the full model and has one state and one control.

2.1 Full model

A model of the longitudinal dynamics is formulated for a stiff driveline (Kiencke and Nielsen, 2005). Gear shifting is considered and the ratio i and efficiency η are functions of the current gear. The engine torque T_e is given by a look-up table from measurements. The states are velocity v and engaged gear g, and the controls are fueling u_{f}, braking u_{b} and gear u_{g}. The road slope is given by $\alpha(s)$ and the brake torque is denoted by T_b. The forces in (1) are then

$$F_p = \frac{1}{c_m r_w}\left(i\eta T_e(v,g,u_{\mathrm{f}}) - T_b(u_{\mathrm{b}})\right) \tag{2a}$$

$$F_d(s,v) = \frac{1}{c_m}\left(F_a(v) + F_r(s) + F_g(s)\right) \tag{2b}$$

where

$$c_m = 1 + \frac{I_l + \eta i^2 I_e}{m r_w^2}$$

is a mass factor. The models of the resisting forces and all model parameters are explained in Table 1 and 2 respectively.

Table 1: Longitudinal forces.

Force	Explanation	Expression
$F_a(v)$	Air drag	$\frac{1}{2}c_w A_a \rho_a v^2$
$F_r(s)$	Rolling resistance	$mg_0 c_r \cos\alpha(s)$
$F_g(s)$	Gravitational force	$mg_0 \sin\alpha(s)$

Table 2: Truck model parameters.

I_l	Lumped inertia	c_w	Air drag coefficient
I_e	Engine inertia	A_a	Cross section area
m	Vehicle mass	ρ_a	Air density
r_w	Wheel radius	c_r	Rolling res. coeff.
g_0	Gravity constant		

The fuel consumption is given by integrating the mass flow of fuel M' (g/m),

$$M' = \frac{n_{cyl}}{2\pi n_r}\frac{i}{r_w}u_{\mathrm{f}} \tag{3}$$

where n_{cyl} is the number of cylinders, n_r is the number of engine revolutions per cycle, and u_{f} is grams of fuel per engine cycle and cylinder.

2.2 Basic model

A basic model is derived as an approximation of the full model for the purpose of analytical calculations later on. A constant gear and no braking is assumed, the state is velocity v and the control is fueling u.

Measurements of engine torque T_e as a function of fueling u for a diesel engine typically show an approximate affine relation, see, e.g., Hellström et al. (2010a) for an experimental validation. Such an approximation can be interpreted as a Willans description (Guzzella and Sciarretta, 2005). Denote an estimated gradient of this relation by c_e, then

$$\Delta u = c_e \Delta T_e \tag{4}$$

holds approximately. For the basic model, it is assumed that the fueling is proportional to the torque with c_e being the constant of proportionality (the drag torque offset d_e is included in the drag forces without changing the model structure). The dependence on the road slope α is approximated to first order (α is typically a few percent). The forces in (1) become

$$F_p = \frac{i\eta}{c_m r_w}\frac{u}{c_e} \tag{5a}$$

$$F_d(s,v) = \frac{1}{c_m}\Big(F_a(v) + F_r + F_g(s)\Big) \tag{5b}$$

where $F_a(v) = \frac{1}{2}c_w A_a \rho_a v^2$, $F_r = mg_0 c_r - \frac{i\eta}{r_w}d_e$, and $F_g(s) = mg_0\alpha(s)$. The control is bounded by

$$0 \le u \le \bar{u} \tag{6}$$

where $\bar{u}$ is maximum fueling. The mass flow of fuel (3) is

$$M' = c_u u, \quad c_u = \frac{n_{cyl}}{2\pi n_r}\frac{i}{r_w} \tag{7}$$

where c_u is a constant.

3 Look-ahead

Look-ahead control utilizes RHC to handle the complexity due to changing conditions. Now the RHC problem is formulated, and based on that suboptimality measures are introduced.

3.1 Receding horizon

Combining Equations (1) and (2), the system model is given by

$$\frac{dx}{ds} = f(x, u, s), \quad x(0) = x_0 \tag{8}$$

where $x \in X$, $u \in U$ are states and controls. The problem over the entire drive mission $s \in [0, S]$ is defined by

$$J^S(x_0) = \min_{u \in U} \int_0^S L(x, u)\, ds \tag{9}$$

where L is the running cost given by (P2).

Denote by J^R the optimal cost for the RHC problem with the horizon length R. Let s_r be the current position and $P = \min\{s_r + R, S\}$. The problem

$$J^R(s_r, x) = \min_{u \in U} \left\{ \phi(x(P)) + \int_{s_r}^P L(x, u)\, ds \right\} \tag{10}$$

where ϕ is a residual cost, is solved repeatedly on-line by some optimization method. The solution is the RHC controller, denoted by μ^R, and the resulting trajectory is the solution for

$$\frac{dx}{ds} = f(x, \mu^R, s), \quad x(0) = x_0 \tag{11}$$

with an associated cost

$$J^S_{\mu^R}(x_0) = \int_0^S L(x, \mu^R)\, ds \tag{12}$$

Thus, $J^S_{\mu^R}$ gives a basis for evaluating a given horizon length R in relation to the full problem given by J^S in (9). The other important performance factor in RHC is the residual cost ϕ in (10). The choice of R and ϕ will be studied in the following.

3.2 Suboptimality measures

To begin with, the basis for studying different horizon lengths is introduced. This foundation is valid independent of the choice of the residual cost ϕ in (10).

The difference between the costs (9) and (12) is the central matter, and it is clear that the relation

$$J^S(x) \le J^S_{\mu^R}(x) \tag{13}$$

holds between these costs. To quantify the difference between them, a measure of the suboptimality imposed by RHC is introduced that is the relative difference between the

costs. Consequently, define the degree of suboptimality for a horizon length R by κ_J^R, where

$$\kappa_J^R = J_{\mu^R}^S(x) \Big/ J^S(x) - 1 \tag{14}$$

Clearly, κ_J^R is non-negative, is zero for the optimal control law for the original problem (9), and $\kappa_J^R \to 0$ when $R \to S$. The suboptimality is decreasing with horizon length so studying κ_J^R for varying R can be used to judge suitable horizon lengths. Note that the measure is independent of how the optimal solution for (10) is obtained.

The application here is problem (P2) where

$$J^S(x) = M^S(x) + \beta T^S(x) \tag{15}$$

To separate the suboptimality in fuel mass M and trip time T, define the measures κ_M^R, κ_T^R by

$$\kappa_M^R = \frac{M_{\mu^R}^S(x)}{M^S(x)} - 1, \quad \kappa_T^R = \frac{T_{\mu^R}^S(x)}{T^S(x)} - 1 \tag{16}$$

analogous to (14). The measures κ_J^R, κ_M^R, κ_T^R are studied quantitatively for (P2) and varying R in Section 6.

4 Fuel equivalents

For an efficient solution of (P1), fuel equivalents have been introduced in Hellström et al. (2010b,a) based on physical intuition. The support for these is substantiated in Section 5 by a mathematical interpretation relating to optimal control theory. The use of fuel equivalents is inspired by the electrical energy equivalents in works by, e.g., Paganelli et al. (2000); Sciarretta et al. (2004).

4.1 Kinetic energy equivalence - residual cost

The residual cost, the other important topic in RHC, is now treated. Starting with the fuel equivalent γ (g/J) that is based on that Equation (4) represents an affine relation between engine torque T_e and fueling u. The scaled gradient,

$$\gamma = \frac{n_{cyl}}{2\pi n_r \eta} c_e \tag{17}$$

defines an equivalence between energy and fuel mass.

In Hellström et al. (2010a), the idea is to calculate kinetic energy into an equivalent fuel mass as an approximation of the fact that kinetic energy can be used to save fuel in the future. The residual cost $\phi(x) = -\gamma e$, where $e = \frac{1}{2} m v^2$ is kinetic energy at the end of the horizon, was proposed. A slightly modified residual cost is obtained by rewriting the basic model for a small Δs. Equations (1),(5),(7), and (17) yield

$$\Delta M = \gamma \left[c_m \Delta e + \Delta p + \left(F_a(v) + F_r \right) \Delta s \right] \tag{18}$$

where p is potential energy and $\Delta p \approx m g_0 \alpha \Delta s$. From (18) it is seen that a change Δe in kinetic energy approximately equals a fuel mass $\gamma c_m \Delta e$. Based on this, the mass factor c_m should be included to yield

$$\phi(x) = -\gamma c_m e \tag{19}$$

but c_m is typically close to one, especially for large masses and higher gears. The value of γ for an example of a typical engine in a heavy diesel truck is 53 g/MJ or 4.6 kWh/L.

4.2 Time equivalence

The reformulation in (P2) is beneficial since the problem has a lower dimension than (P1) and since, with an RHC approach, it avoids the risk of an infeasible constraint. However, the parameter β has to be selected. An approximate value of β can be found by assuming that the constant speed $\hat{v}$ is the solution for the trip length S. Using $S = \hat{v} T_0$ and (18) gives the criterion.

$$J(\hat{v}) = \gamma \left(p(S) - p(0) \right) + \gamma \left(F_a(\hat{v}) + F_r \right) S + \beta \frac{S}{\hat{v}} \tag{20}$$

In a stationary point $J'(\hat{v}) = 0$ which yields $\beta = \gamma \hat{v}^2 F_a'(\hat{v})$. The air drag force according to Table 1 yield

$$\beta = 2\gamma P_a(\hat{v}) = 2\gamma P_a(S/T_0) \tag{21}$$

where $P_a(\hat{v}) = \hat{v} F_a(\hat{v})$ is the air drag power. With β according to (21), $J''(\hat{v})$ is positive for all physically feasible parameters which shows that it gives a minimum for this stationary case. The compromise between fuel mass and trip time is defined by the ratio

$$q = \frac{M}{\beta T} = \frac{1}{2} \left(1 + \frac{F_r}{F_a(\hat{v})} \right) \tag{22}$$

A change in β gives another stationary speed $v(\beta)$ and q. The relative changes in fuel mass and trip time become

$$\kappa_M^\beta = \frac{F_a(v(\beta)) - F_a(\hat{v})}{F_a(\hat{v}) + F_r}, \quad \kappa_T^\beta = \frac{\hat{v}}{v(\beta)} - 1 \tag{23}$$

The slope in the origin of the graph κ_M^β versus κ_T^β becomes $-q^{-1}$ where q is given by (22) and so, close to the origin

$$q \kappa_M^\beta + \kappa_T^\beta = 0 \tag{24}$$

holds. Examples of typical parameters for a heavy diesel truck and 80 km/h give β as 4.5 g/s or 18.5 L/h and q as 1.2. The ratio q thus indicates that an increase in time of 1.2% gives, approximately, a decrease in fuel mass of 1%.

5 Interpretation of fuel equivalents

The fuel equivalents in Section 4 are given a mathematical interpretation by relating them to the Lagrange multipliers used in optimization theory. To accomplish this, first an optimal control problem is formulated and the multipliers for this problem are throughly studied. A related work is Fröberg and Nielsen (2008) where the multiplier for a velocity state is studied.

5.1 Problem formulation

Consider (P1) for the basic model in Section 2.2 and treat the time constraint as an equality constraint since the minimum is attained in the limit for a realistic drive mission:

$$\begin{aligned} &\text{minimize } M \\ &\text{subject to } T = T_0 \end{aligned} \tag{P3}$$

The problem (P3) is specified exactly below by (25)–(28). In the formulation, it is convenient to use position s as independent variable and kinetic energy e as state instead of velocity. The notation in the following is adopted from Bryson and Ho (1975).

The states are time t and kinetic energy e with associated Lagrange multipliers denoted by

$$x = (t, e)^T, \quad \lambda = (\lambda_t, \lambda_e)^T$$

The dynamics is

$$x' = f(x, u, s) = \begin{pmatrix} \sqrt{m/2e} \\ \frac{c_u}{\gamma c_m} u - F_d \end{pmatrix} \tag{25}$$

The running cost is $L = M'$, so (7) gives the objective

$$J = \min_{u \in U} \int_0^S c_u u \, ds \tag{26}$$

with U given by (6). The trip time constraint is

$$\psi(x(S)) = t(S) - T_0 \tag{27}$$

Together with an initial condition

$$x(0) = (0, \frac{1}{2} m v_0^2) \tag{28}$$

the problem (P3) becomes completely specified.

5.2 Solution

The Minimum Principle states that the optimal control minimizes the Hamiltonian H,

$$u^\star = \arg\min_{u \in U} H \tag{29}$$

where $H = L + \lambda^T f$ and

$$\lambda'^T = -\frac{\partial H}{\partial x}, \quad \lambda(S) = \nu^T \frac{\partial \psi}{\partial x} \tag{30}$$

where ν is a constant vector (Bertsekas, 1995, Ch. 3.3).

For the problem (P3), the Hamiltonian is

$$H = L + \lambda^T f = \sigma u + \lambda_t \sqrt{m/2e} - \lambda_e F_d \tag{31}$$

where σ is given by

$$\sigma(s) = \frac{c_u}{\gamma c_m} \left(\gamma c_m + \lambda_e(s)\right) \tag{32}$$

The dynamics of λ (30) is

$$\lambda' = \begin{pmatrix} 0 \\ \frac{\lambda_t}{m} \left(\frac{m}{2e}\right)^{\frac{3}{2}} + \frac{\lambda_e}{c_m} \frac{\partial F_a}{\partial e} \end{pmatrix}, \quad \lambda(S) = \begin{pmatrix} \nu \\ 0 \end{pmatrix} \tag{33}$$

where the fact that $\frac{\partial}{\partial e} F_d(s, e) = \frac{1}{c_m} \frac{\partial}{\partial e} F_a(e)$ has been used.

Since H is linear in u, the solution is at one of the bounds in (6) if $\sigma(s) \neq 0$. If $\sigma(s) = 0$, the solution is singular and can not be determined from the Minimum Principle. To summarize, the possible controls are

$$u^\star = \begin{cases} 0 & \sigma(s) > 0 \\ \hat{u} & \sigma(s) = 0 \\ \bar{u} & \sigma(s) < 0 \end{cases} \tag{34}$$

where $\hat{u}$ is the yet unknown control on a singular arc.

To find $\hat{u}$, the singular arc is studied. Equation (32) immediately gives that if $\sigma(s) = 0$, then

$$\lambda_e(s) = -\gamma c_m \tag{35}$$

If $\sigma(s) = 0$ on a finite interval, it must hold that $\sigma'(s) = 0$. From (32) and (33) together with (35) it then follows that

$$\sigma' = \frac{\lambda_t}{m} \left(\frac{m}{2e}\right)^{\frac{3}{2}} - \gamma \frac{\partial F_a}{\partial e} = 0 \tag{36}$$

which shows that, since λ_t and $\frac{\partial F_a}{\partial e}$ are constant, the kinetic energy is constant on a singular arc (this further implies that $\sigma''(s) = 0$). The control $\hat{u}$ is then given from (25)

$$\hat{u} = \frac{\gamma c_m}{c_u} F_d(s, \hat{v}) \tag{37}$$

where $\hat{v}$ is the constant speed. Singular arcs are possible on road segments with small slopes such that constant speed is feasible since there must be a feasible $\hat{u}$, $0 \leq \hat{u} \leq \bar{u}$.

Solving (36) for λ_t and inserting the air drag force F_a in (5b) shows that, on a singular arc,

$$\lambda_t = 2\gamma P_a(\hat{v}) \tag{38}$$

holds where $P_a(\hat{v}) = \hat{v}F_a(\hat{v})$ is the air drag power. Since $v = \lambda_t$ is constant, the choice of v such that the trip time constraint is satisfied also determines the constant speed $\hat{v}$ on singular arcs.

A complete solution for (P3) is given by solving the two-point boundary value problem given by (25), (28), and (33) where v is determined by the trip time constraint (27).

5.3 Interpretation

The relationships (Bryson and Ho, 1975; Bertsekas, 1995)

$$\lambda^T = \frac{\partial J}{\partial x}, \quad H = -\frac{\partial J}{\partial s} \tag{39}$$

or equivalently

$$dJ = \lambda^T dx - Hds \tag{40}$$

form a general connection between the optimal cost function J and the Lagrange multipliers λ and the Hamiltonian H. The aim here is to investigate physically meaningful interpretations of these quantities.

The control u may be discontinuous if selected according to (34). Moreover, the road slope $\alpha(s)$ is typically known in discrete points α_k where

$$\alpha(s) = \alpha_k, \quad s \in [k\Delta s, (k+1)\Delta s) \tag{41}$$

Jumps in $\alpha(s)$ and $u(s)$ yield jumps in the system dynamics f, and the point at which f changes can be seen as an interior boundary condition. Since, in this case, the condition becomes a function only of position, it leads to that λ is continuous whereas H may be discontinuous (see Bryson and Ho, 1975, Ch. 3.5).

Kinetic energy

The dynamics of λ_e is written as

$$\lambda_e'(s) = \theta\lambda_e(s) + \gamma c_m \theta \left(\frac{\hat{v}}{v(s)}\right)^3, \quad \theta = \frac{c_w A_a \rho_a}{c_m m} \tag{42}$$

by inserting (5b) and (38) into (33). It turns out that the adjoint dynamics is driven by the deviation of the optimal velocity $v(s)$ from the constant level $\hat{v}$ and it is expected that $\lambda_e(s)$ varies around $-\gamma c_m$ if $v(s)$ varies around $\hat{v}$. On a singular arc, $v(s) = \hat{v}$ which implies that λ_e' is zero.

A variation δe on an optimal trajectory gives a changed cost $\delta J = \lambda_e \delta e$ according to (39), i.e., a change in kinetic energy leads to a proportional change in the equivalent fuel consumption with the constant of proportionality being λ_e. In particular, on a singular arc, $\delta J = -\gamma c_m \delta e$ and

$$\left.\frac{\partial J}{\partial e}\right|_{e=\hat{e}} = -\gamma c_m, \quad \hat{e} = \frac{1}{2} m \hat{v}^2 \tag{43}$$

The change in the Hamiltonian (31) due to a change in the road slope at $s = s_1$ becomes, since x and λ are continuous,

$$H(s_1+) - H(s_1-) = -\frac{1}{c_m}\lambda_e(s_1) m g_0 \left(\alpha_k - \alpha_{k-1}\right) \tag{44}$$

The Hamiltonian is therefore stepwise constant

$$H(s) = H_k, \quad s \in [k\Delta s, (k+1)\Delta s) \tag{45}$$

and may be written as

$$H_k = H_0 - \frac{1}{c_m}\sum_{j=1}^{k} \lambda_e(j\Delta s) m g_0 \left(\alpha_j - \alpha_{j-1}\right) \tag{46}$$

for $k = 1, 2, \ldots, S/\Delta s - 1$. According to (40), the change in the optimal cost due to a Δs with $\Delta x = 0$ is $-H$. Potential energy is approximately $m g_0 \alpha(s)\Delta s$ and consequently, $\lambda_e(s)$ determines the proportional change in the cost due to the change in potential energy during $[s, s + \Delta s)$.

Time

When solving (P3), the value of $\nu = \lambda_t = 2\gamma P_a(\hat{v})$ must be found such that the trip time constraint (27) is satisfied. Using the time equivalent β in (21) is the same as choosing a value β, removing the trip time constraint (27) by letting $\psi = 0$, and modify the objective (26) as

$$J = \min_{u \in U} \int_0^S c_u u + \frac{\beta}{\nu}\, ds \tag{47}$$

that is equal to the formulation (P2). This formulation may lead to a trip time $T \neq T_0$. With the original formulation, a variation δt on the optimal trajectory gives a changed cost $\delta J = \nu \delta t$ according to (39) and ν is thus a measure of the increase in the equivalent fuel consumption if the remaining time decreases.

Summary

In conclusion, λ_t determines the constant speed $\hat{v}$ on singular arcs, according to (38), whereas λ_e is the decisive variable for the dynamical behavior, i.e., when the velocity deviates from $\hat{v}$, according to (32),(34),(42). The standard interpretation, given by (39), of the values of the adjoint variables is that they are the gradient of the cost function with respect to the states. In addition, it turns out in (46) that, in the position direction, the cost function varies proportional to the varying potential energy with the constant of proportionality equal to λ_e.

5.4 Residual cost

The residual cost (19) is now interpreted by aid of problem (P3). Consider an RHC approach for solving (P3) by using the objective (47) and $\psi = 0$. The real residual cost

for the objective (47) at position s, with $x = (t, e)$, is

$$J(s,x) = \min_{u\in U} \int_s^S c_u u + \beta t' \, ds \tag{48}$$

Since $\psi = 0$, (30) yields that $\lambda_t = 0$, so it follows from (39) that $J(s,x)$ is a function of s and e. Equation (39) gives that

$$\frac{\partial J}{\partial e} = \lambda_e \tag{49}$$

According to (35), $\lambda_e = -\gamma c_m$ on a singular arc and now, approximate λ_e with this constant value on constrained arcs as well, i.e., $\lambda_e \approx -\gamma c_m$. Integration of (39) with respect to e then gives

$$J(s,x) \approx -\gamma c_m e + C(s) \tag{50}$$

The integration constant $C(s)$ does not affect the optimal solution and can be omitted when choosing a residual cost ϕ. Thus, this connection to optimal control theory supports the choice of the residual cost $\phi(x) = -\gamma c_m e$ in (19). Further, the choice is justified in Hellström et al. (2010a) where it is shown that, without approximations, the real residual cost (48) is dominated by this term.

6 Quantitative study

The choice of horizon length is quantitatively studied by evaluating the suboptimality measures in Section 3.2. The full model in Section 2.1 and three different routes, with the characteristics and the abbreviations in Figure 2, are used. The maximum allowed speed is 89 km/h and β in (P2) is chosen for a cruising speed of $\hat{v} = 84$ km/h. The vehicle parameters are from the experimental setup in Hellström et al. (2009) and represent a truck with a gross weight of 40 t with a relatively small engine of 310 hp. The computation of the optimal cost functions (9) and (10) is done by value iteration (see, e.g., Bertsekas, 1995) by utilizing the algorithm development in Hellström et al. (2010a).

In Figure 3, the measure κ_J^R is shown for different horizon lengths R. It is seen that κ_J^R depends on the route but the rate of decrease, i.e., the relative benefit of increasing R, for around 1–2 km is similar. To study the effect on the fuel-time trade-off, Figure 4 shows κ_M^R versus κ_T^R for increasing R. It is observed that optimality is approached approximately along a line with negative slope. To explain this behavior, note the following relationship between the suboptimality measures obtained by combining (13)–(16):

$$0 \le \kappa_J^R (1+q) = q\kappa_M^R + \kappa_T^R, \quad q = \frac{M^S}{\beta T^S} \tag{51}$$

Now, since κ_J^R tends to zero faster than the other terms, the solution approaches the line $q\kappa_M^R + \kappa_T^R = 0$. By computing J^S in (15) for varying β, it shows that the ratio q is around 1 which explains the observed behavior. The computations also show that Equation (24) gives a good approximation when $\kappa_M^\beta, \kappa_T^\beta$ are a few percent. With a desired suboptimality d in M, it is reasonable, based on (24), to aim for

$$0 \le q\kappa_M^R + \kappa_T^R \le d \tag{52}$$

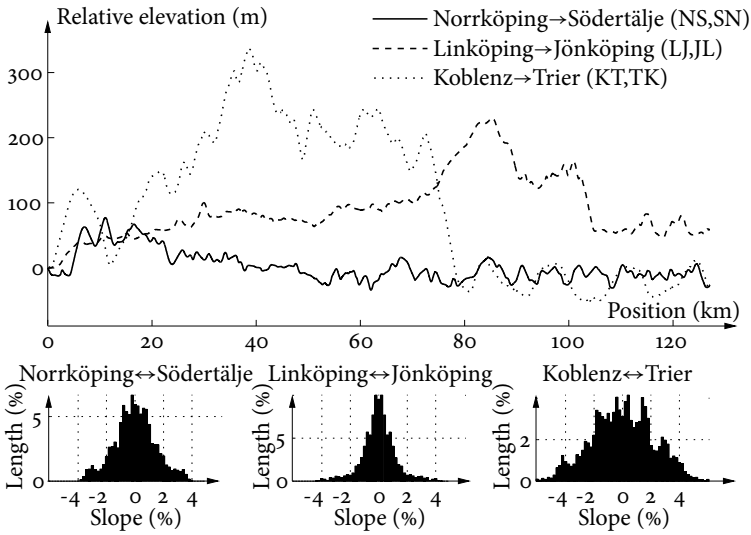

Figure 2: Elevation profiles (in one direction) and distributions of road slope values (in both directions) for two Swedish routes and one German route.

since this is close to an optimal solution with a different β. The optimal trade-off line (24) and the desired area (52) are shown in Figure 4 for $d = 0.5\%$ and q given by (22). These are used to determine horizon lengths with the appropriate compromise between fuel consumption and trip time.

The vehicle mass is now varied by repeating the computations for lower masses down to 20 t. The principle behavior in Figures 3–4 remains the same but the necessary horizon length to reach a certain degree of suboptimality decreases with decreasing mass. This effect is shown in Figure 5 where the necessary horizon length to reach the desired area (52) for q given by (22), in both directions of the respective route, is drawn as a function of vehicle mass.

7 Conclusions

Approximating the residual cost and choosing the horizon length are the two main issues in RHC, and these are addressed here for the look-ahead problem. The support for the residual cost used is strengthened by a mathematical interpretation, in terms of Lagrange multipliers, that confirms the physical intuition. The choice of horizon length is a compromise between complexity and suboptimality, and this compromise is quantified by introducing measures for suboptimality. These are combined into an optimal trade-off line that enables choosing horizon lengths with the appropriate compromise between fuel consumption and trip time. Altogether, the framework for quantitative analysis provide valuable insights into design and tuning for different road characteristics and vehicle mass.

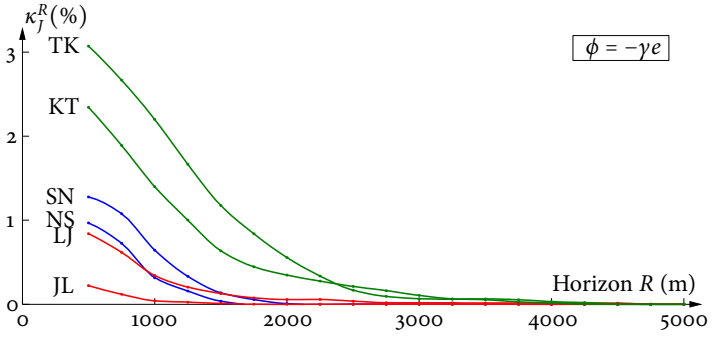

Figure 3: Suboptimality for varying horizon length.

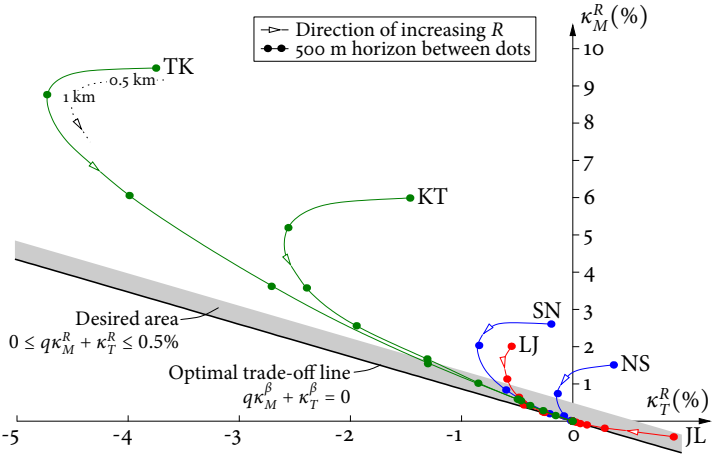

Figure 4: The suboptimality in fuel and time.

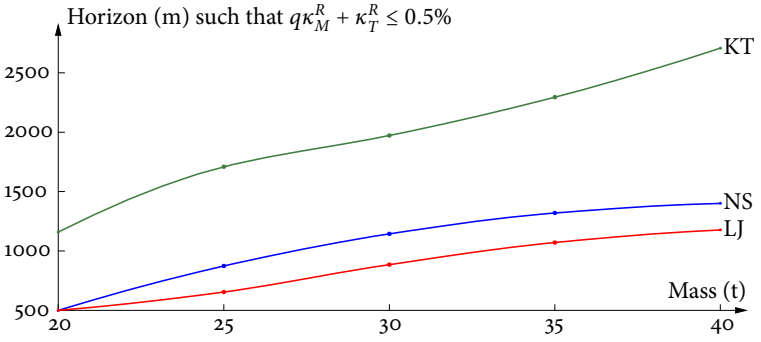

Figure 5: Required horizon to obtain (52) with $d = 0.5\%$.

References

D.P. Bertsekas. *Dynamic Programming and Optimal Control*, volume I. Athena Scientific, Belmont, Massachusetts, 1995.

A.E. Bryson and Y. Ho. *Applied Optimal Control*. Taylor and Francis, 1975.

A. Fröberg and L. Nielsen. Optimal control utilizing analytical solutions for heavy truck cruise control. Technical Report LiTH-ISY-R-2842, Department of Electrical Engineering, Linköping University, Linköping, Sweden, 2008.

L. Guzzella and A. Sciarretta. *Vehicle Propulsion Systems - Introduction to Modeling and Optimization*. Springer-Verlag, Berlin, 2005.

E. Hellström, M. Ivarsson, J. Åslund, and L. Nielsen. Look-ahead control for heavy trucks to minimize trip time and fuel consumption. In *5th IFAC Symposium on Advances in Automotive Control*, Monterey, CA, USA, 2007.

E. Hellström, M. Ivarsson, J. Åslund, and L. Nielsen. Look-ahead control for heavy trucks to minimize trip time and fuel consumption. *Control Engineering Practice*, 17(2): 245–254, 2009.

E. Hellström, J. Åslund, and L. Nielsen. Design of an efficient algorithm for fuel-optimal look-ahead control. *Control Engineering Practice*, in press, 2010a. doi: 10.1016/j.conengprac.2009.12.008.

E. Hellström, J. Åslund, and L. Nielsen. Management of kinetic and electric energy in heavy trucks. In *SAE World Congress*, number 2010-01-1314 in SAE Technical Paper Series, Detroit, MI, USA, 2010b.

W. Huang, D.M. Bevly, S. Schnick, and X. Li. Using 3D road geometry to optimize heavy truck fuel efficiency. In *11th International IEEE Conference on Intelligent Transportation Systems*, pages 334–339, 2008.

U. Kiencke and L. Nielsen. *Automotive Control Systems, For Engine, Driveline, and Vehicle*. Springer-Verlag, Berlin, 2nd edition, 2005.

D. Q. Mayne, J. B. Rawlings, C. V. Rao, and P. O. M. Scokaert. Constrained model predictive control: Stability and optimality. *Automatica*, 36(6):789–814, 2000.

G. Paganelli, T.M. Guerra, S. Delprat, J-J. Santin, M. Delhom, and E. Combes. Simulation and assessment of power control strategies for a parallel hybrid car. *Proceedings of the Institution of Mechanical Engineers – Part D – Journal of Automobile Engineering*, 214 (7):705–717, 2000.

B. Passenberg, P. Kock, and O. Stursberg. Combined time and fuel optimal driving of trucks based on a hybrid model. In *European Control Conference*, Budapest, Hungary, 2009.

A. Sciarretta, M. Back, and L. Guzzella. Optimal control of parallel hybrid electric vehicles. *IEEE Transactions on Control Systems Technology*, 12(3):352–363, 2004.

S. Terwen, M. Back, and V. Krebs. Predictive powertrain control for heavy duty trucks. In *4th IFAC Symposium on Advances in Automotive Control*, Salerno, Italy, 2004.

Paper D

Management of kinetic and electric energy in heavy trucks☆

D

☆ Updated and corrected version of paper accepted for *SAE World Congress*, 2010.

Management of kinetic and electric energy in heavy trucks

Erik Hellström, Jan Åslund, and Lars Nielsen

Linköping University, Linköping, Sweden

Abstract

Hybridization and velocity management are two important techniques for energy efficiency that mainly have been treated separately. Here they are put in a common framework that from the hybridization perspective can be seen as an extension of the equivalence factor idea in the well known strategy ECMS. From the perspective of look-ahead control, the extension is that energy can be stored not only in kinetic energy, but also electrically. The key idea is to introduce more equivalence factors in a way that enables efficient computations, but also so that the equivalence factors have a physical interpretation. The latter fact makes it easy to formulate a good residual cost to be used at the end of the look-ahead horizon. The formulation has different possible uses, but it is here applied on an evaluation of the size of the electrical system. Previous such studies, for e.g. ECMS, have typically used a driving cycle, i.e. a fixed velocity profile, but here the extra freedom to choose an optimal driving pattern is added.

1 Introduction

Hybridization allow recovery of brake energy, optimization of the energy distribution between engine and motor, and reduction of losses due to idling and clutching, and may allow downsizing of the heat engine (Guzzella and Sciarretta, 2005). These possibilities may yield better fuel economy and lower emissions despite the fact that a vehicle with a hybrid powertrain typically is heavier than with a conventional powertrain.

Another upcoming technology is look-ahead control where, with a conventional powertrain, there is a possibility to save fuel by taking information about the upcoming road topography into account. Fuel-optimal algorithms that utilize such information have lately been evaluated experimentally (Hellström et al., 2009). A system that adapts the velocity to the road topography was also recently launched by Daimler Trucks North America in collaboration with Navteq (Daimler Trucks North America press release, 2009).

Combining these two ideas in a hybrid powertrain gives extra degree of freedom in the power flows, and information about the road topography is valuable for selecting the power distribution in an optimal way. The power to mass ratio of heavy trucks leads to that significant downhills, where the vehicle accelerates without engine propulsion, and significant uphills, where the vehicle decelerates despite maximum engine power, are common on highways. Therefore the optimal control law is expected to be position-variant and, for the hybrid case, the energy management of both kinetic and electrical energy is important. These are features that distinguishes the problem from related work on passenger cars (Paganelli et al., 2000; Sciarretta et al., 2004; Back, 2006) and light-duty vehicles (Lin et al., 2003, 2004) where predefined drive cycles are used or time-invariant feedback controllers are derived from stochastic control.

The purpose of this paper is to study fuel-optimal management of kinetic and electric energy in heavy trucks traveling on open roads. The following sections present background on the scenario, the problem objective, and a model for the relevant dynamics. The potential gain in fuel economy is then investigated and it is demonstrated that simultaneous management of kinetic and electrical energy is important. After that, the fuel equivalents are recalled and used for formulating a look-ahead control scheme that efficiently solves the minimum-fuel problem. Finally, powertrains with different sizes of the electrical system are compared to a conventional powertrain by computing the optimal solution.

2 Background

For heavy trucks up to class 7, hybridization has been identified as a technology that could improve fuel economy substantially (Bradley, 2000; An et al., 2000; Vyas et al., 2003). The ideal candidates are vehicles mainly operating in urban areas with stop-and-go conditions, such as transit buses and delivery trucks. For these applications, e.g., engine downsizing and regenerative braking are expected to yield good results.

For the heavy trucks in class 8, weighing more than 15 tonnes, there is less room for improvement. These trucks typically travels on open road at operating points with

high efficiency and significant downsizing requires heavy electrical motors due to the high power requirements (Bradley, 2000; An et al., 2000). On the other hand, they are a large consumer of fuel, e.g., in the U.S. class 8 trucks consume about 68% of all commercial truck fuel used, and 70% of this amount is spent traveling on open road with a trip length of more than 100 miles (Bradley, 2000). Thus, any technology that improves truck efficiency will have the best benefit for this class. The first targets for class 8 trucks are applications where the drive pattern yields an expected good utilization of the hybridization, such as regional delivery or drayage applications (HTUF DiaLog, #09-01). When such hybrid powertrains matures, long-haul applications are further developments.

3 Objective

To achieve cost reductions, the objective is to minimize the fuel mass M required for a drive mission with a given maximum trip time T_0:

$$\begin{aligned} &\text{minimize } M \\ &\text{subject to } T \leq T_0 \end{aligned} \tag{P1}$$

The control inputs are the torques from the combustion engine and from the electrical motor, respectively, together with the brakes, and the gear shifts. The control signals are fueling u_e, electrical motor voltage u_m, brake torque u_r, and gear selection u_g. The road slope is a function of position, and it is therefore natural to use spatial coordinates. A model may then have, e.g., velocity and state of charge as states. A straightforward way to handle the trip time constraint is to include time as an additional state.

4 Truck model

A model for the dynamics of a hybrid electrical truck is formulated (Kiencke and Nielsen, 2005; Guzzella and Sciarretta, 2005). For the longitudinal motion, kinetic energy is used as state. This has been shown to be beneficial in the case of a conventional powertrain since it allows for simple integration and linear interpolation on coarse grids (Hellström et al., 2010). It is later shown that this formulation is suitable for a hybrid powertrain as well.

4.1 Longitudinal motion

The prime movers are a combustion engine and an electrical motor. The torques from the engine T_e and the motor T_m torque are given by

$$T_e = f_e(\omega, u_e), \quad T_m = f_m(\omega, u_m) \tag{1}$$

where ω is the rotational speed, u_e is the engine fueling, u_m is the motor voltage, f_e is a lookup table originating from measurements, and f_m is specified below. The torque

Table 1: Longitudinal forces.

Force	Explanation	Expression
F_a	Air resistance	$\frac{1}{2}c_w A_a \rho_a v^2$
F_r	Rolling resistance	$mgc_r \cos\alpha$
F_g	Gravitational force	$mg \sin\alpha$

from the engine and motor is assumed to be combined between the crankshaft and the transmission by direct coupling. The torque at the flywheel is then

$$T_t = T_e + T_m \tag{2}$$

The components of the driveline, such as propeller shafts and drive shafts, are assumed stiff and no clutches are modeled. The combined conversion ratio of the transmission and final drive, denoted by i, and their efficiency, denoted by η, are functions of the gear number u_g. The models of the resisting forces are given in Table 1.

Use the relation $v = \frac{r_w}{i}\omega$ where r_w is the effective wheel radius and the mass factor

$$c_m = 1 + \frac{i^2\eta I_1 + I_2}{mr_w^2}$$

where I_1, I_2 are lumped inertia before and after the transmission respectively. The dynamics for the velocity v is then

$$\frac{dv}{dt} = \frac{1}{c_m m}\left(\frac{i\eta}{r_w}T_t - \frac{u_r}{r_w} - \left(F_a + F_r + F_g\right)\right) \tag{3}$$

where all model parameters are explained in Table 2. By introducing kinetic energy $e = \frac{1}{2}mv^2$ and noting that $\frac{de}{ds} = mv\frac{dv}{ds} = m\frac{dv}{dt}$ where s is position, the model is finally written as

$$c_m\frac{de}{ds} = \frac{i\eta}{r_w}T_t - \frac{u_r}{r_w} - \left(F_a + F_r + F_g\right) \tag{4}$$

4.2 Buffer dynamics

The amount of energy in the electrical buffer is denoted by b. The dynamics is governed by the power P_b, and the convention is that when P_b is positive, energy flows from the

Table 2: Truck model parameters.

$I_{1,2}$	Lumped inertia	c_w	Air res. coefficient
m	Vehicle mass	A_a	Cross section area
r_w	Wheel radius	ρ_a	Air density
g	Gravity constant	c_r	Rolling res. coeff.

buffer, and energy is stored in the buffer when P_b is negative. The dynamics becomes

$$\frac{db}{dt} = v\frac{db}{ds} = -P_b \tag{5}$$

The power P_b equals the motor power. Thus

$$\eta_m P_b = \omega T_m \tag{6}$$

where η_m is the motor efficiency that is less than unity when P_b is positive and larger than unity when P_b is negative.

An electrochemical battery is used as the buffer in the evaluation later on. The battery is modeled by an internal resistance model (Johnson, 2002). This is an equivalent circuit that consists of a voltage source, with open-circuit voltage U_{oc}, in series with a resistor with resistance R_i. The battery voltage U is

$$U = U_{oc} - R_i I_b \tag{7}$$

where the current I_b is determined by

$$I_b = \frac{1}{2R_i}\left(U_{oc} - \sqrt{U_{oc}^2 - 4R_i P_b}\right) \tag{8}$$

The battery voltage is limited to an interval $U \in [U_{\min}, U_{\max}]$ which yields limits for the maximum current and power for discharging and charging respectively.

4.3 Fuel consumption

The mass flow of fuel $\dot{m}$ is determined by the fueling level u_e and the engine speed ω,

$$\dot{m} = \frac{n_{cyl}}{2\pi n_r}\omega u_e = \frac{n_{cyl}}{2\pi n_r}\frac{i}{r_w} v u_e \tag{9}$$

where n_{cyl} is the number of cylinders and n_r is the number of engine revolutions per cycle. The consumed fuel mass per unit distance is $\dot{m}/v$.

5 Recovering brake energy

The fuel economy can be improved by reducing the brake energy. A preliminary analysis is made to investigate the potential gain and the requirements on a storage system in terms of energy, power, and efficiency. It is demonstrated that, with an additional energy buffer, management of both kinetic and buffer energy is important.

The scenario considered is highway driving on open road where braking typically is required for limiting the speed with respect to legal and safety requirements. Figure 1 shows two routes from Sweden and one from Germany. From the elevation profile and road slope distribution it is seen that these routes have different characteristics, and this leads to different usage of the brakes.

The numerical results in this section are obtained with a 360 hp conventional powertrain controlled by a cruise controller (CC), and a gross weight of 40 tonnes.

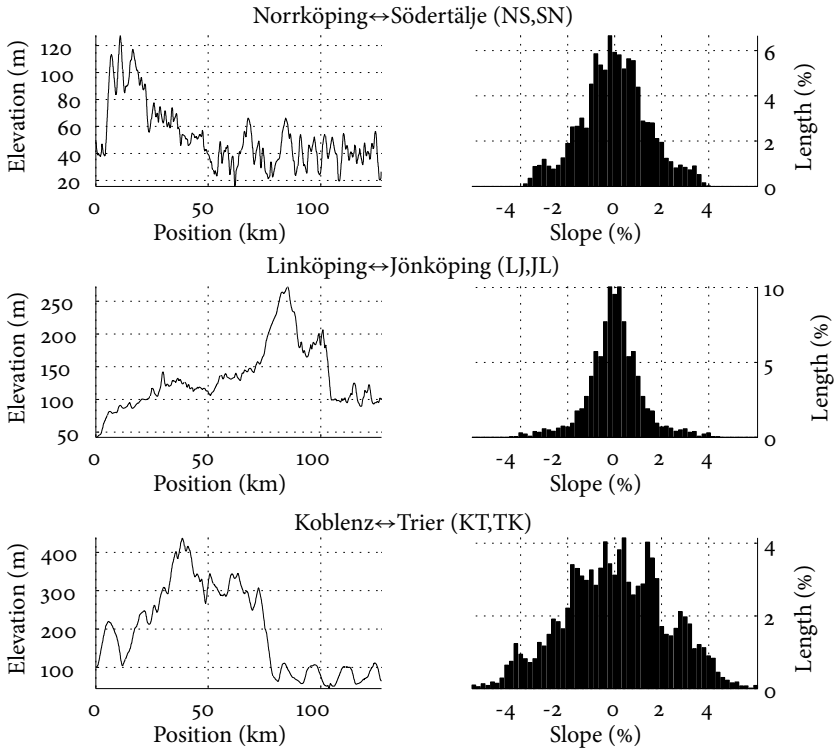

Figure 1: Elevation profile (in one direction) and distribution of road slope values (in both directions) for three different routes.

5.1 Potential gain

In Figure 2 the energy requirements for traveling the routes in Figure 1 back and forth are shown. The set speed is 80 km/h and the extra speed allowed in downhills is varied along the horizontal axis. The percentages of brake energy in relation to the total propulsive energy show the maximum gain in fuel economy with reduced braking. The values differ much and have the intuitively negative correlation with the extra speed allowed in downhills.

5.2 Brake power

The required brake power for a certain speed for a given slope is given by the forces in Table 1. A 40 ton truck in a 2% downhill requires about 70 kW brake power to keep 90 km/h and 260 kW in a 4% downhill. The distribution of the brake power for traveling the routes in Figure 1 back and forth are shown in Figure 3. The set speed is 84 km/h with 5 km/h extra speed allowed in downhills.

A generator covering the power range in Figure 3 would weigh several hundred

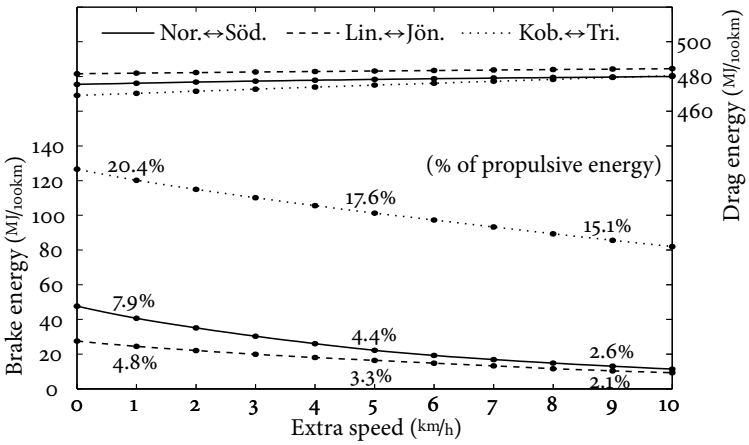

Figure 2: Energy consumed by drag and brake forces with CC and different values for the extra speed allowed in downhills.

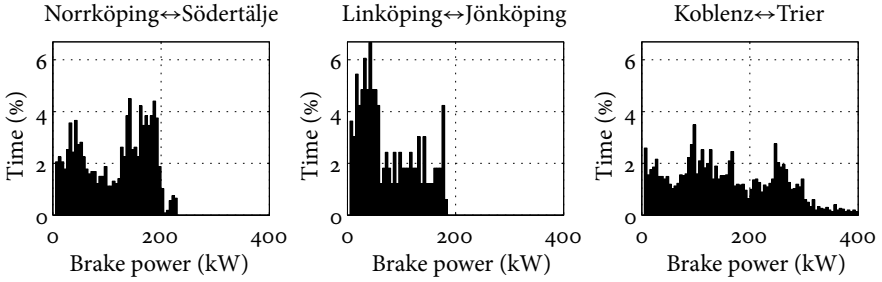

Figure 3: Distribution of brake power for three routes.

kilograms considering a reasonable specific power. There are also constraints, depending on the placement, that limit the physical size of the motor. However, any size of the generator is useful for reducing the energy wasted in braking, the question is if it is beneficial for reducing the fuel consumption despite the additional mass.

5.3 Storage system

Reducing the brake energy on highways can be achieved by using kinetic energy as a buffer or adding a device for regenerative braking. Utilizing kinetic energy requires that there is an interval in which the velocity is allowed to vary and some energy is lost due to increased air resistance. Devices for recovering energy may be of different types such as electrochemical or electrostatic. Losses occur when charging and discharging the buffer, and the mass of the device will increase the rolling resistance.

A 40 ton truck in a 2% downhill requires, per kilometer, about 0.78 kWh brake energy to keep 90 km/h and 2.9 kWh in a 4% downhill. This corresponds to the capacity of a

3.9 kWh and 14.4 kWh battery respectively with a 20% usable charge range. A significant amount of energy can also be stored as kinetic energy. With the same numbers as above, a velocity interval 80 ± 5 km/h correspond to a buffer of about 0.7 kWh which is equivalent to the capacity of a 3.5 kWh battery.

Efficiency

Utilizing kinetic energy as a buffer is, intuitively, more efficient than a device for regenerative braking. Here, a simplified analysis is done to compare these strategies quantitatively. Consider a road segment of length L_1, with sufficiently steep slope α for the vehicle to accelerate without engine propulsion and assume that $T_e = 0$ and $\cos\alpha \approx 1$.

Assume that the recovering device is capable of absorbing the sufficient amount of energy ΔW in order to keep constant kinetic energy e_0. With the drag forces $F_d(e) \approx F_r + F_a$, the amount becomes

$$\Delta W = (F_g(\alpha) + F_d(e_0))L_1 \tag{10}$$

which is a negative quantity in a steep downhill. The stored energy is $-\eta_s \Delta W$ where η_s is the storage efficiency. Given that the efficiency is equal when discharging, then $-\eta_s^2 \Delta W$ is the amount of energy that can be used in the future. If this energy is used to overcome the driving resistance on a level road, then

$$-\eta_s^2 \Delta W = F_d(e_0)L_2 \tag{11}$$

holds where L_2 is the length of level road.

Now, consider the case of using kinetic energy as buffer instead. For this case, the model (4) can be written as

$$e'(s) = c_1 - c_2 e(s) \tag{12}$$

where $c_1 = -\frac{mg}{c_m}(c_r + \sin\alpha)$, $c_2 = \frac{c_w A_a \rho_a}{c_m m}$. The solution for (12) yields that the kinetic energy in the end of the downhill is

$$e_1 = e(L_1) = \frac{c_1}{c_2} + (e_0 - \frac{c_1}{c_2})\exp(-c_2 L_1) \tag{13}$$

and that after the distance L_3 on the level road where

$$L_3 = \frac{1}{c_2}\log\frac{c_1 - c_2 e_1}{c_1 - c_2 e_0} \tag{14}$$

the initial kinetic energy e_0 is reached. Thus, the stored kinetic energy can be used overcome the driving resistance for the distance L_3 on level road.

The two strategies can now be compared by requiring that the vehicle should travel the same distance, i.e., $L_2 = L_3$. Solving (10) and (11) for the efficiency gives

$$\eta_s^2 = \frac{1}{-\frac{F_g(\alpha)}{F_d(e_0)} - 1}\frac{L_3}{L_1} \tag{15}$$

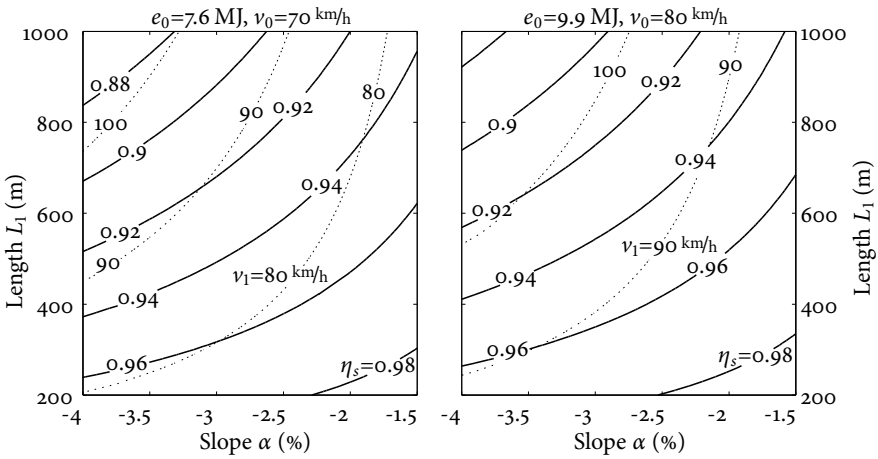

Figure 4: The device efficiency η_s (solid lines) and the speed v_1 (km/h) at the end of the hill (dashed lines).

where L_3 is given by (14). Equation (15) indicates the required efficiency for the two strategies to be equally efficient. Figure 4 shows η_s as a function of the downhill slope α and length L_1 for two different initial conditions e_0. The velocity v_1 corresponding to the kinetic energy e_1 at the end of the hill is also shown. Typical parameters of a truck with a gross weight of 40 tonnes have been used.

A realistic value of η_s^2 for a recovery device is about 60% (Guzzella and Sciarretta, 2005), so $\eta_s \approx 77\%$ which is lower than η_s in Figure 4. Note also that the additional mass of a device is not taken into account nor the fact that allowing a higher speed yields a shorter trip time. However, when the allowed velocity interval is not sufficient to absorb all energy there are possibilities to recover energy with a device. Examples are in longer or steeper downhills where the velocity must be limited for safety or legal reasons. For a fuel-optimal solution, the simultaneous management of kinetic and buffer energy is thus important.

6 Look-ahead control

Look-ahead control is a method where future conditions are known, here focusing on the road topography ahead of the vehicle. The minimum-fuel solution, given the information about the future, is found through dynamic programming (DP) (Bellman and Dreyfus, 1962; Bertsekas, 1995).

6.1 DP algorithm

The models (4)–(5) are first discretized in order to obtain a discrete process model

$$x_{k+1} = F_k(x_k, u_k)$$

where x_k, u_k denotes the state and control vectors of dimension two (e, b) and four (u_e, u_m, u_r, u_g) respectively. The drive mission is divided into M steps and the problem is to find

$$J_0^*(x_0) = \min_{u_0,\ldots,u_{M-1}} \zeta_M(x_M) + \sum_{k=0}^{M-1} \zeta_k(x_k, u_k) \tag{16}$$

where ζ_k and ζ_M defines the running cost and the terminal cost respectively. The running cost $\zeta_k(x_k, u_k)$ is defined by (P2) in Section 7.3. The terminal cost $\zeta_M(x_N)$ is treated in the following by introducing a residual cost.

By introducing an approximate residual cost, (16) is transformed into a problem over a shorter look-ahead horizon of $N < M$ steps. Rewrite Equation (16) as

$$\min_{u_0,\cdots,u_{N-1}} J_N^*(x_N) + \sum_{k=0}^{N-1} \zeta_k(x_k, u_k) \tag{17}$$

where the residual cost at stage N,

$$J_N^*(x_N) = \min_{u_N,\ldots,u_{M-1}} \zeta_M(x_M) + \sum_{k=N}^{M-1} \zeta_k(x_k, u_k) \tag{18}$$

is replaced with an approximation $\tilde{J}_N^*(x_N)$, see (26).

The DP solution for this problem is to solve the functional equation

$$J_k(x_k) = \min_{u_k} \{\zeta_k(x_k, u_k) + J_{k+1}(F_k(x_k, u_k))\} \tag{19}$$

for $k = N-1, N-2, \ldots, 0$ starting from

$$J_N(x_N) = \tilde{J}_N^*(x_N) \tag{20}$$

being the terminal cost. When finished, $J_0^*(x_0) = J_0(x_0)$ is the minimum cost.

When evaluating $J_{k+1}(F_k(x_k, u_k))$ in (19), interpolation is generally needed and bilinear interpolation is used for this purpose. It is shown in Section 9 that this is an appropriate method.

7 Fuel equivalents

To facilitate an efficient solution of (P1) fuel equivalents are introduced. These relates, approximately, a change in each of the degrees of freedom to a change in the criterion, that is the fuel mass. The degrees of freedom are time, kinetic energy, and buffer energy.

The time equivalent is used to reformulate the problem (P1) into a problem of lower dimension. The other equivalents are later combined into a residual cost that depends on the states, i.e., kinetic energy and state of charge. The equivalence between fuel and kinetic energy was used in Hellström et al. (2010). The equivalence factors between fuel and charge are, e.g., used in the well known ECMS-type of control strategies (Paganelli et al., 2000; Sciarretta and Guzzella, 2007).

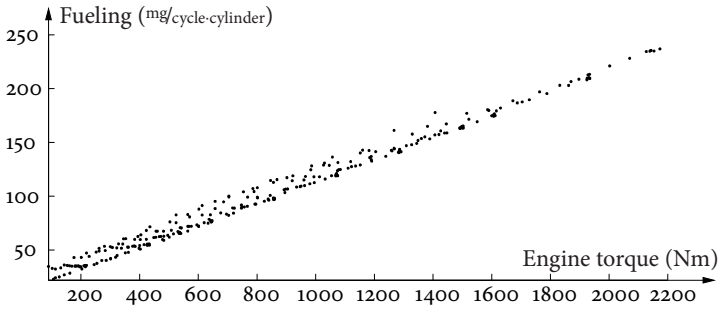

Figure 5: The relation between fueling and engine torque for a diesel engine.

7.1 Kinetic energy

Measurements of the relation between engine torque and injected fuel mass per cycle and cylinder, for a diesel engine with typical characteristics, are shown in Figure 5. As can be seen, this function is approximately an affine function and using the method of least squares, the gradient can be calculated. By multiplying the quantities by the scaling factors $2\pi n_r$ and n_{cyl}, respectively, the relation between work per cycle delivered to the transmission and total fuel mass per cycle is obtained. The gradient of the scaled function is denoted by γ (g/J), and it indicates how much additional fuel ΔM is needed, approximately, in order to deliver a given amount of work ΔW, i.e.,

$$\Delta M \approx \gamma \Delta W \tag{21}$$

For a given increase of the kinetic energy Δe, the additional fuel required is

$$\Delta M \approx \frac{\gamma}{\eta} \Delta e \tag{22}$$

where η is the driveline efficiency.

The value of γ can be interpreted as the inverse of the product of the indicated engine efficiency and the fuel heating value. The approximation (21) is then the so called Willans description (Guzzella and Sciarretta, 2005).

7.2 Buffer energy

Denote the efficiency of the electrical energy path η_b. Consider a given change Δb of the energy level in the buffer. The energy $\eta_b \Delta b$ is then delivered to the transmission if discharging or the energy $\Delta b/\eta_b$ is consumed if charging. The equivalence between fuel and buffer energy is now obtained by combining this with (21) which yields

$$\Delta M \approx \begin{cases} \gamma \eta_b \Delta b & \text{if discharging} \\ \frac{\gamma}{\eta_b} \Delta b & \text{if charging} \end{cases} \tag{23}$$

For example, consider a battery as the buffer. Then η_b includes the efficiency of the motor and for discharging and charging the battery. A given change in the state of charge Δq yields that the energy delivered or absorbed is

$$\Delta b = UQ_0\Delta q \approx U_{oc}Q_0\Delta q \tag{24}$$

7.3 Time

The objective is to minimize the fuel mass on a drive mission with a given trip time as stated in (P1). Now consider adjoining the trip time to the criterion in (P1) yielding

$$\text{minimize } M + \beta T \tag{P2}$$

where β is a scalar representing the trade-off between fuel consumption and trip time. With this alternative formulation, it is no longer necessary to introduce time as a state. Thus the problem (P2) has a lower dimension than (P1). However, there is an additional issue tuning the parameter β.

The solution for (P2) gives a trip time $T(\beta)$. An approximate value of β can be found by considering a vehicle traveling at the speed v for the length Δs on level road. The criterion in (P2) is $J(v) = \Delta M + \beta\Delta T$ where $\Delta T = \frac{\Delta s}{v}$ and, by using (21),

$$\Delta M = \gamma\Delta W = \frac{\gamma}{\eta}F(v)\Delta s$$

where $F(v) = F_a(v) + F_r + F_g$ is the sum of the resisting forces in Table 1. In a stationary point $J'(v) = 0$, it holds that $\beta = \frac{\gamma}{\eta}v^2F'(v)$ and thus

$$\beta = 2\frac{\gamma}{\eta}P_a(v) \tag{25}$$

where $P_a(v) = vF_a(v)$ is the power required to resist the air drag. With this value $J''(v)$ is positive for all physically feasible parameters which shows that (25) gives a minimum for this stationary case.

8 Residual cost

An approximation of the residual cost (18) makes it possible to solve the optimization problem over a truncated horizon, see Section 6.1. The basic idea in the approximation is that it is assumed that kinetic energy and buffer energy can be calculated to an equivalent fuel energy and conversely, at the final stage N of the horizon, using (22) and (23). This reflects that energy at the end of the horizon can be used to save fuel in the future.

For the buffer it must be decided whether discharging or charging should be considered since the fuel equivalent in (23) are different in these cases. If the energy level b at the end of the horizon is less than a desired value, denoted by b_0, the cost should reflect the fuel required for charging the amount $b_0 - b$. Conversely, if b is larger than b_0

the cost should be the fuel equivalent for discharging $b - b_0$. Using (22) and (23), the residual cost becomes

$$\tilde{J}_N^*(x_N) = C - \frac{\gamma}{\eta} e - \begin{cases} \frac{\gamma}{\eta_b} b & b < b_0 \\ \gamma \eta_b b + D & b \geq b_0 \end{cases} \tag{26}$$

where C, D are constants. The crucial issue for the residual cost is that the relative cost between different states is approximated well. Therefore, C can be omitted and D is selected so that (26) is continuous which will allow interpolation between the linear segments for charging and discharging.

When considering a battery, the residual cost may be expressed with the battery state of charge q by using (24):

$$\tilde{J}_N^*(x_N) = -\frac{\gamma}{\eta} e - \begin{cases} \frac{\gamma}{\eta_b} U_{oc} Q_0 q & q < q_0 \\ \gamma \eta_b U_{oc} Q_0 q + D & q \geq q_0 \end{cases} \tag{27}$$

where q_0 denotes the desired state of charge at the end of the horizon.

A simple approach to determine the efficiencies of the electrical path is to assign them a constant value based on, e.g., the average efficiency for a drive mission. For ECMS, the charge equivalence factor for a mission has also been determined without explicit assumptions about the efficiencies by simulating the model with different control trajectories in a systematic way, see Sciarretta et al. (2004). These factors are key parameters in ECMS since they are used as approximations for the adjoint variable in order to determine the optimal control. Errors may, e.g., lead to excessive violations of constraints on the state of charge (Guzzella and Sciarretta, 2005). The DP algorithm is not as sensitive as ECMS to the approximation since the factors are used only for the residual cost at the end of the horizon although the sensitivity certainly increases with shorter horizon lengths. In the following section, it is shown that assuming constant efficiencies yields a reasonable approximation for the value function.

9 Interpolation and discretization

A numerical example is presented to gain insight into features of the problem for typical parameters. The second hybrid system in Table 3 is used and the road segment comes from measurements of the route from Norrköping to Södertälje, see Figure 6.

Figure 7 shows the value function $J(s, e, b)$, for a given kinetic energy e, every 500 m as a function of the electrical energy b. In Figure 8, the value function is shown for a given electrical energy b as a function of the kinetic energy e. The characteristics in these figures are observed for other e and b as well. The cost at s=6 km is the residual cost (27). It can be seen that the form of the value function is approximately maintained throughout the horizon and that it is dominated by the piece-wise linear residual cost function. The distance between the lines is smaller in the downhill segments than in the uphill segments, e.g, around 2 and 3 km. The switching point between the linear segments in Figure 7 is for the position 6 km placed at b equal to 50% state of charge, but occurs for different b at other positions.

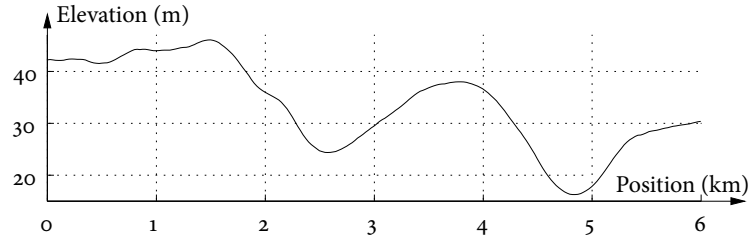

Figure 6: Road segment.

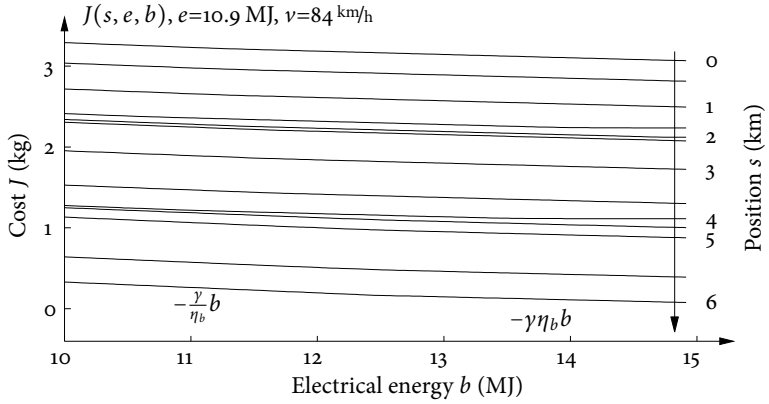

Figure 7: The value function for different positions, for a given value of kinetic energy, as a function of the electrical energy.

In order to get similar resolution of the value function in e and q, it is natural to select a discretization resolution in energy for the grid. The number of grid points in the respective state will then vary with the allowed sets for the kinetic energy and electrical energy for a given position.

The value function $J(s, e, q)$ at a given position s is dominated by a piece-wise linear function in e and q. For the optimal solution, it is the deviations from this function that are important. Since the errors from bilinear interpolation are zero on the dominating linear parts, except for close to the switching point, a rather coarse discretization grid can be used together with interpolation.

The look-ahead control scheme consists of the described DP algorithm utilizing the fuel equivalents and residual cost that are introduced above. The algorithm is feasible to run on an ordinary computer mainly due to the fact that the formulation makes it possible to use a coarse grid and linear interpolation.

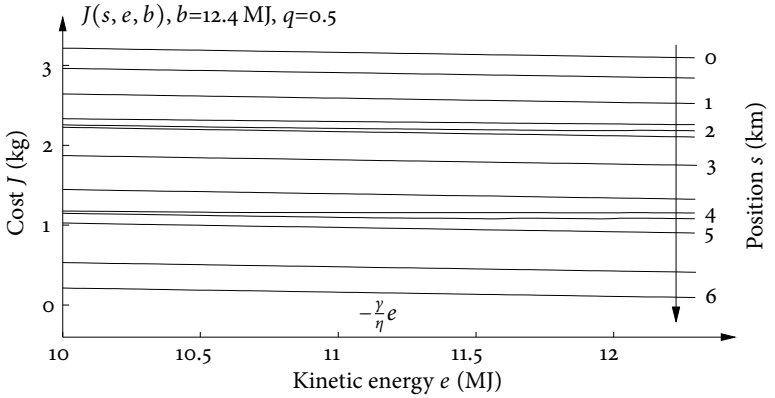

Figure 8: The value function for different positions, for a given value of electrical energy, as a function of the kinetic energy.

10 Design study

A study is carried out where different powertrain designs are compared by computing the minimum-fuel solution.

10.1 Designs

Data on four Euro 5 diesel engines and other vehicle parameters were provided by Scania. The maximum power of the engines ranges from 320 hp to 440 hp in 40 hp steps. The 320 hp engine is an inline 5-cylinder 9-litre engine and the others are inline 6-cylinder 13-litre engines.

The configurations are one conventional powertrain with look-ahead control (LC) using only kinetic energy as a buffer, and three parallel hybrid powertrains (HLC1, HLC2, HLC3) with increasing degree of hybridization. The 320 hp engine is used in all of these configurations. The hybrids have a motor with maximum power of 40, 80, and 120 hp respectively. The main characteristics of the electrical configurations are given in Table 3. The basic assumptions for these are the following. The battery has a specific power of 1 kW/kg and a specific energy 0.1 kWh/kg at cell level. At pack level these values are reduced by a factor of 2. The motor has an average efficiency of 85% and a continuous power rating with a specific power of 0.7 kW/kg. This corresponds to, e.g., a reasonable motor and high-power lithium-ion battery targeted for hybrid electric vehicles (Stewart et al., 2008; Guzzella and Sciarretta, 2005). These configurations yield a degree of hybridization (the ratio between motor and engine power) that ranges from 13% to 38%.

The characteristics of the motor is modeled by a constant efficiency and an ideal power profile that is parametrized by maximum power P_m and the speed ω where maximum torque and power are delivered, see Figure 9. The characteristics are symmetrical in generator mode.

Table 3: Three hybrid system configurations.

Design	Battery power (kW)	energy (kWh)	Motor power (kW)	Total mass (kg)
HLC1	35	3.5	29.4	111
HLC2	69	6.9	58.8	223
HLC3	104	10.4	88.3	334

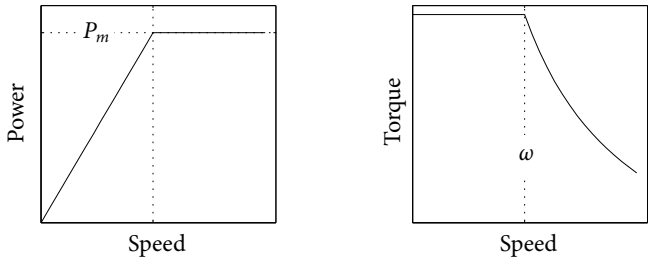

Figure 9: Ideal motor characteristics.

10.2 Baseline controller

The four designs are compared to a vehicle with a conventional powertrain controlled by a cruise controller (CC) without look-ahead. The comparison is made between powertrains with the same maximum power, e.g., HLC1 is compared to a conventional 360 hp powertrain controlled by CC.

The CC determines fueling, braking levels through inversion of the system, see, e.g., Fröberg and Nielsen (2008). The set speed determines the fueling level and the brakes are applied when reaching the set speed plus the extra speed allowed. Gears are selected based on engine speed and load.

10.3 Results

The DP algorithm is applied back and forth on the three routes seen in Figure 1. The algorithm parameters are constant for all runs. The allowed velocity interval is $[79,89]^{\text{km/h}}$ where the lower limit is extended when it is not reachable. The allowed state of charge interval is [40,60]%. The parameter β is selected for a cruising speed of approximately 84 $^{\text{km/h}}$ on level road through (25). The vehicle mass for the LC configuration is 40 tonnes, and for HLC the mass in Table 3 is added. For CC an extra mass of 110 kg is added when the larger 6-cylinder engines are used. The CC set speed is about 84 $^{\text{km/h}}$ and the brakes are applied when the speed reaches 5 $^{\text{km/h}}$ above the set speed.

The CC set speed is adjusted to make the time difference small in order to make a fair comparison of the fuel consumption. It is noted, for all of the hybrid designs on all routes, that the corresponding conventional truck has comparable trip time with lower cruising speed. This is due to the limited capacity of the battery and the additional mass

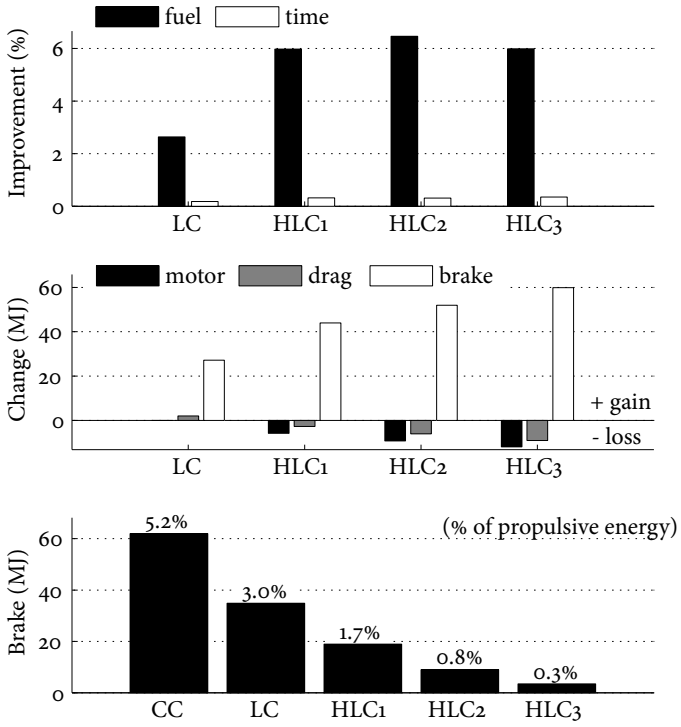

Figure 10: The Norrköping–Södertälje route.

for the hybrid truck. The consequence is added air resistance, and this effect amplifies with the size of the electrical system. The added rolling resistance, due to the extra mass, further increases the additional drag forces for the hybrid designs.

The results from the road between Norrköping and Södertälje are shown in Figure 10. The LC reduces the brake energy with a large amount. When adding a hybrid system the amount of brake energy is further reduced but this is counteracted by losses in the motor and increased drag. In total, the fuel economy is improved and the largest gain is achieved with HLC2. Similar results show on the road between Linköping and Jönköping, see Figure 11.

The results from the road between Koblenz and Trier, see Figure 12, have different characteristics. Comparing the setups from left to right in the figure, fuel consumption is reduced when adding all hybrid systems. Furthermore, there is a significant amount of energy spent on braking even with the largest HLC3 configuration.

10.4 Discussion

Different characteristics of the optimal solution appear for the various designs. These differences are connected to the characteristics of the road topography since they influ-

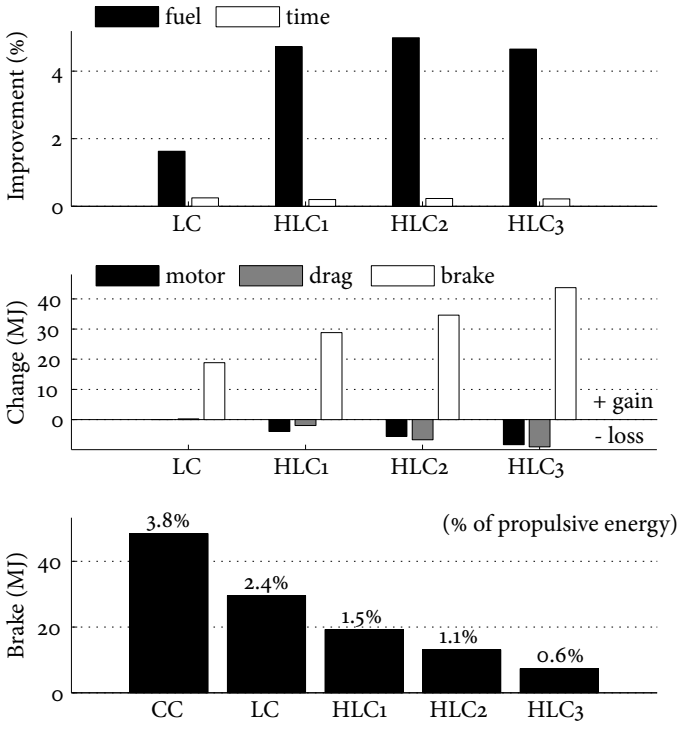

Figure 11: The Linköping–Jönköping route.

ence the brake usage. To utilize most of the brake energy, the buffers of kinetic energy and electrical energy must have sufficient capacity.

Considering the designs studied here, the buffers show to be sufficient for the routes in Figure 10 and 11. The third route, between Koblenz and Trier, has noticeably different characteristics than the two other routes studied, as can be seen in Figure 1 and 2. The route has larger elevation variations, more steep slopes, and the amount of brake energy is considerably larger than the other two routes. The gain from more hybridization is increasing but the relative gain decreases.

In general, there are many factors for the design of a hybrid system like operating conditions such as start-and-stop. From the long haulage perspective, however, it seems that a rather modest hybrid system achieves most of the gain.

11 Conclusions

The potential gains in fuel economy for a heavy truck by reducing brake energy on open roads are significant and dependent on the characteristics of the road topography. A hybrid system can recover brake energy, and for such a truck the simultaneous management of kinetic and electrical energy is important. The reason is that if the velocity is

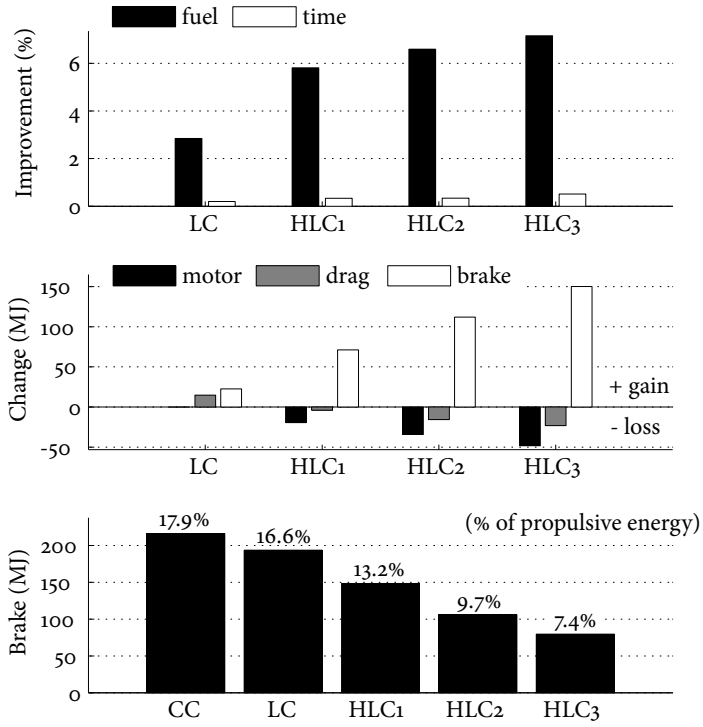

Figure 12: The Koblenz–Trier route.

allowed to vary, even within a narrow interval, kinetic energy becomes an energy buffer of considerable size due to the large mass of a truck. Further, utilizing kinetic energy is an efficient way of short-term energy storage.

It shows that the formulation for an efficient look-ahead algorithm, previously used for management of kinetic energy, works well in the extended framework including management of electrical energy. The study of different powertrain designs reveals that fuel economy is improved by look-ahead control with a conventional powertrain, and that a hybrid powertrain may yield additional improvements. With a hybrid system further reductions of the brake energy are possible but these are counteracted by losses in the motor and increased drag. It is shown how the optimal trade-off between size and capacity depend on the road characteristics, and also that a modestly sized electrical system achieves most of the gain.

References

F. An, F. Stodolsky, A. Vyas, R. Cuenca, and J.J. Eberhardt. Scenario analysis of hybrid class 3-7 heavy vehicles. In *SAE World Congress*, number 2000-01-0989 in SAE Technical Paper Series, 2000.

M. Back. *Prädiktive Antriebsregelung zum energieoptimalen Betrieb von Hybridfahrzeugen*. PhD thesis, Universität Karlsruhe, Karlsruhe, Germany, 2006.

R.E. Bellman and S.E. Dreyfus. *Applied Dynamic Programming*. Princeton University Press, Princeton, New Jersey, 1962.

D.P. Bertsekas. *Dynamic Programming and Optimal Control*, volume I. Athena Scientific, Belmont, Massachusetts, 1995.

R. Bradley. Technology roadmap for the 21st century truck program. Technical Report 21CT-001, U.S. Department of Energy, December 2000.

Daimler Trucks North America press release, 2009. Freightliner Trucks Launches RunSmart Predictive Cruise for Cascadia. http://daimler-trucksnorthamerica.com/, March 19, 2009.

A. Fröberg and L. Nielsen. Efficient drive cycle simulation. *IEEE Transactions on Vehicular Technology*, 57(2), 2008.

L. Guzzella and A. Sciarretta. *Vehicle Propulsion Systems - Introduction to Modeling and Optimization*. Springer-Verlag, Berlin, 2005.

E. Hellström, M. Ivarsson, J. Åslund, and L. Nielsen. Look-ahead control for heavy trucks to minimize trip time and fuel consumption. *Control Engineering Practice*, 17(2): 245–254, 2009.

E. Hellström, J. Åslund, and L. Nielsen. Design of an efficient algorithm for fuel-optimal look-ahead control. *Control Engineering Practice*, in press, 2010. doi: 10.1016/j.conengprac.2009.12.008.

HTUF DiaLog, #09-01. Hybrid Truck Users Forum DiaLog. http://www.htuf.org/, February 2009.

V.H. Johnson. Battery performance models in ADVISOR. *Journal of Power Sources*, 110:321–329, 2002.

U. Kiencke and L. Nielsen. *Automotive Control Systems, For Engine, Driveline, and Vehicle*. Springer-Verlag, Berlin, 2nd edition, 2005.

C. Lin, H. Peng, J.W. Grizzle, and J. Kang. Power management strategy for a parallel hybrid electric truck. *Control Systems Technology, IEEE Transactions on*, 11(6):839–849, 2003.

C. Lin, H. Peng, and J.W. Grizzle. A stochastic control strategy for hybrid electric vehicles. In *American Control Conference*, volume 5, pages 4710–4715, 2004.

G. Paganelli, T.M. Guerra, S. Delprat, J-J. Santin, M. Delhom, and E. Combes. Simulation and assessment of power control strategies for a parallel hybrid car. *Proceedings of the Institution of Mechanical Engineers – Part D – Journal of Automobile Engineering*, 214 (7):705–717, 2000.

A. Sciarretta and L. Guzzella. Control of hybrid electric vehicles. *IEEE Control Systems Magazine*, 27(2):60–70, 2007.

A. Sciarretta, M. Back, and L. Guzzella. Optimal control of parallel hybrid electric vehicles. *IEEE Transactions on Control Systems Technology*, 12(3):352–363, 2004.

S.G. Stewart, V. Srinivasan, and J. Newman. Modeling the performance of lithium-ion batteries and capacitors during hybrid-electric-vehicle operation. *Journal of The Electrochemical Society*, 155(9):A664–A671, 2008.

A. Vyas, C. Saricks, and F. Stodolsky. The potential effect of future energy-efficiency and emissions-improving technologies on fuel consumption of heavy trucks. Technical Report ANL/ESD/02-4, Argonne National Lab., March 2003.

Linköping studies in science and technology, Dissertations
Division of Vehicular Systems
Department of Electrical Engineering
Linköping University

No 1 Magnus Pettersson, *Driveline Modeling and Control*, 1997.

No 2 Lars Eriksson, *Spark Advance Modeling and Control*, 1999.

No 3 Mattias Nyberg, *Model Based Fault Diagnosis: Methods, Theory, and Automotive Engine Applications*, 1999.

No 4 Erik Frisk, *Residual Generation for Fault Diagnosis*, 2001.

No 5 Per Andersson, *Air Charge Estimation in Turbocharged Spark Ignition Engines*, 2005.

No 6 Mattias Krysander, *Design and Analysis of Diagnosis Systems Using Structural Methods*, 2006.

No 7 Jonas Biteus, *Fault Isolation in Distributed Embedded Systems*, 2007.

No 8 Ylva Nilsson, *Modelling for Fuel Optimal Control of a Variable Compression Engine*, 2007.

No 9 Markus Klein, *Single-Zone Cylinder Pressure Modeling and Estimation for Heat Release Analysis of SI Engines*, 2007.

No 10 Anders Fröberg, *Efficient Simulation and Optimal Control for Vehicle Propulsion*, 2008.

No 11 Per Öberg, *A DAE Formulation for Multi-Zone Thermodynamic Models and its Application to CVCP Engines*, 2009.

No 12 Johan Wahlström, *Control of EGR and VGT for Emission Control and Pumping Work Minimization in Diesel Engines*, 2009.

No 13 Anna Pernestål, *Probabilistic Fault Diagnosis with Automotive Applications*, 2009.


LINKÖPINGS UNIVERSITET
LINKÖPINGS UNIVERSITET